MOLECULAR FEATURES OF REGULATORY T CELLS IN HEALTH AND DISEASE

by

Catherine Ann Konopacki

A Dissertation

Presented to the Faculty of the Louis V. Gerstner, Jr.

Graduate School of Biomedical Sciences,

Memorial Sloan-Kettering Cancer Center

in Partial Fulfillment of the Requirements for the Degree of

Doctor of Philosophy

New York, NY

May, 2018

_____ _____

Alexander Y. Rudensky PhD Date

Dissertation Mentor

DEDICATION

I would like to dedicate this thesis to my parents, Teresa Nicewicz-Konopacka and Peter Konopacki.

ABSTRACT

Regulatory T (Treg) cells reside in lymphoid organs and barrier tissues where they control different types of inflammatory responses. Treg cells are also found in human cancers, and studies in animal models suggest that they contribute to cancer progression. However, properties of human intratumoral Treg cells and those present in corresponding normal tissue remain largely unknown. Here, we analyzed features of Treg cells in untreated human breast carcinomas, normal mammary gland, and peripheral blood. Tumor-resident Treg cells were potently suppressive and their gene-expression pattern resembled that of normal breast tissue, but not of activated peripheral blood Treg cells. Nevertheless, a number of cytokine and chemokine receptor genes, most notably CCR8, were upregulated in tumor-resident Treg cells in comparison to normal tissue-resident ones. Our studies suggest that targeting CCR8 for the depletion of tumor-resident Treg cells might represent a promising immunotherapeutic approach for the treatment of breast cancer.

The highly conserved transcription factors Foxp3 and Foxp1 are present in the same protein complexes in Treg cells and can homo- or heterodimerize. We sought to gain insight into the shared and independent functions of Foxp3 and Foxp1 in Treg cells. We identified significant overlap of Foxp3 and Foxp1 bound DNA sequences, and also identified sequences bound exclusively by Foxp3. Foxp1 deficiency in Treg cells resulted in reduced Foxp3 mRNA and protein levels, reduced Foxp3 binding genome-wide, and concomitant dysregulation of expression of key Foxp3 target genes including *Ctla4* and *Il2ra*. Foxp1-deficient Treg cells were impaired in their suppressor function leading to an increase of cytokine production by $CD4^+$ and $CD8^+$ T cells and lymphadenopathy. Similar to previous reports describing Foxp1 deficiency in $CD4^+$ and $CD8^+$ T cells, Foxp1 deficiency in Treg cells led to a cell-intrinsic increase in proliferation and apoptosis, and Foxp1 deficient Treg cells were severely disadvantaged in a competitive setting *in vivo*.

ACKNOWLEDGMENTS

I would like to thank my mentor, Dr. Sasha Rudensky, for providing me with the training, support and independence needed to complete this work, Drs. George Plitas and Yuri Pritykin for two wonderful collaborations, Stanislav Dikiy and Drs. Alejandra Mendoza and Jesse Green for providing me with the sanity needed to complete this dissertation, Drs. Yury Rubtsov, Takatoshi Chinen and Sergio Lira for mouse strains, Drs. Yongqing Feng and Joris van der Veeken for help regarding ChIP-seq and other experimental procedures, Dr. Wei Hu for technical advice related to protein biochemistry, Drs. Olivier Elemento, Harman Bussemaker and Sean Davis for biostatistics training, Dr. Dmitry Chudakov for collaboration, the Flow Cytometry and Integrated Genomics Cores at MSKCC, and Drs. Sharlene Madera, Carlos Carmona-Fontaine and Paula Bos for training and advice during my laboratory rotations and beyond.

I would like to thank my thesis committee members, Drs. Christina Leslie and Ming O. Li for providing me the support needed to complete my dissertation. In particular, I would like to thank Drs. Christina Leslie and Yuri Pritykin for computational analyses and discussion, and Dr. Ming Li for critical and thoughtful guidance. I would also like to thank my External Advisor and my Thesis Chair, Drs. Steven Josefowicz and Andrea Scheitinger for critically reviewing this thesis.

I would like to thank all members of the Rudensky lab, with whom I have become very close friends during my tenure in the lab. They are an amazing and supportive group of people, and I have learned a great deal from them. I would also like to thank several members of the Dr. David Scheinberg and Dr. Charles Sawyers laboratories, including Ron Gejman, and Drs. Emily Casey, Tao Dao and Neel Shah for insightful discussion throughout the years. Importantly, I would like to thank my family and friends. You have been incredibly supportive over the past few years and I feel honored and humbled to have you all in my life.

I would like to thank our graduate school, particularly Drs. Ken Marians, Tom Kelly, Harold Varmus, and our benefactor Louis V. Gerstner. If it weren't for their vision, initiative and generosity, our graduate program would not exist today. Additionally, I would like to thank Linda Burnley, Iwona Abramek, Maria J. Torres, Ivan Gerena and David McDonagh for their assistance and moral support over the years.

I would like to thank the mice that were used in these experiments.

Most importantly, I would like to thank the specimen donors at MSKCC and the TCGA.

TABLE OF CONTENTS

LIST OF TABLES x

LIST OF FIGURES xi

LIST OF ABBREVIATIONS xiii

CHAPTER 1: INTRODUCTION 1

Regulatory T Cells and Immune Homeostasis 1

Immunity in the Context of Solid Tumors 4

Forkhead Box Transcription Factors 7

Introduction to the Thesis 9

CHAPTER 2: Regulatory T Cells Exhibit Distinct Features In Human Breast Cancer 11

INTRODUCTION 11

RESULTS 14

Breast Tumors Have an Increased Presence of Treg Cells 14

More Aggressive Breast Cancers Are Enriched for Treg Cells 17

Shared and Distinct Features of Breast Tumor and Normal Parenchyma-Resident Treg Cells 21

CCR8 Is Expressed by Intratumoral Treg Cells 32

CCR8 Ligand CCL1 Is Expressed by Intratumoral Myeloid Cells 34

High CCR8 Expression Marks Highly Activated and Proliferative Tumor Treg Cells and Is Associated with Poor Survival 39

DISCUSSION 43

CHAPTER 2: Forkhead Family Member Foxp1 Regulates Foxp3 Function in Regulatory T Cells 47

INTRODUCTION 47

RESULTS 50

Foxp1 and Foxp3 Share a Majority of Binding Sites that are Enriched for Forkhead and Ets Family Consensus Sequences 50
Sequences Bound Exclusively by Foxp3 are Associated Predominantly with Differentially Upregulated Genes in Activated Treg Cells. 52
Foxp3 DNA binding and protein abundance are reduced in the context of Foxp1 deficiency 59
Foxp1 Deficiency Causes Treg Cell Activation and Effector Cytokine Production 65
Foxp1 deficiency causes Treg cell functional impairment 70
Foxp1 Deficient Treg Cells are Severely Disadvantaged in a Competitive Setting and have Increased Apoptotis 76
IL-2 Signaling is Impaired in Foxp1 Deficient Treg cells and is Rescued by Constitutive Stat5 Activation *In Vivo* 77
DISCUSSION 81
CHAPTER 4: CONCLUSION 85
CHAPTER 5: MATERIALS AND METHODS 87
Human Samples 87
Mice 87
Tissue Lymphocyte Isolation 89
Flow Cytometry 89
In Vitro Assays with Human Cells 90
Ex Vivo Stimulation 91
Ex Vivo IL-2 Responsiveness 91
Ex Vivo Apoptosis 91
CellTrace Labeling and Cell Culture 93
Treg Cell Transduction 93

Adoptive Transfer 93
In Vivo Suppression Assay 94
RNA Sequencing 94
Chromatin Immunoprecipitation and Sequencing 95
Nuclear Complex Co-IP 96
Statistical Analysis 96
Bioinformatic Analyses – Human Samples 98
RNA-seq 98
Bioinformatic Analyses – Mouse Samples 98
Genome 98
RNA-seq 99
ChIP-seq 99
REFERENCES 102

LIST OF TABLES

Table 2.1. Clinical Characteristics of the Patients Whose Tumor Specimens were Used in this Study. 16

Table 3.1. Differential Gene Expression Between Naïve and Activated Treg or Tconv Cells for a Subset of Genes that were Bound by Foxp3 and not Foxp1. 58

Table 3.2. Differential Gene Expression Between Naïve or Activated Foxp1 Sufficient and Deficient Treg cells for a Subset of Genes that were Bound by Foxp3. 64

Table 4.1. Genotyping Primer Sequences. 88

Table 4.2. Primer Sequences for CCR8 and Ligand Quantitative RT-PCR. 92

Table 4.3. Runx1 ChIP-qPCR Primer Sequences. 97

LIST OF FIGURES

Figure 2.1. Experimental Approach. 13

Figure 2.2. Treg Cells Densely Populate Human Breast Tumors. 15

Figure 2.3. Treg Cell Frequency Correlates with Grade and Type of Human Breast Cancer. 18

Figure 2.4. Tumor-Resident Treg Cells Are Activated and Potently Suppressive. 19

Figure 2.5. Tumor-Infiltrating Treg and Non-Treg CD4 Cells Are Transcriptionally Similar to Tissue-Resident Cells. 23

Figure 2.6. TCR-β Repertoires of Tumor and NBP Treg and Tconv Cells Are Oligoclonal and Non-overlapping. 25

Figure 2.7. Tumor Treg Specific Genes Identified by RNAseq are Highly Expressed by Tumor Treg Cells at the Protein Level. 27

Figure 2.8. CD177 is Highly Expressed by a Subset of Tumor Treg Cells in Several Types of Cancer. 30

Figure 2.9. Analysis of Gene Expression and TCR Oligoclonality of Intratumoral $CD177^+$ and $CD177^-$ Treg Cells. 31

Figure 2.10. CCR8 Expression by Tumor-Resident Treg Cells Is Specific and Functional. 33

Figure 2.11. The CCR8 Ligand CCL1 is Expressed by $CD11b^+CD14^+$ Myeloid Cells in Breast Tumors. 35

Figure 2.12. CCR8 Signaling Does not Affect Treg Cell Suppressor Function *In Vitro*. 37

Figure 2.13. CCR8 is Expressed by a Minor Subset of Treg Cells in Axillary Lymph Nodes of Stage III Breast Cancer Patients. 38

Figure 2.14. Treg CCR8 Expression Correlates with Clinic-Pathologic Features of Human Breast Cancer and Is Associated with Poor Disease Free and Overall Survival. 41

Figure 2.15. Ratio of Chemokine Receptor mRNA to Foxp3 mRNA does not Correlate with Survival Outcome in the TCGA Dataset. 42

Figure 3.1. Experimental Approach for Genomics Experiments. 49

Figure 3.2. Foxp1 and Foxp3 Share a Majority of Binding Sites that are Enriched for Forkhead and Ets Family Consensus Sequences. 51

Figure 3.3. Sequences Bound Exclusively by Foxp3 are Associated Predominantly with Differentially Upregulated Genes in Activated Treg Cells. 55

Figure 3.4. Analysis of Genes Associated with Foxp3-only Peaks. 57

Figure 3.5. Generation of the Conditional *Foxp1* Allele. 61

Figure 3.6. Foxp3 DNA Binding and Protein Abundance are Reduced in the Context of Foxp1 Deficiency. 62

Figure 3.7. Foxp1 Deficiency Causes Treg Cell Activation and Effector Cytokine Production. .. 66

Figure 3.8. Comparison of $Foxp3^{YFP\text{-}Cre}Foxp1^{f/f}$ to $CD4^{Cre}Foxp1^{f/f}$. 69

Figure 3.9. Foxp1 Deficiency Causes Treg Cell Functional Impairment. 71

Figure 3.10. *In Vivo* Suppression Assay Analysis. 73

Figure 3.11. Foxp1 Deficient Treg Cells are Severely Disadvantaged in a Competitive Setting and have Increased Apoptotis. 74

Figure 3.12. IL-2 Signaling is Impaired in Foxp1 Deficient Treg Cells and is Rescued by Constitutive Stat5 Activation *In Vivo*. 79

Figure 3.13. Foxp1 Presence in Treg Cells Enables Foxp3 Binding to Additional Sites Genome-wide. 83

LIST OF ABBREVIATIONS

ADP	Adenosine diphosphate
APC	Antigen presenting cell
ATP	Adenosine triphosphate
BCR	B cell receptor
BSA	Bovine serum albumin
DC	Dendritic Cell
DFS	Disease-free survival
EMSA	Electrophoretic mobility shift assay
ER^+	Estrogen receptor positive
FBS	Fetal Bovine Serum
Fox	Forkhead box
GO	Gene Ontology
$Her2^+$	Her2 amplified
IDO	indoleamine 2,3-dioxygenase
IPEX	Immune dysregulation, polyendocrinopathy, enteropathy, X-linked
IRB	Institutional Review Board
NBP	Normal breast parenchyma
NK	Natural killer cell
NKT	Natural killer T cell
NYBC	New York Blood Center
OS	Overall survival
PBMC	Peripheral blood mononuclear cells
PCR	Polymerase chain reaction
PMA	phorbol 12-myristate-13-acetate

TCGA The Cancer Genome Atlas

Tconv Foxp3^{-} CD4^{+} T cell

TCR T cell receptor

TNBC Triple negative breast cancer

TRE TPA-responsive element

Treg Regulatory T cell

CHAPTER 1: INTRODUCTION

Regulatory T Cells and Immune Homeostasis

Our immune system is comprised of a variety of effector cells and molecules that serve to protect our bodies from various infectious agents and the damage they cause. The immune response functions by first recognizing the presence of an infection, then mounting an immune effector response to contain and eliminate the infection, and finally by forming an immunological memory of the infection so that it will be prepared to respond more rapidly and robustly to subsequent exposure to the same infectious agent [1]. The immune response needs to be carefully regulated so that it does not itself do damage to the body, and several mechanisms have evolved to enable self-regulation by the immune system. Failure of such regulation contributes to autoimmune disease [2].

The innate immune system provides initial discrimination between self and non-self. Innate immune cells rely on a constrained repertoire of receptors to recognize pathogens. Macrophages, neutrophils and dendritic cells (DCs) express pathogen recognition receptors that recognize pathogen-associated molecular patterns, such as mannose-rich oligosaccharides, peptidoglycans, and lipopolysaccharides in the bacterial cell wall, as well as unmethylated CpG DNA, which is common to many pathogens but not present in the body's own cells [1].

The adaptive immune system is comprised of B and T cells that express an enormously diverse range of B cell receptors (BCRs) and T cell receptors (TCRs) respectively. Each B and T lymphocyte matures bearing a unique variant of antigen receptor [1]. Every nucleated cell in the body expresses a cell surface protein termed the major histocompatibility complex I (MHC I) that is specialized to present peptides derived from cytosolic proteins to the $CD8^+$ subset of T cells. Certain cells of the innate immune system termed antigen presenting cells (APCs) express a second cell surface protein termed the MHC II that is specialized to present peptides derived from

extracellular proteins to the $CD4^+$ subset of T cells. These innate immune cells are also capable of cross-presenting peptides derived from extracellular proteins on MHC I to $CD8^+$ T cells. APCs induce expression of a second type of cell surface protein upon activation in response to infection, CD80 or CD86 [3]. These proteins interact with a co-stimulatory cell surface protein CD28 expressed by T cells and this interaction, combined with the interaction of TCR with MHC/peptide complex, is required for T cell activation. During T cell development in the thymus, the TCR is formed by random rearrangements of *TCRα* and *TCRβ* gene segments. Thymocytes expressing an αβTCR are positively selected in the thymic cortex so that only clones that recognize self-peptide presented by MHC with moderate affinity differentiate [1]. Avidity for MHC/self-peptide determines CD4 or CD8 lineage differentiation [4]. T cells that fail to bind the MHC/peptide complex die by apoptosis, termed death by neglect. Thymocytes then migrate into the thymic medulla and interact with APC MHC/peptide complexes. The majority of thymocytes that interact too strongly die by apoptosis, termed negative selection, but some cells escape negative selection and are tolerized and rendered anergic in the periphery through chronic TCR engagement without co-stimulation [1]. Positive and negative selection during T cell development produces a diverse population of non-self reactive T cells that exit the thymus and circulate in the periphery.

A subset of $CD4^+$ T cells that is exposed to strong TCR signal during negative selection, in the context of certain other cell-extrinsic and intrinsic cues, will induce expression of a transcription factor, Foxp3 [5-10]. Foxp3 regulates expression of many pro-survival molecules, conferring a selective survival advantage to these cells, enabling them to differentiate into a subset of T cells called Treg cells [3]. Treg cells can also differentiate from $CD4^+Foxp3^-$ conventional T (Tconv) cells in the periphery [11, 12]. In this case, Tconv cells expressing non-self reactive TCRs that recognize certain foreign antigens, such as food or intestinal or skin microbiota, with high affinity but under suboptimal activation conditions may induce Foxp3

expression and differentiate into Treg cells [13]. Suboptimal activation conditions that have been shown to induce Foxp3 in Tconv cells include weak costimulation due to increased Ctla-4 signaling, and TCR signaling in the presence of tolerogenic cytokines, such as TGF-β [14]. The *Foxp3* locus contains several highly conserved non-coding sequences (CNS) that are critical for Foxp3 induction in different contexts [15]. The CNS3 element is required for Foxp3 induction in thymocytes [15]. CNS2 is required for heritable maintenance of Foxp3 expression but is not necessary for its induction [15]. Likewise, CNS1 is dispensable for Treg cell induction in the thymus but is required for Treg cell generation from Tconv cells in the periphery [15]. Loss of Foxp3 expression, either through genetic manipulation in mice or through mutations in the gene locus in immune dysregulation, polyendocrinopathy, enteropathy, X-linked (IPEX) syndrome patients or in scurfy mice results in severe autoimmunity whose direct cause is a lack of Treg cells [16-22]. Foxp3-expressing Treg cells are therefore crucial for maintaining immune homeostasis.

Treg cells maintain immune homeostasis in a variety of ways. They produce and secrete immunomodulatory cytokines such as TGF-β and IL-10 that inhibit differentiation, proliferation and activation of cytotoxic T cells and Tconv cells and suppress their production of inflammatory cytokines [23, 24]. Treg cells express high levels of Il2r-α, which forms the high-affinity IL-2 receptor with Il2r-β and Il2r-γ. High IL-2 receptor expression by Treg cells depletes local IL-2, causing cytokine-deprivation mediated apoptosis of Tconv cells that express much lower levels of the receptor [25]. Treg cells express the ectonucleotidase CD39 that converts extracellular adenosine triphosphate (ATP) to adenosine diphosphate (ADP), and CD73 that converts extracellular ADP to adenosine [26, 27]. Adenosine is an immunosuppressive molecule that inhibits T cell proliferation, promotes production of immunosuppressive molecules by APCs, inhibits natural killer (NK) cell activity, and increases Treg cell immunomodulatory activity. A reduction in extracellular ATP inhibits ATP-driven DC maturation [26]. Treg cells express co-

inhibitory molecules such as Ctla-4, Lag-3 and PD-1 highly, which can interact with receptors on DCs and inhibit DC maturation [28-30]. Ctla-4 ligation of CD80 and CD86 on DCs triggers expression of indoleamine 2,3-dioxygenase (IDO), an enzyme that catabolizes tryptophan and has a role in induction of tolerance [30].

The immune system has evolved to recognize foreign pathogens accurately, mount an effective response to clear them and form long-lasting memory. T cell development in the thymus is designed to generate a diverse pool of naïve non-self reactive T cells. Despite this, auto-reactive T cells do develop. Treg cells are critical for suppression of autoimmunity and maintenance of self-tolerance.

Immunity in the Context of Solid Tumors

Cancer is defined as uncontrolled division of abnormal cells. Cells can begin to divide uncontrollably as a result of viral infection, through prolonged exposure to an inflammatory environment conducive to tumorigenesis, or upon accumulation of DNA mutations. The immune system prevents virus-induced tumor formation by eliminating or suppressing viral infections. The immune system also serves to resolve pathogenic infections to prevent establishment of chronic inflammatory environments[31]. In the vast majority of cases when the DNA in a cell has sustained damage, DNA repair proteins will be activated and cells will remain at the G1/S stage until the damage is repaired or will undergo apoptosis if DNA damage is irreparable. In some cases cells may mutate or lose p53 or other genes involved in the DNA damage response, enabling cell cycle progression [32]. The immune system can specifically identify and eliminate such cancerous or pre-cancerous cells on the basis of their expression of tumor-specific antigens or molecules induced by cellular stress in a process called tumor immune surveillance [31].

Despite tumor immune surveillance, tumors do develop in the presence of a functional immune system. When the immune system does not completely clear all malignant cells, variants

that are able to resist, avoid or suppress the antitumor immune response will continue to proliferate and form a progressively growing tumor [33]. Many tumor cell-specific factors have been shown to contribute to immune suppression, including activation of T cells in the absence of co-stimulation leading to T cell anergy, expression of T cell inhibitory molecules, tumor antigen loss or downregulation of MHC I molecules by tumor cells, secretion of soluble immunomodulatory cytokines and enzymes such as TGF-β and IDO by tumor cells, and tumor resistance to cytotoxic pathways, through overexpression of the anti-apoptotic protein BCLXL or by mutating *Fas*, *Dr5* or *Bax* [34, 35] [36] [37]. Furthermore, Rapid cellular division during tumor growth can lead to localized hypoxia [38]. Effector T cells require glycolysis for their survival and function and face metabolic competition in a hypoxic tumor microenvironment [39]. Conversely, Treg cells, which rely on lipid oxidation rather than glycolysis, may be better able to survive in the tumor microenvironment [40]. Hypoxia also induces PD-L1 expression on cancer cells, protecting them from cytotoxic T cell mediated lysis [41].

Solid tumors are a mixture of tumor cells, hematopoietic cells and non-hematopoietic stromal cells. Besides tumor cell mediated immune suppression, stromal cells in the tumor microenvironment can also actively suppress antitumor immunity by several mechanisms, including expression of inhibitory receptors, production of molecules that induce T cell apoptosis and secretion of immunosuppressive factors [42]. Stromal cells can also hinder immune infiltration into tumors. Dysfunctional endothelial cells in tumors produce leaky and highly irregular blood vessels, resulting in low nutrient availability, necrosis and localized hypoxia and preventing immune cell migration into tumors [38, 42]. Fibroblasts secrete chemokines that selectively repel cytotoxic T cells and recruit immunosuppressive cells [43].

Analysis of the tumor microenvironment in patients with a variety of solid tumors has revealed that tumors can be categorized into major groups based on their pattern of immune cell infiltration. The first category of tumors shows high T cell infiltration, a broad chemokine profile

and a type I interferon signature indicative of innate immune activation [44]. There also exist tumors for which immune cells are excluded at the periphery, potentially through mechanisms mediated by stromal cells. Lastly, there are tumors that are completely devoid of immune infiltrate, with a so-called desert immune landscape [45]. A pioneering study by Galon et al. showed that disease free survival (DFS) for patients with colorectal tumors that have high density of $CD3^+$ T cells and $CD45RO^+$ antigen experienced T cells in the tumor center and at the invasive margin is significantly higher than DFS for patients with low density of these cell types in their tumors, regardless of tumor stage [46]. The immunoscore, first proposed to classify malignant colorectal tumors based on their level of immune infiltrate, is now appreciated as a more important predictor of cancer progression than tumor stage or its pathological grade [46].

Over the past decade, cancer immunotherapy to enhance anti-tumor immunity has emerged as a very promising therapeutic strategy. However, it has been observed that some T-cell-inflamed tumors respond to immunotherapy and others do not. Expression of multiple inhibitory molecules by tumor cells can compensate for checkpoint blockade therapy targeting one inhibitory receptor. Some patients who do not respond to immunotherapy may have exhausted T cells that cannot mount an anti-tumor response. Two recent studies show that non-responders and patients that developed resistance to checkpoint blockade therapy had tumors with genomic defects in interferon pathway genes [47, 48] suggesting that interferon signaling is important in anti-tumor immunity. Regulatory T cell or immunosuppressive APCs within solid tumors may also inhibit effector T cell activation in the context of immunotherapy.

Further characterization of the immune cells present in the tumor microenvironment is crucial, both to improve existing immunotherapies and enable development of new ones, but also to increase our understanding of why certain tumors are strongly infiltrated by immune cells and others are not. Tumors that are completely devoid of immune cells are not responsive to immunotherapy, so there is a clear need for novel therapeutic strategies for this subset of patients.

Recently, it was shown that lack of antigen expression does not explain the non-T cell-inflamed tumor microenvironment phenotype in melanoma, as non-T cell-inflamed tumors express similar frequency of non-synonymous mutations as tumors with T cell infiltration [49]. These data suggest that strategies to overcome the barrier of T cell migration into solid tumors might ultimately enable immunotherapy efficacy in non-T cell inflamed tumors.

Forkhead Box Transcription Factors

The conserved family of Forkhead box (Fox) proteins is a functionally diverse group of transcription factors that have critical roles both during embryonic development and in differentiated cells. This family is defined by a conserved 110 amino acid DNA binding domain that is almost perfectly conserved between *D. melanogaster* Forkhead and the mammalian Fox transcription factors [50]. The Forkhead domain forms three alpha helices and three beta sheets flanked with two loops or wings, based on x-ray crystallography and nuclear magnetic resonance studies, giving the three-dimensional structure a winged-helix appearance [50]. This winged-helix structure facilitates binding of Fox proteins to the major groove of DNA sequences containing consensus binding sites [51]. Fox proteins recognize sites with the core sequence 5' RTAAAYA 3' [52]. Cell-type specific and temporally regulated expression of Fox proteins, post-translational modification that alters their activity, differential DNA binding affinity of different family members, recruitment of distinct cofactors and modified DNA binding affinity and specificity due to interactions with other proteins all contribute to the ability of Fox transcription factors to exert unique functions *in vivo*, despite recognizing nearly identical DNA sequences [53-55].

The Fox proteins are further categorized into 19 subgroups on the basis of sequence homology within and outside of the winged-helix/Forkhead domain [56]. The Foxp subfamily consists of four members in humans and in mice, Foxp1-4 that are expressed in distinct and overlapping cell types [57]. *Foxp1* is most similar to the *D. melanogaster Foxp* gene, whereas the

other three genes likely originated through serial duplications [58]. All four Foxp proteins contain a zinc finger structure and a leucine zipper motif N-terminal to the Forkhead domain.

Foxp1, Foxp2 and Foxp4 regulate important aspects of development in heart, lung, neural and thymic tissues. Foxp1 mutant embryos have severe defects in cardiac morphogenesis, including outflow tract septation defects, thinning of ventricular myocardium and lack of proper ventricular septation [59-62]. These defects lead to embryonic death at E14.5 [61]. Foxp2 is involved in speech and language development, while Foxp2 and Foxp4 together coordinate neural stem cell and precursor cell differentiation during neurogenesis [63, 64]. Foxp1 and Foxp2 cooperate to regulate lung and esophageal development [65]. Foxp1 has been implicated as a tumor suppressor due to its loss in breast, lung, stomach, colon, prostate, liver, renal and endometrial tumors [57]. Foxp4 is downregulated in kidney tumors and commonly mutated in prostate cancer[57].

Several Foxp family members have known roles in the hematopoetic system. Foxp3 is the lineage-specific transcription factor in Treg cells. Foxp1 has essential roles in B and T lymphocyte development [66, 67]. Foxp1 also regulates the quiescence of naïve T cells in a cell-intrinsic manner and acute deletion of Foxp1 results in proliferation and activation of naïve T cells and increased follicular helper T cell differentiation [68-71]. In advanced tumors, Foxp1 upregulation in CD8+ T cells drives their unresponsiveness by preventing proliferation and effector cytokine production [72]. Foxp4 may regulate memory recall responses [73].

There is sequence divergence in the flanking sequences around the Forkhead domain among the family members, which could enable distinct target recognition and regulation by each Foxp protein [74]. Indeed, radioactive electrophoretic mobility shift assays (EMSA) using truncated Foxp3 and Foxp1 proteins showed that Foxp3 binds the nucleotide sequence 5’(G/a)TAAACA 3’, while Foxp1 binds the sequence 5’ AA(C/t)A(C/t)AAATA 3’ [75]. The

sequences of Foxp member genes *Foxp1*, *Foxp2* and *Foxp4* are more closely related, while *Foxp3* is much smaller [57, 76]. These transcription factors therefore likely interact with distinct binding partners *in vivo*. Foxp3 ChIP-seq experiments in primary Treg cells have shown that the Forkhead motif exists only in a small subset of Foxp3 bound DNA sequences, suggesting the importance of cofactors in Foxp3 mediated gene regulation [77].

The Foxp transcription factors require dimerization through their leucine zipper motif to bind DNA and are capable of homo- and hetero-dimerization [57]. Mutation of the highly conserved leucine residues within the leucine zipper domain disrupts protein-protein interactions and inhibits transcriptional regulation by Foxp dimers [78-80]. Overexpression studies have demonstrated that Foxp1, Foxp2, and Foxp4 can homo- and heterodimerize, and that Foxp3 can form heterodimers with Foxp1 [78, 79]. Foxp family heterodimerization may therefore offer yet another level of regulation of DNA sequence recognition.

Introduction to the Thesis

This thesis begins by specifically addressing how the breast tumor environment regulates Treg cell phenotype[81]. A plethora of data exist comparing gene expression of tumor infiltrating immune cells to that of circulating immune cells and support the idea that the tumor environment drives massive gene expression changes in immune cells. However, significant work has also been done to characterize tissue resident immune cells and has revealed significant gene expression changes in cells that reside in tissues as compared to their counterparts in the circulation. An open question that we sought to address in this thesis was whether the tumor environment imprints distinct transcriptional and functional features upon Treg cells or whether these cells are similar to activated Treg cells found in corresponding normal tissues. We therefore characterized tumor and tissue resident Treg cells from breast cancer patients.

Treg cell density in multiple different solid tumor types is correlated with worse prognosis and transient depletion of Treg cells in tumor-bearing mice has been shown to delay tumor growth and metastasis, providing strong evidence for the role of Treg cells in cancer progression and providing rationale for targeting them in cancer patients. Systemic Treg cell targeting leads to severe inflammation and is not a tractable therapeutic strategy, so mechanisms to specifically deplete tumor resident Treg cells or block their suppressor function will have therapeutic potential.

In the second part of this thesis, we assessed the effect of Foxp1 deletion on the function and phenotype of Treg cells. We became interested in investigating the role of Foxp1 in Treg cells because of its well-characterized functions in T cell development and in effector T cell quiescence, because of its presence in Foxp3 transcription factor complexes in Treg cells, and because of its known ability to form heterodimers with Foxp3. These multiple lines of evidence pointed to a role of Foxp1 in Treg cell biology and led us to investigate its function in this context. We were also very interested in understanding how Foxp1 and Foxp3 are able to exert unique functions *in vivo*, despite being predicted to recognize identical DNA sequences. One recent study directly assessed Foxp3 and Foxp1 DNA binding *in vitro* and found that they have preference for distinct DNA sequences, but *in vivo* relevance of these findings is unknown [75]. We thus characterized Foxp3 and Foxp1 transcription factor occupancy genome-wide in Treg cells to identify unique and shared binding sites and to determine if these factors had distinct sequence specificities *in vivo*.

CHAPTER 2: REGULATORY T CELLS EXHIBIT DISTINCT FEATURES IN HUMAN BREAST CANCER

INTRODUCTION

Treg cells expressing the transcription factor Foxp3 play an essential role in controlling autoimmunity and maintain immunological tolerance[3]. Treg cells are present in secondary lymphoid organs, peripheral blood, and in non-lymphoid organs, most prominently at barrier sites including skin, lung, gastrointestinal tract, and liver. Under inflammatory conditions, however, Treg cells can be recruited to inflammatory insult sites throughout the body. In addition to secondary lymphoid organs, Treg cells can exert their suppressor function in non-lymphoid tissues as evidenced by specific tissue lesions in mice with selectively impaired Treg cell migration[82].

Suppression of distinct types of inflammatory responses by Treg cells is tailored by their sensing of cytokines and other cues resulting in activation of some of the same transcription factors involved in elaboration of pro-inflammatory effector responses[83]. Besides sensing distinct types of inflammation, Treg cells residing in non-lymphoid organs can sense unknown tissue cues and exhibit distinct features. Treg cells have also been found in increased numbers in diverse experimental mouse tumors and in human cancers[84, 85]. While breast carcinomas have not traditionally been considered immunogenic, evidence of tumor-infiltrating lymphocytes and their subset composition paralleling disease progression suggest that the underlying interactions of these tumors with immune cells are important [86]. Specifically, the clinical relevance of tumor-infiltrating T cells has been intensively studied [87]. An increased ratio of $CD4^+$ to $CD8^+$ T cells correlates with lymph node metastases and reduced overall survival [88]. Increased

presence of Treg cells in breast tumor biopsies is associated with an invasive phenotype and diminished relapse-free as well as overall survival [89-91].

It is thought that Treg cells can facilitate tumor growth and metastasis based on the observed regression of established tumors in experimental models of Treg cell depletion [92-95]. Transient ablation of Treg cells results in marked reductions in primary and metastatic tumor growth in a poorly immunogenic, oncogene-driven model of mammary carcinoma [96]. Despite the potential major importance of Treg cells in tumor progression and metastasis and their role as therapeutic targets as established by mouse studies, the properties of Treg cells present in human tumors remain largely unknown. Specifically, it is not clear whether the tumor environment imprints distinct transcriptional and functional features upon Treg cells or whether these cells are similar to activated Treg cells found in corresponding normal tissues or in the peripheral blood.

To address these questions, we explored the functional and transcriptional properties of Treg cells present in breast carcinomas from a large cohort of newly diagnosed patients using flow cytometric and RNA-seq analysis and compared them to peripheral blood or normal breast parenchyma (NBP)-resident Treg cells (Figure 2.1). Our analyses indicated that tumor and normal tissue-resident Treg cells exhibit largely shared transcriptional features, distinct from those of activated Treg cells in peripheral blood. Nevertheless, tumor-resident Treg cells exhibit increased expression of genes involved in cell activation and cytokine and chemokine signaling including highly augmented expression of chemokine receptor CCR8. CCR8 was also highly expressed by Treg cells present in a number of other cancer types. Analysis of breast cancer gene expression datasets revealed a strong association of CCR8 mRNA amounts normalized to Foxp3, but not Foxp3 mRNA amounts alone, with poor prognosis, implicating highly activated CCR8 expressing Treg cells in breast cancer progression. These findings provide rationale for the therapeutic targeting of Treg cells through a CCR8 depleting antibody in breast cancer, where Ctla-4 and PD-1 focused checkpoint blockade has met limited success so far.

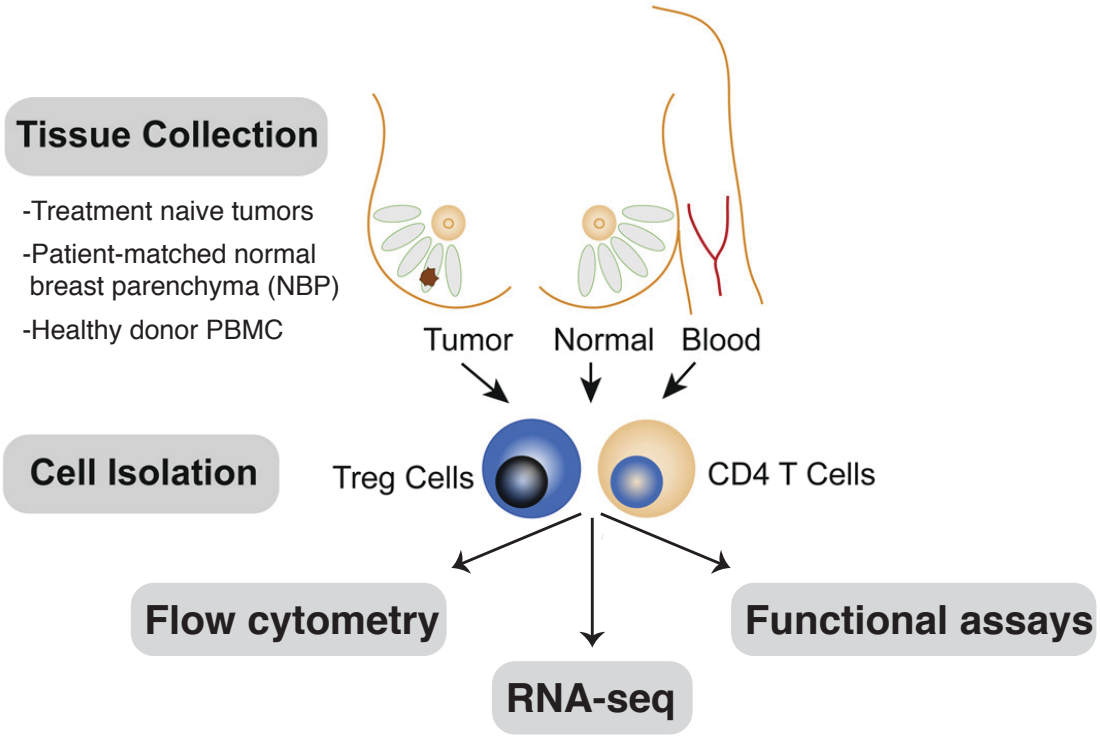

Figure 2.1. Experimental Approach.

Human primary breast tumor, NBP, and peripheral blood mononuclear cells (PBMC) were freshly isolated. Treg cells and CD4 T cells were analyzed by flow cytometry, RNA-seq and in functional assays.

RESULTS

Breast Tumors Have an Increased Presence of Treg Cells

Treg cells variably infiltrate human breast cancers and their frequency in the tumor microenvironment has clinical significance [97-100]. To determine the composition of T cell subsets-resident in primary human breast tumors, we evaluated tissue-resident lymphocytes from tumors, NBP, and lymphocytes from peripheral blood by multi-color flow cytometry. The tissue samples were immediately procured from operative specimens of treatment-naive patients undergoing surgery for primary breast cancer (Table 2.1). NBP-resident cells were isolated from patients undergoing prophylactic mastectomies with no radiographic evidence of disease. Blood samples were from patients undergoing surgery, as well as from buffy coats from healthy donors. The frequency of Treg cells among all tumor-infiltrating leukocytes varied widely (Figure 2.2D). As compared to NBP and peripheral blood, tumor-resident T cell populations exhibited a distinct prevalence and distribution of T cell subsets with an increased abundance of $Foxp3^+$ Treg cells (Figure 2.2A). This pattern was observed in multiple patients as evidenced by increased percentage of Treg cells within both $CD4^+$ and total $CD3^+$ T cell populations, as well as by a markedly decreased ratio of cytotoxic $CD8^+$ T cells to Treg cells (Figure 2.2B). Furthermore, we found that the ratio of $CD4^+$ to $CD8^+$ T cells was markedly different between tumor and NBP with NBP having a greater proportion of $CD8^+$T cells (Figure 2.2C). Our finding was consistent with previously reported analysis of freshly isolated lymphocytes from a small set of normal and malignant breast tissue samples [101]. It is noteworthy that we observed near perfect correlation of high amounts of Foxp3 with high CD25 expression in tumor and NBP-resident Treg cells with no detectable Foxp3 found in $CD8^+$ or $CD4^+$ Tconv cells. This enabled highly efficient fractionation of tumor associated Treg and non-Treg cells based on CD25 expression. Our results suggest that the T cell composition in the human tumor microenvironment is distinct from tissue and favors a more immunoregulatory phenotype.

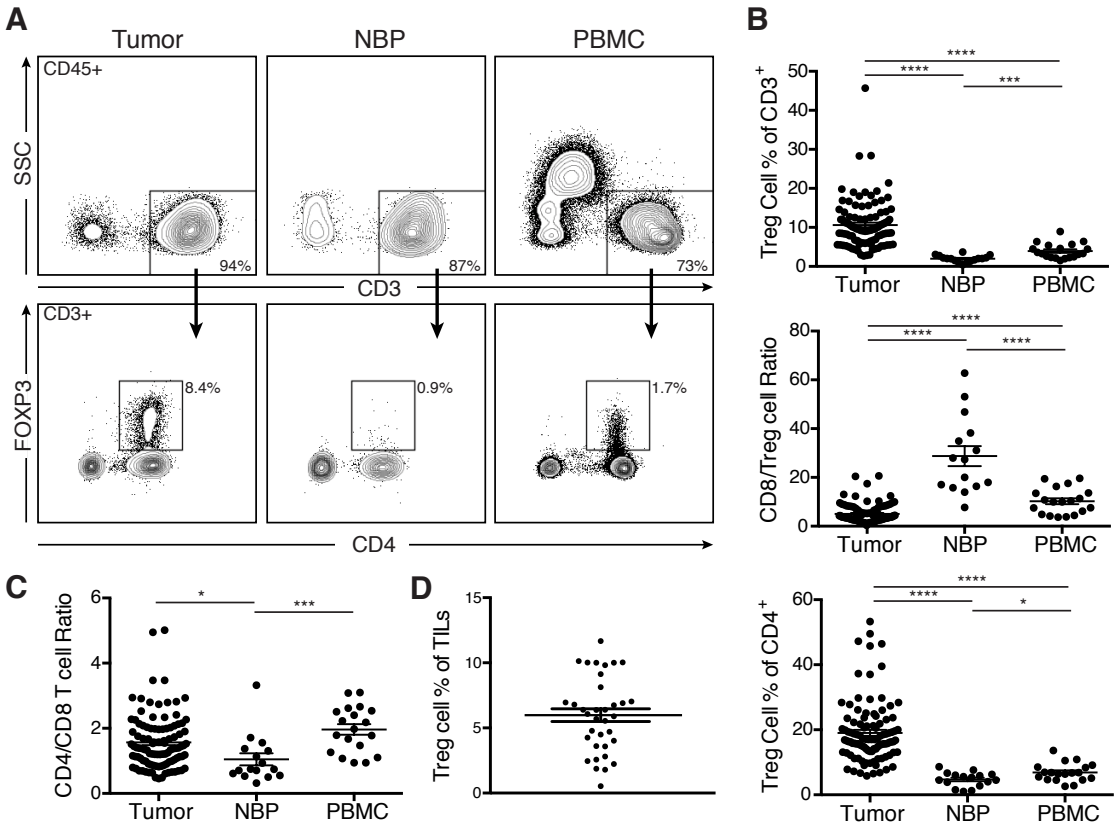

Figure 2.2. Treg Cells Densely Populate Human Breast Tumors.

Freshly isolated human primary breast tumor, NBP, and peripheral blood mononuclear cells (PBMC) were analyzed by flow cytometry. (A) Representative flow cytometric analysis of lymphocytes from tumor, NBP, and PBMC isolated from a patient with primary breast cancer. (Data are representative of findings in samples analyzed from 105 patients.) (B) Scatterplots indicating the cumulative frequency of Treg cells among all T cells and the $CD8^+$:Treg cell ratio. **c,** Ratio of $CD4^+$ to $CD8^+$ T cells in tumor, NBP, and PBMC. Data represent the analysis of over 100 individual patients; error bars represent SEM; $^*p < 0.05$; $^{**}p < 0.01$, $^{***}p < 0.001$, ns: non-significant (unpaired two-tailed Student's t test). (D) Cumulative frequency of Treg cells among all tumor-infiltrating leukocytes.

Table 2.1. Clinical Characteristics of the Patients Whose Tumor Specimens were Used in this Study.

Description of patient age, tumor stage, nodal stage, cancer subtype and tumor grade for each patient.

Variable		N=105
Age (median)		50 (24-88)
Tumor Stage	T1 T2 T3	52 (49.5%) 50 (47.6%) 3 (2.10%)
Nodal Stage	N0 N1 N2 N3	71 (67.6%) 28 (26.7%) 2 (1.9%) 4 (3.8%)
Subtype	ER+ Her2+ TNBC	78 (74.3%) 10 (9.5%) 19 (18.1%)
Tumor Grade	1 2 3	8 (7.6%) 38 (36.2%) 59 (56.2%)

More Aggressive Breast Cancers Are Enriched for Treg Cells

To explore whether any particular clinical correlates were associated with heightened presence of Treg cells, we analyzed the distribution of T cell subsets among the clinically defined surrogates for the molecular subtypes of breast cancer including estrogen receptor positive (ER^+), Her2 amplified ($Her2^+$), and triple negative breast cancer (TNBC). In addition, we utilized histologic grade as a variable to gain further insight into the relationship between T cell composition and tumor biology. We found that TNBC had a higher proportion of $CD4^+$ T cells than the other subtypes of breast cancer and that Treg cells were particularly prominent in TNBC (Figure 2.3A). Although $CD4^+$ to $CD8^+$ T cell ratio alone could not distinguish between tumors of low to high histologic grade, an increased frequency of Treg cells correlated with higher grade tumors (Figure 2.3A). Further analysis of tumor-infiltrating Treg cells for expression of a cell-division-associated marker Ki67 revealed that higher-grade tumors were characterized by higher Treg cell proliferative activity. However, the latter did not correlate with biologic subtype (Figure 2.3B). Notably, Treg cells were markedly more proliferative than either conventional $CD4^+$ or $CD8^+$ T cells in breast tumors and NBP and Treg cells isolated from breast tumors were more proliferative than Treg cells isolated from NBP (Figure 2.4A). A comparison of expression of Ctla-4 and CD25, two known markers indicative of Treg cell activation, between breast tumor, NBP, and peripheral blood Treg and Tconv cells also revealed that tumor-resident Treg cells exhibited an activated phenotype consistent with their increased proliferative activity (Figure 2.4B). Previous studies of human Treg cells isolated from autoimmune lesions suggested that these tissue-resident Treg cells exhibit impaired in vitro suppressor capacity raising questions as to whether tumor-resident Treg cells are capable of suppression. Thus, we isolated Treg cells from breast cancers and assessed their ability to suppress proliferation of naive peripheral blood

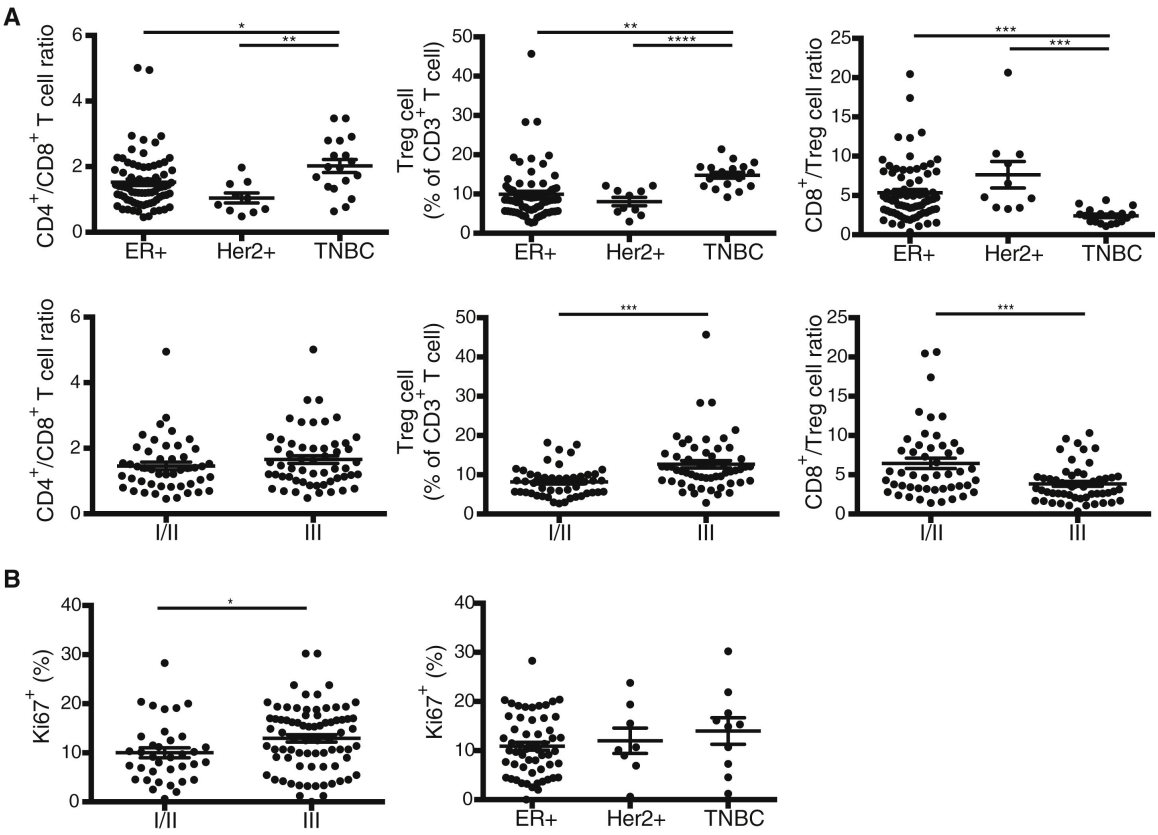

Figure 2.3. **Treg Cell Frequency Correlates with Grade and Type of Human Breast Cancer.**

(A) Scatterplots representing the frequency of T cell subsets based on biologic subtype (ER^+, estrogen receptor > 1% positive Her2 non-amplified; $Her2^+$, Her2 amplified either by 3+ staining on immunohistochemistry or FISH Her2-to-CEP17 ratio > 2.3; TNBC, ER < 1%, PR < 1%, Her2 non-amplified) and based on histologic grade. (B) Scatterplots representing the frequency of proliferating Treg cells in tumors based on histologic grade and biologic subtype. Frequencies are the percentage of Treg cells that are $Ki67^+$. Data represent the analysis of over 100 individual patients; error bars represent SEM; $^*p < 0.05$; $^{**}p < 0.01$, $^{***}p < 0.001$, ns non-significant (unpaired two-tailed Student's t test). The 57 high-grade tumors included 33 ER+, 18 TNBC, and 6 $Her2^+$ samples.

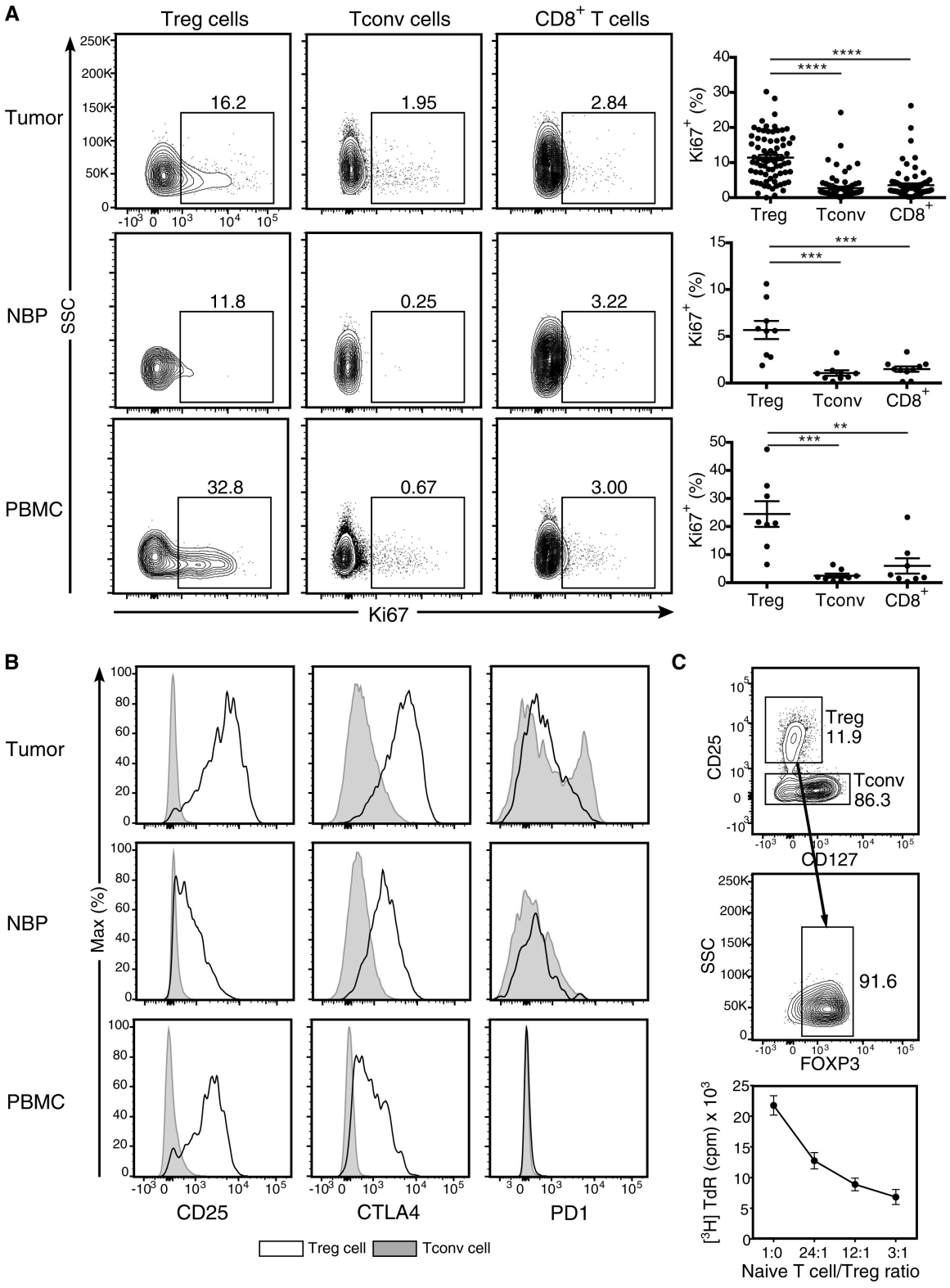

Figure 2.4. Tumor-Resident Treg Cells Are Activated and Potently Suppressive.

(Figure description continued on next page)

Figure 2.4 – (continued)

(A) Representative flow cytometric analysis of lymphocytes from tumor, NBP, and peripheral blood isolated from a patient with primary breast cancer and summary plot indicating the proportion of lymphocytes from tumor, NBP and periphe3ral blood that are $Ki67^{+}$. Data represent the analysis of over 70 individual patients; error bars represent SEM; $^{*}p < 0.05$; $^{**}p < 0.01$, $^{***}p < 0.001$, ns non-significant (unpaired two-tailed Student's t test). (B) Mean fluorescence intensity (MFI) of staining for activation markers on cells gated on Treg (open histograms) and Tconv cells (shaded histograms) in breast tumor, NBP, and peripheral blood. Individual dots represent data are from individual tumor specimens.(C) Tumor-resident $CD4^{+}CD25^{hi}$ Treg cells were flow cytometry isolated and their capacity to suppress proliferation of naive Tconv cells in vitro was assessed by ^{3}H-thymidine incorporation on day 4 (n = 3, plot is representative of three independent experiments).

$CD4^+$ T cells isolated from buffy coats. We found that in agreement with their observed activated phenotype, $CD25^{hi}CD4^+$ Treg cells isolated from breast tumors were also strongly suppressive (Figure 2.4C). Thus, more advanced grades of different types of breast cancer and the more aggressive TNBC type are associated with a heightened presence of activated Treg cells with potent suppressor function.

Shared and Distinct Features of Breast Tumor and Normal Parenchyma-Resident Treg Cells

Next, we sought to explore whether the tumor microenvironment imparts distinct features on Treg cells and on Tconv cells. Alternatively, it was possible that the transcriptional features of these cell subsets in the tumor resembled those in NBP or in peripheral blood. Thus, we employed RNA-seq analysis to assess genome-wide gene expression features of purified $CD25^{hi}CD4^+$ Treg and effector $CD25^-CD4^+$ T cells isolated from breast tumors and from NBP. Activated $CD45RO^+$Treg cells and Tconv cells were isolated from buffy coats to match the activated phenotype of the corresponding cell subsets found in the tumor and NBP. The gene-expression patterns of tumor-resident Treg and Tconv cells were very similar to those of NBP-resident Treg and Tconv cells, respectively, but distinct from those of the corresponding activated or memory T cell cells isolated from peripheral blood (Figures 2.5A–2.5C). Thus, residence in a non-lymphoid tissue, regardless of whether it is healthy or has undergone oncogenic transformation, serves as a major determinant of gene-expression characteristics of tumor and tissular Treg and Tconv cells.

The observation that breast tumor and tissue Treg cells and breast tumor and tissue Tconv cells were transcriptionally very similar led us to ask whether Treg and Tconv populations in breast tumors are largely shaped by local expansions of pre-existing tissue-resident cells. It was

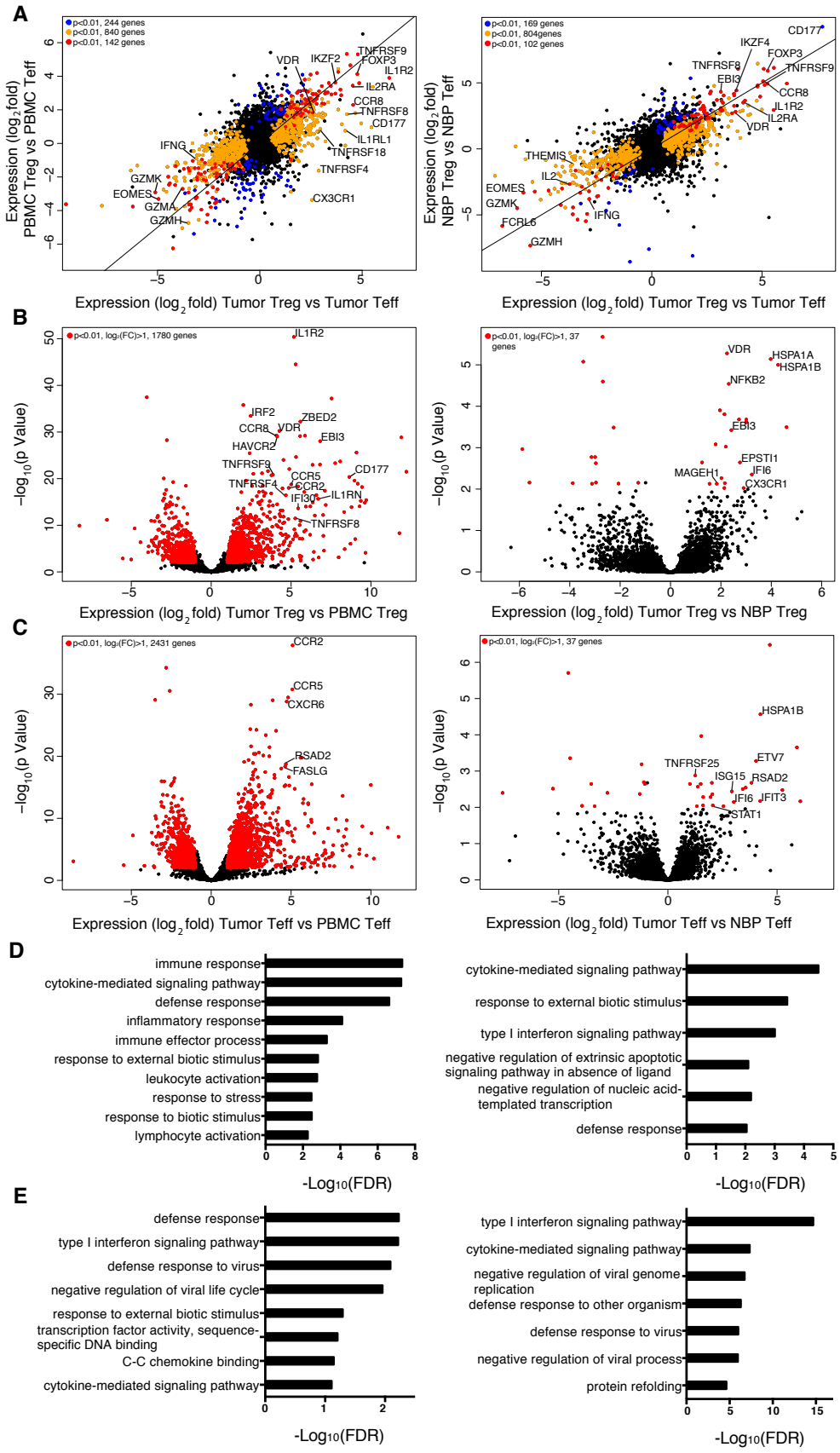
A
p<0.01, 244 genes
p<0.01, 840 genes
p<0.01, 142 genes
Expression (log2fold) PBMC Treg vs PBMC Teff
Expression (log2 fold) Tumor Treg vs Tumor Teff
p<0.01, 169 genes
p<0.01, 804genes
p<0.01, 102 genes
Expression (log2fold) NBP Treg vs NBP Teff
Expression (log2 fold) Tumor Treg vs Tumor Teff
B
p<0.01, log2(FC)>1, 1780 genes
−log10(p Value)
Expression (log2 fold) Tumor Treg vs PBMC Treg
p<0.01, log2(FC)>1, 37 genes
Expression (log2 fold) Tumor Treg vs NBP Treg
C
p<0.01, log2(FC)>1, 2431 genes
Expression (log2 fold) Tumor Teff vs PBMC Teff
p<0.01, log2(FC)>1, 37 genes
Expression (log2 fold) Tumor Teff vs NBP Teff
D
immune response
cytokine-mediated signaling pathway
defense response
inflammatory response
immune effector process
response to external biotic stimulus
leukocyte activation
response to stress
response to biotic stimulus
lymphocyte activation
-Log10(FDR)
cytokine-mediated signaling pathway
response to external biotic stimulus
type I interferon signaling pathway
negative regulation of extrinsic apoptotic signaling pathway in absence of ligand
negative regulation of nucleic acid-templated transcription
defense response
-Log10(FDR)
E
defense response
type I interferon signaling pathway
defense response to virus
negative regulation of viral life cycle
response to external biotic stimulus
transcription factor activity, sequence-specific DNA binding
C-C chemokine binding
cytokine-mediated signaling pathway
-Log10(FDR)
type I interferon signaling pathway
cytokine-mediated signaling pathway
negative regulation of viral genome replication
defense response to other organism
defense response to virus
negative regulation of viral process
protein refolding
-Log10(FDR)

Figure 2.5. Tumor-Infiltrating Treg and Non-Treg CD4 Cells Are Transcriptionally Similar to Tissue-Resident Cells.

(A) Left shows genes differentially expressed in tumor-resident Treg cells versus tumor-resident Tconv cells compared to genes differentially expressed in peripheral blood Treg cells versus Tconv cells (n = 4, n = 6, n = 6, n = 4, respectively). Right shows genes differentially expressed in tumor-resident Treg cells versus Tconv cells compared to genes differentially expressed in NBP Treg cells versus NBP Tconv cells (n = 8, n = 9, n = 4, n = 5, respectively). The indicated cell subpopulations were sorted based on CD4, CD25 CD45RO and CD127 expression. Gene expression was measured by RNA-seq using IonTorrent (left) and Illumina HiSeq (right) platforms; differential gene-expression analysis was performed with the DESeq2 package, where p values represent FDR. A normalized gene count cutoff of 50 was used. Genes down- or upregulated in tumor-resident Treg cells are shown in orange ($p < 0.01$), while genes down- or upregulated in peripheral blood or NBP Treg cells are shown in blue ($p < 0.01$). Genes down- or upregulated in both tumor and peripheral blood or NBP Treg cells are shown in red ($p < 0.01$). The numbers of genes differentially expressed are indicated. (B, C)**.** Left shows volcano plot comparing the p value versus fold-change for genes from tumor-resident Treg (B) and Tconv cells (C) relative to peripheral blood Treg (B) and Tconv cells (C) (n = 4, n = 6, respectively for both comparisons). Right shows volcano plot comparing the p value versus fold-change for genes from tumor-resident Treg (B) and Tconv cells (C) relative to NBP Treg (n = 8, n = 5, respectively) (B) and Tconv cells (n = 9, n = 6, respectively) (C). Genes labeled in red are significantly differentially expressed between tumor and peripheral blood or NBP Treg and Tconv cells ($p < 0.01$). (D, E). Gene set enrichment analysis was performed using the GOrilla bioinformatics tool for significantly upregulated genes in tumor Treg cells relative to peripheral blood Treg cells on left or NBP Treg cells on right (p value < 0.05, mean normalized read count > 50) as the target gene set and all genes expressed in the RNA-seq data as the background set (expressed genes are defined as genes with mean normalized read count > 20).

also conceivable that Treg and Tconv cells are recruited into the tumor from draining lymph nodes or peripheral blood and subsequently undergo phenotypic changes in response to the local environment. Thirdly, it was possible that local conversion of Tconv cells into Treg cells within breast tumors largely contribute to the increased presence of Treg cells in breast tumors as compared to NBP. To distinguish between these possibilities, we extracted TCR-β CDR3 sequences from the RNA-seq data using MiXCR software [102]. Comparative analysis of TCR repertoires of peripheral blood and tumoral Treg and Tconv cells was performed to determine their overlaps within individual patients using VDJtools software [103]. These analyses revealed low TCR repertoire overlap between normal tissue and tumor Treg cell subsets, suggesting that local expansion of tissue-resident Treg cells was unlikely the primary origin of intratumoral Treg cells (Figure 2.6A). Low TCR repertoire overlap between intratumoral Treg and Tconv cells, which was comparable to that between Treg and Tconv cells in NBP, argued against prominent conversion of Tconv to Treg cells within tumors (Figure 2.6A). Furthermore, both normal tissue and tumor Treg subsets contained large expanded clones, similarly to the activated $CD45RO^+$ but not to the resting $CD45RA^+$ peripheral blood Treg cells (Figure 2.6B). These results were consistent with the possibility that the majority of Treg cells in breast tumors were recruited from the periphery, after which their features were affected by the local environment.

Gene ontology (GO) analysis of differentially expressed genes showed that tumor-resident Treg cells, when compared to activated Treg cells from peripheral blood, were enriched for cytokine signaling, defense response, inflammatory response and lymphocyte activation categories, among others (Figure 2.5D, left panel). The gene-expression pattern of tumor-resident Tconv cells was enriched for a type I interferon signaling gene signature (Figure 2.5E, left panel). Notably, many chemokine receptors, including CCR5, CCR8, CCR10, CX3CR1, CXCR3, and CXCR6 were robustly and differentially expressed by tumor-resident Treg cells at the mRNA and

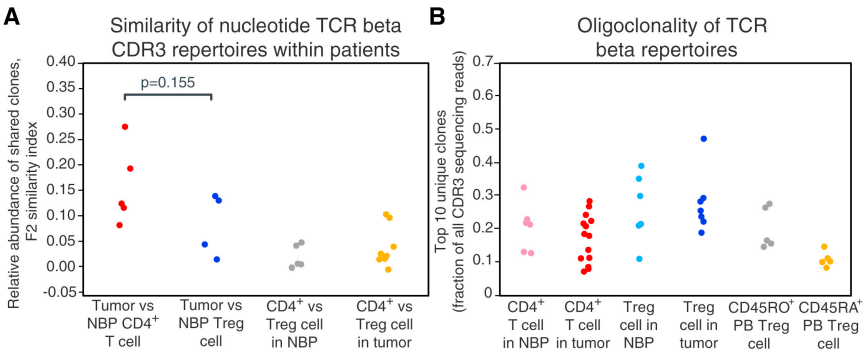

Figure 2.6. TCR-β Repertoires of Tumor and NBP Treg and Tconv Cells Are Oligoclonal and Non-overlapping.

(A) Within-patient similarity of TCR-β CDR3 repertoires between Treg and Tconv cells in breast tumors and NBP was assessed by measuring relative abundance of clones shared between the pairs of samples and displayed as F2 similarity index. P values were calculated using an unpaired two-tailed Student's t test. (B) Fraction of the TCR-β CDR3 repertoire occupied by the ten most abundant clones. Please also see Figure 2.9.

protein levels. Other chemokine receptors, such as CCR4, were highly expressed by both tumor and peripheral blood Treg cells, or were downregulated in tumor-resident Treg cells at the mRNA and protein level (CCR7 and CCR9). The wide array of chemokine receptors and cytokine receptors expressed by intratumoral Treg cells suggests that these cells are able to respond to a variety of local factors. As in Treg cells, certain chemokine receptors, such as CCR5, CCR2, CXCR3, and CXCR6 were highly expressed by tumor Tconv cells at the mRNA and protein level. Certain chemokine receptors, such as CCR8, were found to be highly expressed by tumor Treg cells and were much less abundant in Tconv cells, while others were more abundant in Tconv cells, suggesting that Treg and Tconv cells may rely on both unique and shared pathways to guide their migration to, and retention within the breast tumors environment (Figures 2.5B and 2.5C, left panels, Figure 2.7).

Several genes and their products known to be upregulated upon Treg cell activation and associated with increased suppressor function were more highly expressed by Treg cells in breast tumors when compared to peripheral blood Treg cells. These included CD39 (*ENTPD1*), CD25 (*IL2RA*), ST2 (*IL1RL1*), and Epstein-Barr virus Induced 3 (*EBI3*). We also found that intratumoral Treg cells exhibited heightened expression of interleukin 1 receptor type II (*IL1R2*), encoding a decoy IL-1 receptor (Figures 2.5A and 2.5B, left panels). Of these genes, a subset was more highly expressed by Treg cells in tumor as compared to NBP-resident Treg cells, including *EBI3*, *OX40*, and *IL1R2*. Likewise, several genes encoding proteins implicated in T cell effector function were differentially expressed by Tconv cells isolated from breast tumors when compared to peripheral blood Tconv cells [104]. These include the transcription factor eomesodermin (*EOMES*), and several genes encoding effector molecules, including granzyme K (*GZMK*), and interferon-γ (*IFNG*). Certain genes associated with T cell exhaustion in Tconv cells, *PDCD1*, *TIGIT*, and *TIM3*, were differentially expressed by tumor Tconv when compared to those in peripheral blood.

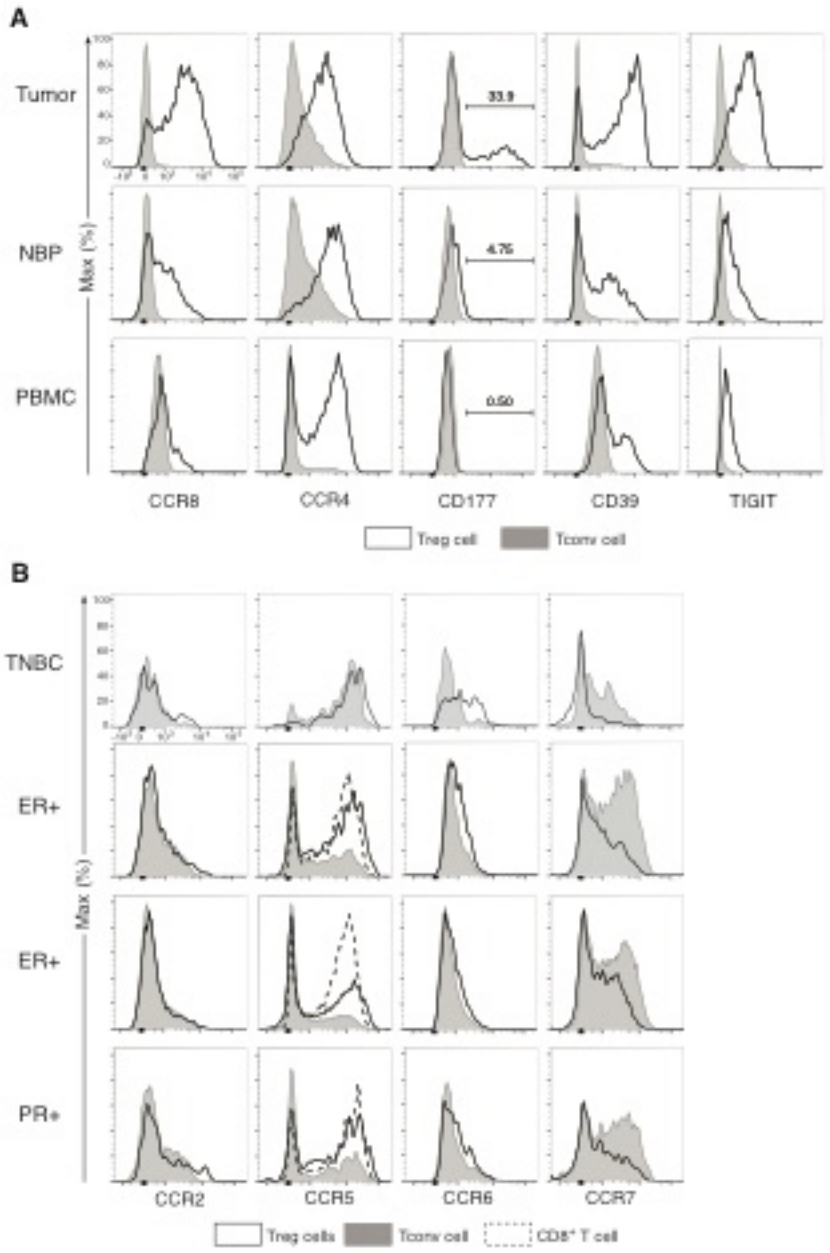

Figure 2.7. Tumor Treg Specific Genes Identified by RNAseq are Highly Expressed by Tumor Treg Cells at the Protein Level.

(A) Expression of several genes found to be differentially expressed in tumor Treg cells by RNAseq analysis was measured at the protein level by flow cytometry. MFI of genes gated on Treg cells (open histograms) and Tconv cells (shaded histograms) in breast tumor, NBP and peripheral blood. Plots represent data from individual specimens.

(figure description continued on next page)

Figure 2.7 – (continued)

(B) Expression of chemokine receptors found to be differentially expressed in tumor Treg or Tconv cells relative to peripheral blood T cells by RNA-seq analysis was measured at the protein level by flow cytometry. MFI of staining for indicated chemokine receptors gated on Treg cells (open histograms), Tconv cells (shaded histograms) and CD8+ T cells (dashed histograms) in ER+, PR+ and TNBC breast tumors.

In addition, we found several genes not previously associated with Treg cells or T cells differentially and robustly expressed by tumor Treg cells including melanoma antigen family H1 gene (*MAGEH1*) and *CD177*. MAGEH1 belongs to the type II MAGE protein family, whose members are expressed in multiple types of tissues and might act as an E3 ubiquitin ligase, which might potentially regulate Treg cell function or survival within tumors [105]. CD177 is a receptor for PECAM1, expressed by a subset of human and mouse neutrophils and implicated in neutrophil extravasation and potentially survival [106]. CD177 was highly expressed by a subset of intratumoral Treg cells representing 10%–50% of total Treg cells in individual tumor samples. In contrast, markedly fewer Treg cells found in NBP expressed CD177 and in lower amounts than in those found in tumors (Figure 2.7A). Furthermore, our flow cytometric studies showed increased CD177 expression by Treg cells in lung cancer, colorectal cancer, and melanoma (Figure 2.8). To further examine whether CD177 expression marks a distinct subset of intratumoral Treg cells, we performed RNA-seq analyses of flow cytometrically purified $CD177^+$ and $CD177^-$ $CD25^{hi}CD4^+$ Treg cells isolated from five breast tumors. $CD177^+$ and $CD177^-$tumor Treg cells were transcriptionally similar to each other (Figure 2.9). Furthermore, no correlation was found between the proportion of Treg cells that are $CD177^+$ and histologic grade, nodal status, or biologic subtype (data not shown). However, analysis of TCR-β CDR3 repertoires extracted from RNA-seq data revealed that $CD177^+$ Treg cells contained large clonal expansions that were not prominent in the $CD177^-$ populations (Figure 2.8B). These observations suggest that CD177 expression is induced in a subset of Treg cells in response to strong TCR stimulation and a yet to be identified accessory signal.

We identified *CCR8* as the most robustly and differentially expressed chemokine receptor in breast tumor-resident Treg cells as compared to peripheral blood Treg cells or Tconv cells found in either peripheral blood or breast tumors (Figures 2.5A and 2.5B). Flow cytometric analyses

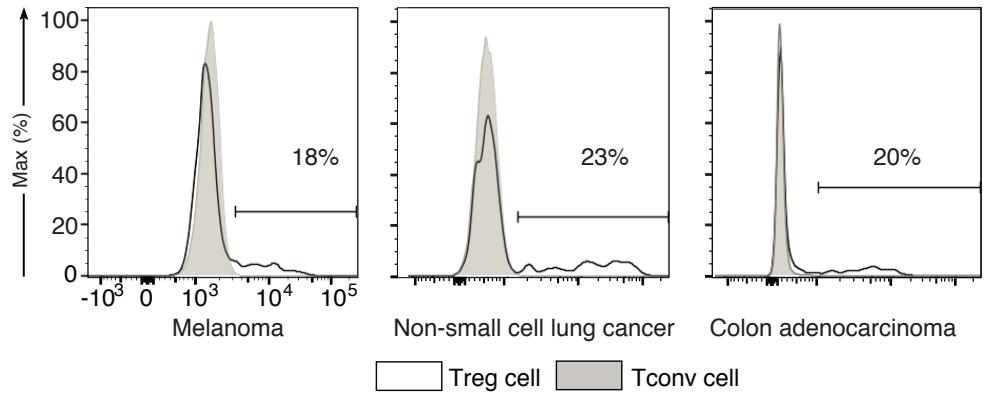

Figure 2.8. CD177 is Highly Expressed by a Subset of Tumor Treg Cells in Several Types of Cancer.

Flow cytometric analysis of CD177 expression by intratumoral T cells. The data are shown as MFI of CD177 staining of single cell suspension dissociated gated on Treg cells (open histograms) and Tconv cells (shaded histograms) in colorectal adenocarcinoma, melanoma and non-small cell lung cancer.

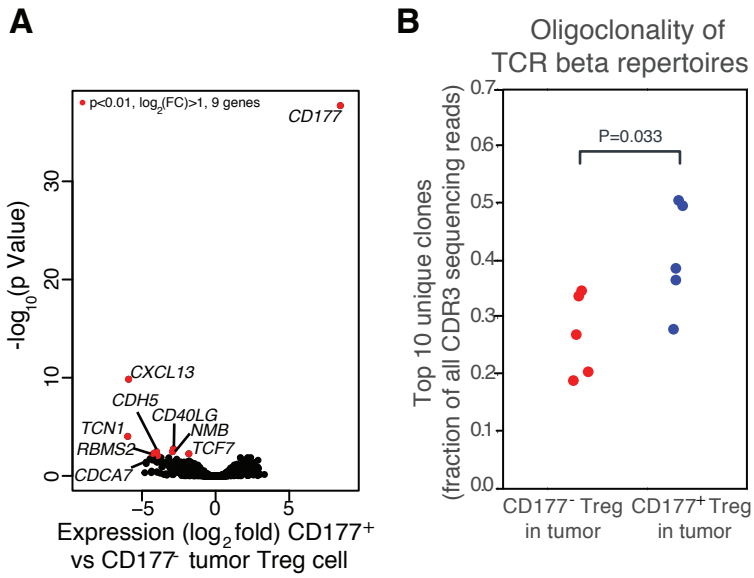

Figure 2.9. Analysis of Gene Expression and TCR Oligoclonality of Intratumoral CD177$^+$ and CD177$^-$ Treg Cells.

(A) Volcano plot comparing the p-value versus fold-change for gene expression in patient matched CD177$^+$ versus CD177$^-$ tumor resident Treg cells (n=5). Genes labeled in red are significantly differentially expressed ($p<0.01$). (B) Frequency of the TCR beta CDR3 repertoire occupied by the 10 most abundant clones in CD177$^+$ and CD177$^-$ intratumoral Treg cells. P-value was calculated using a paired two-tailed Student's t test.

showed that at a protein level, CCR8 was differentially expressed by the entire tumor-resident Treg cell population (Figure 2.6A). In contrast, CCR2, which was highly and differentially expressed by intratumoral Treg cells when compared to peripheral blood Treg cells, was equivalently expressed by intratumoral Tconv cells at the protein level (Figure 2.6B). Similarly, CCR5, which was differentially expressed by tumor Treg cells, was also highly expressed by a subset of intratumoral Tconv cells and by the majority of intratumoral CD8 T cells (Figure 2.6B). The robust and differential expression of CCR8 by intratumoral Treg cells provides an opportunity for selective depletion of Treg cells as an immunotherapeutic approach for the treatment of breast cancer.

CCR8 Is Expressed by Intratumoral Treg Cells

To assess CCR8 protein expression by diverse types of hematopoietic and non-hematopoietic cells present within the tumor, we analyzed dissociated tumor cell preparations by flow cytometry. We found that CCR8 was expressed exclusively by $CD45^+$ cells and that within all $CD45^+$ cells, CCR8 is largely expressed by $Foxp3^+$ Treg cells (Figure 2.10A; data not shown). Further analyses showed that in addition to robust expression by tumor-resident Treg cells and approximately 50% lower expression by Treg cells residing in the NBP, ~50% of intratumoral natural killer T (NKT) cells expressed high amounts of CCR8, whereas NK cells, $CD8^+$, γδT cells, myeloid cells, and the bulk of $CD4^+$ Tconv cells found in the tumor, NBP, and peripheral blood did not (Figures 2.10B and 2.10C). Although human cord blood NKT cells have been reported to express CCR8, we did not observe any staining in peripheral blood NKT cells (data not shown, [107]). To assess whether CCR8 expression on tumor-resident Treg cells is unique to breast cancer or a general feature of Treg cells present in solid tumors of diverse tissue origin, we analyzed tumor-infiltrating T cells by flow cytometry and found that CCR8 was more highly expressed by Treg cells than Tconv cells in several types of cancer, including lung and colorectal cancer, in melanoma and in angiosarcoma (Figure 2.10D; data not shown). Analysis of axillary

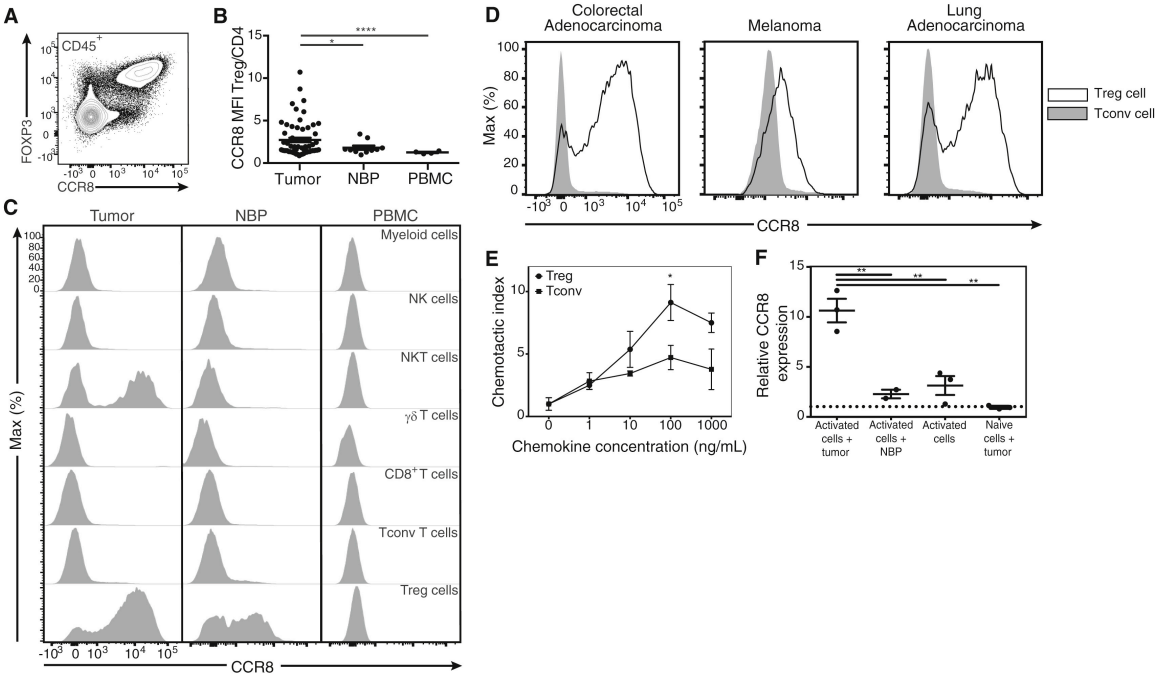

Figure 2.10. CCR8 Expression by Tumor-Resident Treg Cells Is Specific and Functional.

(A) CCR8 staining of $CD45^+$ cells from a human breast tumor. (B) MFI of CCR8 expression on multiple cell types in tumor, NBP, and peripheral blood isolated from a patient with primary breast cancer. (C) Summary plot of MFI ratio of CCR8 expression on Treg cells to Tconv cells in breast tumors, NBP and peripheral blood. Data represent the analysis of over 70 individual patients; error bars represent SEM; $^*p < 0.05$; $^{**}p < 0.01$, $^{***}p < 0.001$, ns non-significant (unpaired two-tailed Student's t test). (D) MFI of CCR8 expression gated on Treg cells (open histograms) and Tconv cells (shaded histograms) in colorectal adenocarcinoma, melanoma, and lung adenocarcinoma. (E) $CD3^+$ T cells were isolated by flow cytometry from a primary breast tumor and their migratory capacity was assessed in in vitro transwell migration assays. Plot is representative of five independent experiments; error bars represent SEM; $^*p < 0.05$; $^{**}p < 0.01$, $^{***}p < 0.001$, ns non-significant (unpaired two-tailed Student's t test). (F) Effect of breast tumor soluble factors on CCR8 expression by Treg cells was assessed by culturing tumor slices and naive Treg cells isolated from peripheral blood in transwell chambers separated by a 0.4 μm membrane. CCR8 mRNA in Treg cells was measured by qPCR on day 5 with *ADAR* as a reference gene and calibrated to expression in non-activated Treg cells. Data represent three independent experiments; error bars represent SEM; $^*p < 0.05$; $^{**}p < 0.01$, $^{***}p < 0.001$, ns non-significant (unpaired two-tailed Student's t test).

lymph nodes from three patients with nodal metastases from breast cancer revealed a minor subset of Treg cells expressing CCR8 (Figure 2.5). These $CCR8^+$ Treg cells might be cells that were poised to migrate into or recently emigrated out of the breast tumor or might represent Treg cells that were residing within the nodal metastases.

CCR8 Ligand CCL1 Is Expressed by Intratumoral Myeloid Cells

Because the ability of Treg cells to migrate to a specific tissue is essential for their capacity to suppress inflammation, we sought to assess the expression and cellular source of the two known cognate CCR8 ligands, CCL1 and CCL18, in breast tumors [108]. First, analysis of the Cancer Genome Atlas (TCGA) breast cancer dataset, which includes whole tumor RNA-seq data and clinical correlates for over 1,000 patients [109] showed that CCL1 mRNA amounts were markedly higher in breast, lung, colorectal, and melanoma tumors as compared to adjacent normal tissue (Figure 2.11A). To identify cell types producing CCR8 ligands in breast tumors, we performed RNA-seq analysis of $CD11b^+CD14^+$ myeloid cells isolated from breast tumors and peripheral blood and found that both CCL1 and CCL18 mRNAs were differentially expressed by intratumoral myeloid cells (Figure 2.11B). To further substantiate these results and to expand our analysis to additional cell subsets, we performed CCL1 qPCR on purified fibroblasts, endothelial cells, and myeloid cells isolated from breast tumors and found heightened CCL1 and CCL18 mRNA expression by myeloid cells, but not by other cell types analyzed (Figure 2.11C).

We next sought to determine the functionality of CCR8 expressed by tumor-infiltrating Treg cells by testing their chemotactic response to CCL1. We found that $CD25^{hi}CD4^+$ Treg cells flow cytometrically sorted from breast tumors were capable of migrating more robustly than $CD25^-CD4^+$ Tconv cells toward CCL1 mediated chemotactic cues (Figure 2.10E). To determine whether CCR8 signaling can markedly alter Treg cell suppressor function, we assessed the ability

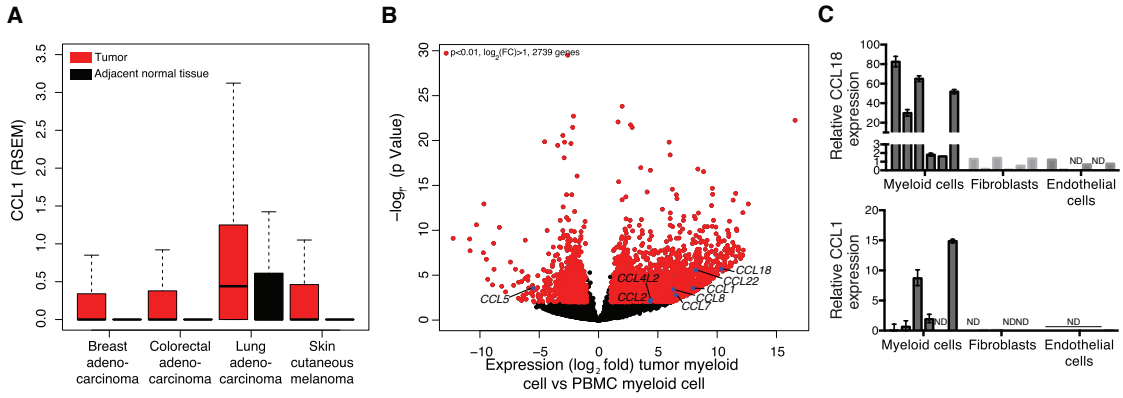

Figure 2.11. The CCR8 Ligand CCL1 is Expressed by CD11b^{+}CD14^{+} Myeloid Cells in Breast Tumors.

Boxplots comparing CCL1 normalized mRNA level in breast, colorectal and lung adenocarcinomas or melanomas versus adjacent normal tissues. (B) Volcano plot comparing the p-value versus fold-change for genes from intratumoral CD11b^{+}CD14^{+} myeloid cells relative to CD11b^{+}CD14^{+} myeloid cells isolated from peripheral blood of healthy donors (n=7, n=4, respectively). Genes labeled in red are significantly differentially expressed ($p<0.01$). (C) CD11b^{+}CD14^{+} myeloid cells, CD90^{+}CD31^{-} fibroblasts and CD31+ endothelial cells were FACS purified from breast tumors and CCL1 and CCL18 mRNA levels were quantified by qPCR with RP2 as a reference gene and calibrated to expression in peripheral blood T cells.

of purified intratumoral Treg cells to suppress in vitro proliferative responses of naive $CD4^+$ T cells upon TCR cross-linking in the presence of CCL1. We found that CCR8 ligand provision had no appreciable effect on the suppressive capacity of Treg cells (Figure 2.12).

To test whether the breast tumor environment has the ability to potentiate CCR8 expression in Treg cells, we stimulated CCR8-negative peripheral blood Treg cells with CD3 and CD28 antibodies upon co-culture with tumor or NBP explants separated by a diffusible membrane. We found that stimulation of "naïve" Treg cells isolated from buffy coats in the presence of tumor explants strongly induced CCR8, whereas Treg cells activated in the presence of NBP or alone induced CCR8 to a much lesser degree (Figure 2.10F). Treg cells cultured with tumor or NBP explants without activation failed to induce CCR8. These data suggest that components of the tumor microenvironment might lead to the induction of CCR8 on Treg in tumors or tumor draining lymph nodes and might contribute to the retention of Treg cells within tumors. We obtained a three samples of involved tumor-draining axillary lymph nodes from patients with stage III breast cancer and found that only a small subset of Treg cells expressed CCR8, relative to robust expression in patient-matched tumors, further supporting the idea that the breast tumor microenvironment may induce CCR8 expression on Treg cells or preferentially recruit $CCR8^+$ Treg cells (Figure 2.13). The strong type I interferon signature in intratumoral T cells led us to test whether type I interferon signaling is able to induce CCR8 on peripheral blood Treg cells. We found that activation of Treg cells in presence of IFN-α inhibited the modest induction of CCR8 upon Treg cell activation (data not shown).

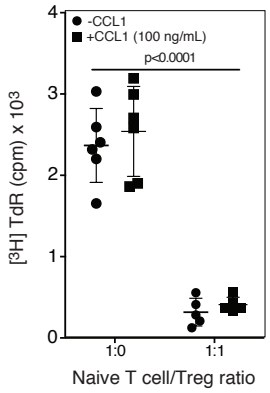

Figure 2.12. CCR8 Signaling Does not Affect Treg Cell Suppressor Function *In Vitro*.

Tumor resident $CD4^{+}CD25^{hi}$ Treg cells were FACS isolated and their capacity to suppress in vitro proliferation of naïve Tconv cells induced by plate-bound CD3 and CD28 antibodies in presence of recombinant CCL1 in vitro was assessed by ^{3}H-thymidine incorporation on day 4 (n=3, plot is representative of two independent experiments).

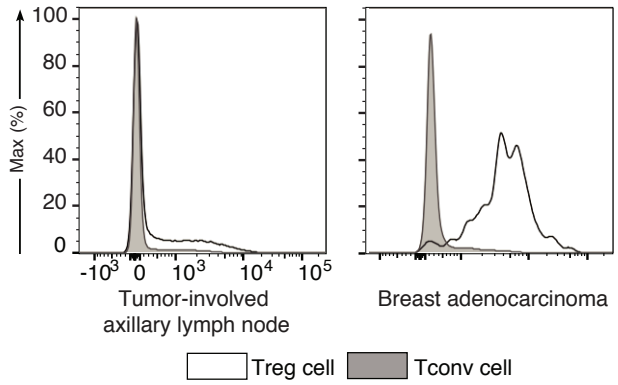

Figure 2.13. CCR8 is Expressed by a Minor Subset of Treg Cells in Axillary Lymph Nodes of Stage III Breast Cancer Patients.

Representative flow cytometric analysis of CCR8 expression by Treg cells in an involved axillary lymph node from a breast cancer patient. MFI of CCR8 gated on Treg cells (open histograms) and Tconv cells (shaded histograms). The results represent one of three independent experiments (three patients total).

High CCR8 Expression Marks Highly Activated and Proliferative Tumor Treg Cells and Is Associated with Poor Survival

To determine whether CCR8 expression by tumor-infiltrating Treg cells has clinical relevance, we correlated the expression of CCR8 on Treg cells with available clinicopathologic correlatives of breast cancer outcomes in our patient samples. We found that CCR8 expression on tumor-infiltrating Treg cells assessed by flow cytometry did not vary based on the biologic subtype of breast cancer, but that high CCR8 expression on tumor-resident Treg cells was associated with higher-grade tumors (Figure 2.14A, data not shown). Several functional Treg cell activation markers, including Ctla-4, CD25, and Foxp3, were more highly expressed by $CCR8^{high}$ tumor Treg cells (Figure 2.14B). Consistent with a requirement of Treg cell activation for induction of CCR8 expression in tumor explant co-cultures, we found CCR8 expression correlated strongly with tumor Treg cell proliferative activity assessed by Ki67 staining (Figures 2.14C–2.14E).

Because high CCR8 expression on tumor-resident Treg cells was associated with higher-grade tumors in the analyzed cohort of patients, we sought to determine whether CCR8 expression by Treg cells in breast cancer correlated with disease prognosis. Because CCR8 was expressed almost exclusively by $Foxp3^{+}$ Treg cells in the analyzed cohort of patients, we turned to the TCGA breast cancer bulk tumor RNA-seq dataset. We first sought to determine whether CCR8 expression correlated with Foxp3 expression in this large cohort of patients. We found a strong positive correlation between normalized CCR8 and Foxp3 mRNA amounts (Figure 2.14F). Furthermore, we found that CCR8 and Foxp3 mRNA amounts were markedly higher in breast tumors than in patient-matched adjacent NBP, in full agreement with our observation that breast tumors contain a higher density of Treg cells than NBP (Figure 2.14G). When breast cancer patients were stratified into two distinct groups based on median CCR8/Foxp3 mRNA ratio, a high CCR8/Foxp3 mRNA ratio was significantly associated with decreased overall survival (OS)

and disease-free survival (DFS, Figure 2.14I). To determine whether CCR8/Foxp3 mRNA ratio is an independent prognostic factor for survival after taking into account other clinical variables, we performed multivariate survival analyses. We found that CCR8/FOXP3 mRNA ratio was no longer associated with OS after adjusting for age, stage, and subtype (data not shown). This is not unexpected because we found subtype strongly associated with CCR8 to FOXP3 mRNA ratio and also with OS. Notably, when patients were stratified into two groups based on median Foxp3 mRNA amount alone, a high Foxp3 mRNA amount was not associated with worse survival outcome (Figure 2.14H). Because CCR2, CCR4, and CCR5 mRNAs are also highly expressed by tumor Treg cells, we assessed whether expression of these chemokine receptors in breast tumors was associated with survival. We found a strong positive correlation between normalized CCR2, CCR4 or CCR5, and Foxp3 mRNA amounts, but when patients were stratified into two groups based on median chemokine receptor/Foxp3 mRNA ratio, a high chemokine receptor/Foxp3 mRNA was not associated with worse survival outcome in any case (Figure 2.15). Similarly, when patients were stratified into two groups based on median mRNA amount of CCR2, CCR4, or CCR5 alone, high chemokine receptor expression was not associated with worse survival outcome (data not shown). Interpretation of this result is complicated due to expression of these chemokine receptors by other cell types. In summary, high CCR8 expression by Treg cells might mark a subset of highly activated and suppressive cells, which, when present in breast tumors, is associated with decreased survival. These results implicate activated CCR8 expressing Treg cells in the pathogenesis of human breast cancer.

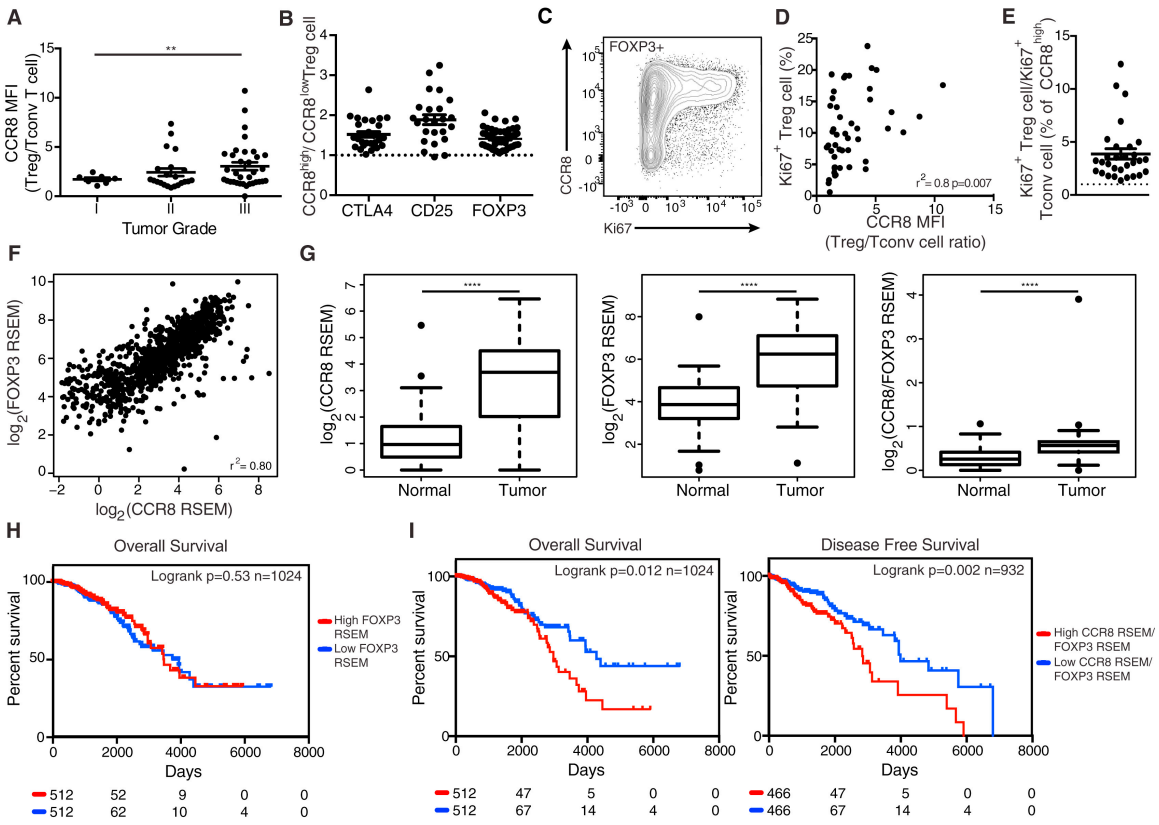

Figure 2.14. Treg CCR8 Expression Correlates with Clinic-Pathologic Features of Human Breast Cancer and Is Associated with Poor Disease Free and Overall Survival.

(A) Summary plot of MFI ratio of CCR8 expression on Treg cells to Tconv cells in breast tumors based on histologic grade. Data represent the analysis of 61 individual patients; error bars represent SEM; ∗p < 0.05; ∗∗p < 0.01, ∗∗∗p < 0.001, ns non-significant (unpaired two-tailed Student's t test). (B) MFI ratio of various Treg cell activation marker expression by CCR8high versus CCR8low Treg cells in individual breast tumors. Data represent the analysis of 57 individual patients. (C) CCR8 and Ki67 staining of CD4+Foxp3+ T cells from a human breast tumor. (D) Correlation of MFI ratio of CCR8 expression on Treg cells to Tconv cells and % of Ki67+ Treg cells in individual breast tumors. Data represent the analysis of 48 individual patients. (E) Ratio of percent of CCR8high Treg cells that are Ki67+ to percent of CCR8low Treg cells that are Ki67+ in individual breast tumors. Data represent the analysis of 30 individual patients. (F) Correlation of CCR8 and FOXP3 normalized mRNA expression in the TCGA breast cancer dataset (Spearman's r2 = 0.80, n = 1,024). mRNA normalization was estimated by the TCGA using the RSEM (RNA-seq by expectation maximization) method. (G) Boxplots comparing CCR8, FOXP3, or CCR8 to FOXP3 ratio normalized mRNA amount in breast tumors versus adjacent NBP. Data represent the analysis of 111 individual patients; ∗p < 0.05; ∗∗p < 0.01, ∗∗∗p < 0.001, ∗∗∗∗p < 0.0001, ns non-significant (paired two-tailed Student's t test). (H) Overall survival of breast cancer patients stratified by median tumor FOXP3 normalized mRNA amount (log rank p = 0.53, n = 1,024, Mantel-Cox test). (I) Overall survival (log rank p = 0.012, n = 1,024, Mantel-Cox test) and disease-free survival (log rank p = 0.002, n = 932, Mantel-Cox test) of breast cancer patients stratified by median tumor CCR8/FOXP3 normalized mRNA ratio.

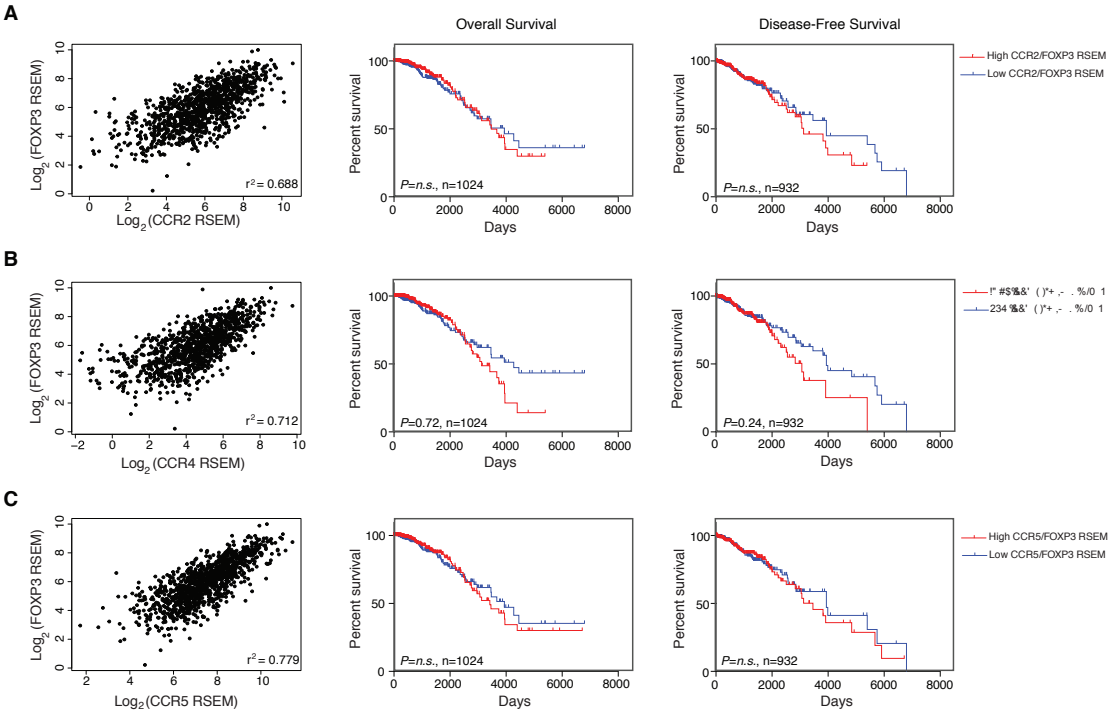

Figure 2.15. Ratio of Chemokine Receptor mRNA to Foxp3 mRNA does not Correlate with Survival Outcome in the TCGA Dataset.

Analysis of breast cancer TCGA data for relative expression of indicated genes normalized against Foxp3 mRNA expression. Spearman correlation (n=1024), overall survival (n=1024, Mantel-Cox test) and disease-free survival (n=932, Mantel-Cox test) of breast cancer patients in the TCGA dataset stratified by median tumor (A) CCR2/FOXP3, (B) CCR4/FOXP3, (C) CCR5/FOXP3 normalized mRNA ratios.

DISCUSSION

The presence of Treg cells in the tumor microenvironment has recently emerged as a characteristic feature of human tumors including breast carcinomas [110-113]. Here, through the analysis of primary tumors surgically removed from over 100 treatment-naive patients, we found that Treg cells were abundant in human breast cancers as compared to normal breast parenchyma and peripheral blood. In addition, their frequency is increased in the more aggressive triple-negative subset of breast cancers and also correlates with higher-grade lesions across all subsets. These findings support the notion that Treg cells can directly contribute to the natural progression of cancer rather than accumulating merely as an indirect consequence of other mechanisms underlying cancer progression.

Studies in mice have revealed that tissue-resident Treg cells differ from their counterparts residing in the secondary lymphoid organs [114]. Some of these distinguishing characteristics mirror the gene-expression features of the particular niche within which the Treg cells reside. In contrast to mice, it remains unknown whether in humans Treg cells residing in non-lymphoid organs or tissues are markedly different in their gene-expression patterns from those in peripheral blood. The unique metabolic nature of the tumor microenvironment including relative hypoxia, scarcity of nutrients, and heightened lactate production raises the possibility that this environment imparts specific properties on Treg cells distinct from those in normal tissue or from activated circulating Treg cells, enabling Treg cells to optimally support tumor growth. An alternative possibility is that active recruitment of Treg cells from circulation might lead to intratumoral Treg cells that largely resemble activated peripheral blood Treg cells. Finally, it is possible that tumor-resident Treg cells are similar to those found in normal tissue with few, if any distinguishing features. Our RNA-seq analysis of highly purified Treg cells from breast carcinomas showed major differences in gene expression when compared to activated peripheral blood Treg cells. In contrast, Treg cells from breast carcinomas shared the bulk of features characteristic of normal

breast-tissue-resident Treg cells. The remaining differences between the two subsets pointed to heightened activation and proliferation of Treg cells in tumors. The gene-expression profile of tumor-resident Treg cells (and Tconv cells) closely mirrored that of their normal breast parenchyma-resident counterparts. These findings suggest that, despite many fundamental differences, the normal breast tissue and breast tumor environment attract and impact tissue-resident Treg cells through overlapping sets of cues and mechanisms. This observation raises the possibility that local expansion of pre-existing tissue-resident Treg cells might account for the high Treg cell density in breast tumors. However, comparison of TCR repertoires revealed low clonal overlap between normal tissue and tumor Treg cell subsets arguing against this hypothesis. Furthermore, a small number of genes were markedly upregulated on tumor Treg cells relative to normal breast Treg cells. GO pathway enrichment analysis revealed that these genes were enriched for cytokine-mediated signaling and type I interferon response pathways. We also found *MAGEH1* gene, previously identified in several cancer types including melanoma, to be upregulated by intratumoral Treg cells. Although its function remains to be explored, *MAGEH1* expression has also been observed in Treg cells isolated from colorectal cancer and lung adenocarcinoma-resident Treg cells [115].

The enhanced state of activation of intratumoral Treg cells might reflect more potent TCR stimulation, which is required for Treg cell activation, proliferation, and suppressor function [116]. We also found chemokine signaling and cell migration as a major single category of genes enriched in intratumoral Treg cells. Treg cell expression of homing receptors defines distinct populations that can direct migration to a range of tissues or sites of inflammation [117]. Trafficking receptors and molecules that have been reported to be expressed by Treg populations found in non-lymphoid and inflamed tissues include CCR2, CCR4, CCR5, CCR6, CCR8, CCR9, CCR10, CXCR3, several integrins, selectin ligands, and GPCRs [118]. Coordinated expression of these receptors and ligands enables the homing of Treg cells to non-lymphoid organs and might

contribute to other aspects of Treg cell function [119]. Characterization of homing receptors expressed by Treg and effector T cells within tumors might help shift the effector to suppressor cell balance. This has been demonstrated experimentally for CCR4, whose ligands CCL17 and/or CCL22 can be expressed by tumor cells or tumor associated myeloid cells [120-122].

It is unlikely that targeting a single chemokine receptor will mitigate the migration or retention of Treg cells in the tumor microenvironment as there is considerable overlapping functionality and promiscuity of ligand binding between the different chemokine receptors. The differential expression of chemokine receptors between Treg cells and T effector cells, however, raises the opportunity to develop selective depletion strategies [123]. Although we found that CCR4 was highly expressed by activated Treg cells in peripheral blood, normal breast tissue and breast tumors, it was also present on activated effector $CD4^+$ T cells, albeit in somewhat lower amounts. Accordingly, diminution in both Treg and effector $CD4^+$ T cells was observed in patients treated with a CCR4 depleting antibody ([124].G.P. and A.Y.R., unpublished observations). High expression of CCR8, facilitated by yet-to-be identified factors present in the tumor environment, was a unique feature of intratumoral Treg cells with markedly lower amounts observed in normal breast-tissue-resident Treg cells and negligible expression by Treg cells in peripheral blood. Importantly, CCR8 was not found on effector αβT, NK and γδT cells, and myeloid cells in the tumor with the exception of CCR8 expression by ~50% of NKT cells. The biologic importance of high CCR8 expression by intratumoral Treg cells in breast cancer was strongly suggested by the observed correlation of high CCR8/Foxp3 mRNA expression ratio in 1,024 tumor samples with markedly decreased disease free and overall survival, whereas high Foxp3 expression alone failed to reach statistical significance. While CCR8 represents a promising means by which to selectively deplete Treg cells in the tumor microenvironment with likely less efficient depletion in normal tissue secondary to the different expression amounts, the role of CCR8 in Treg cell function remains unclear.

Another noteworthy finding was high expression of CD177, another cell adhesion and migration-related protein, by a subset of intratumoral Treg cells in breast cancer patients as well as in lung cancer and melanoma (Figure 2.6). CD177 is a glycosyl-phosphatidylinositol (GPI)-linked cell surface glycoprotein expressed by neutrophils that has not been previously linked to T cells. Although the biological role of CD177 expression by Treg cells restricted to human tumors remains to be explored, it is reasonable to assume that CD177 likely enables interactions of the positive Treg cell subset with its ligand PECAM-1 and might endow these cells with distinct functionality.

In conclusion, our studies show that the tissue of residence, i.e., normal breast parenchyma, rather than tumor environment itself, largely defines distinct properties of intratumoral Treg cells. Nevertheless, breast tumor-resident Treg cells exhibited few distinct features including high amounts of chemokine receptor CCR8. The latter was also expressed by Treg cells in diverse cancers of mesenchymal and epithelial origin, including melanoma, lung and colorectal cancer, and angiosarcoma. High CCR8/Foxp3 mRNA ratio, but not high Foxp3 amount alone correlated with poor prognosis suggesting that CCR8 expression by Treg cells likely plays a role in breast cancer progression either by itself or by marking highly activated pathogenic intra-tumoral Treg cells. Our results suggest that CCR8 may serve as a promising target for cancer immunotherapy.

CHAPTER 2: FORKHEAD FAMILY MEMBER FOXP1 REGULATES FOXP3 FUNCTION IN REGULATORY T CELLS

INTRODUCTION

The conserved family of Forkhead box proteins is a functionally diverse group of transcription factors that regulate a variety of biological processes both during embryonic development and in differentiated cells. The Foxp subfamily consists of four members in humans and in mice, Foxp1-4. All four Foxp proteins contain a zinc finger structure and a leucine zipper motif N-terminal to the Forkhead domain [57]. The Foxp transcription factors require dimerization through their leucine zipper motif to bind DNA and are capable of homo- and hetero-dimerization [57]. Foxp1, 2 and 4 regulate important aspects of development in heart, lung, neural and thymic tissues [59-62, 65]. Foxp1 has essential roles in B and T lymphocyte development and also regulates the quiescence of naïve T cells in a cell-intrinsic manner [67-71].

Foxp3 is the lineage-specifying transcription factor of Treg cells, and its stable expression is essential for establishment and maintenance of Treg cell transcriptional and functional programs [20, 125]. Treg cells are a subset of $CD4^+$ T cells with immunosuppressive function that are critical for suppression of inflammatory responses to self-antigens, allergens, and intestinal microbiota and are essential for resolution of immune homeostasis following infection. Loss-of-function mutations in the *Foxp3* gene cause genetic deficiency of Treg cells and result in fatal multi-organ autoimmune diseases [12, 18, 19].

Biochemical studies have shown that Foxp3 can homodimerize and heterodimerize with Foxp1 and that endogenous Foxp3 exists as part of a large protein complex that includes Foxp1 [78, 80]. Immunofluorescence microscopy has revealed that Foxp3 and Foxp1 co-localize at

many sites within the nucleus of human $CD4^+CD25^+$ T cells [78]. Importantly, a single amino acid deletion within the leucine zipper domain of Foxp3 (E251) found in IPEX patients does not prevent association with the large protein complex but does disrupt the ability of Foxp3 to homodimerize and heterodimerize with Foxp1 and disrupts its ability to associate with and regulate transcription of certain known direct targets, such as the IL-2 promoter [78]. Foxp1 knockdown in Foxp3-expressing Jurkat T cells partially relieves Foxp3-mediated repression of IL-2 production [78]. Combined, these data strongly suggest that Foxp1-Foxp3 heterodimerization is important for Treg cell function, though the extent of Foxp1 transcriptional regulation in Treg cells remains undefined.

The documented importance of Foxp1 in T cell differentiation and Foxp1 interactions with Foxp3 prompted us to investigate the role of Foxp1 in Treg cell biology. We circumvented CD4 and CD8 T cell activation and studied the function of Foxp1 in Treg cells through the use of a Foxp3 mediated deletion model system. To further define the mechanisms underlying the role of Foxp1 in the Treg cell transcriptional program, we generated a conditional allele of Foxp1 (Figure 3.1). Foxp1 deficiency in Treg cells resulted in a genome-wide reduction of Foxp3 binding and altered gene expression of a number of Treg cell signature genes. Mice with a Treg cell specific deficiency of Foxp1 did not display overt autoimmunity, but did exhibit Treg cell dysfunction driven in part by loss of Il2r-α expression and resultant impairment of IL-2 signaling. Foxp1 thus functions to maintain Treg cell suppressor function and may play a direct role in Foxp3 mediated transcriptional regulation of a subset of genes.

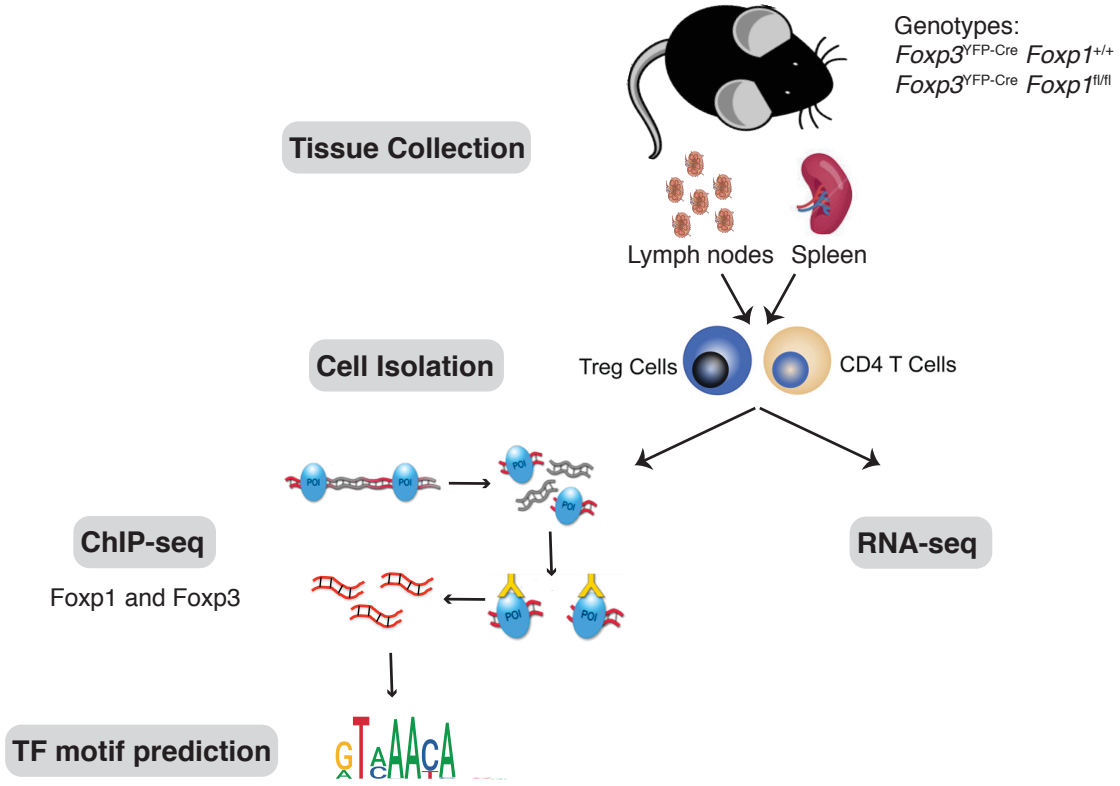

Figure 3.1. Experimental Approach for Genomics Experiments.

Treg cells and CD4 T cells were isolated from spleens and lymph nodes of *Foxp3*$^{YFP\text{-}Cre}$ *Foxp1*$^{+/+}$ and *Foxp3*$^{YFP\text{-}Cre}$ *Foxp1*$^{f/f}$ mice and were subjected to ChIP-seq. HOMER was used to identify enriched DNA binding motifs. YFP^{+} Treg cells were isolated from spleens and lymph nodes of *Foxp3*$^{YFP\text{-}Cre/+}$ *Foxp1*$^{+/+}$ and *Foxp3*$^{YFP\text{-}Cre/+}$ *Foxp1*$^{f/f}$ heterozygous female mice and were subjected to RNA-seq.

RESULTS

Foxp1 and Foxp3 Share a Majority of Binding Sites that are Enriched for Forkhead and Ets Family Consensus Sequences

To determine whether Foxp3 and Foxp1 bound similar sites in T cells, we performed ChIP-seq in Treg and Tconv cells. We identified 7174 significantly bound Foxp3 peaks and 3071 significantly bound Foxp1 peaks in Treg cells ($p<0.01$, Figure 3.2A). While more than half of Foxp3 bound sites were in intronic and intergenic regions, less than 30% of Foxp1 bound sites were in such regions. Rather, Foxp1 binding was primarily at promoters in Treg cells (Figure 3.2B). 1980 peaks were bound by both Foxp1 and Foxp3. ChIP signal for both Foxp3 and Foxp1 at the summits of these shared peaks was not significantly different from ChIP signal at peak summits bound only by one of the two transcription factors (Figure 3.2C,D). To identify motifs enriched within the Foxp3 and Foxp1 peaks, we performed de novo motif discovery with Homer [126]. This analysis identified the canonical Forkhead motif as the most significantly enriched motif in Foxp3 and Foxp1 peaks. This is in contrast to a previous Foxp3 ChIP-seq study that found Forkhead motifs to be less enriched than Ets, Runx and C-not motifs at Foxp3 bound sequences [77]. 8.97% of Foxp3 peaks and 18.45% of Foxp1 peaks contained the canonical 5' GTAAACA 3' Forkhead motif (Figure 3.2E,F). We were unable to find any sequence features that would enable us to distinguish between Foxp3 and Foxp1 binding to sequences containing the canonical Forkhead motif. The Forkhead motif occurred only once in the vast majority of peaks in which it was found. Therefore, the hypothesis recently put forth by Koh *et al*. that both proteins in Foxp3 homo or heterodimers bind simultaneously to DNA at two adjacent Forkhead motifs is unlikely to be true *in vivo* [75]. It has also been recently proposed that Foxp3 can mediate long-range chromatin interactions by forming a domain-swapped dimer and bridging two separate pieces of DNA, which would require only one Forkhead motif per DNA piece [127]. It is also possible that one dimer member mediates the interaction with DNA at a given time.

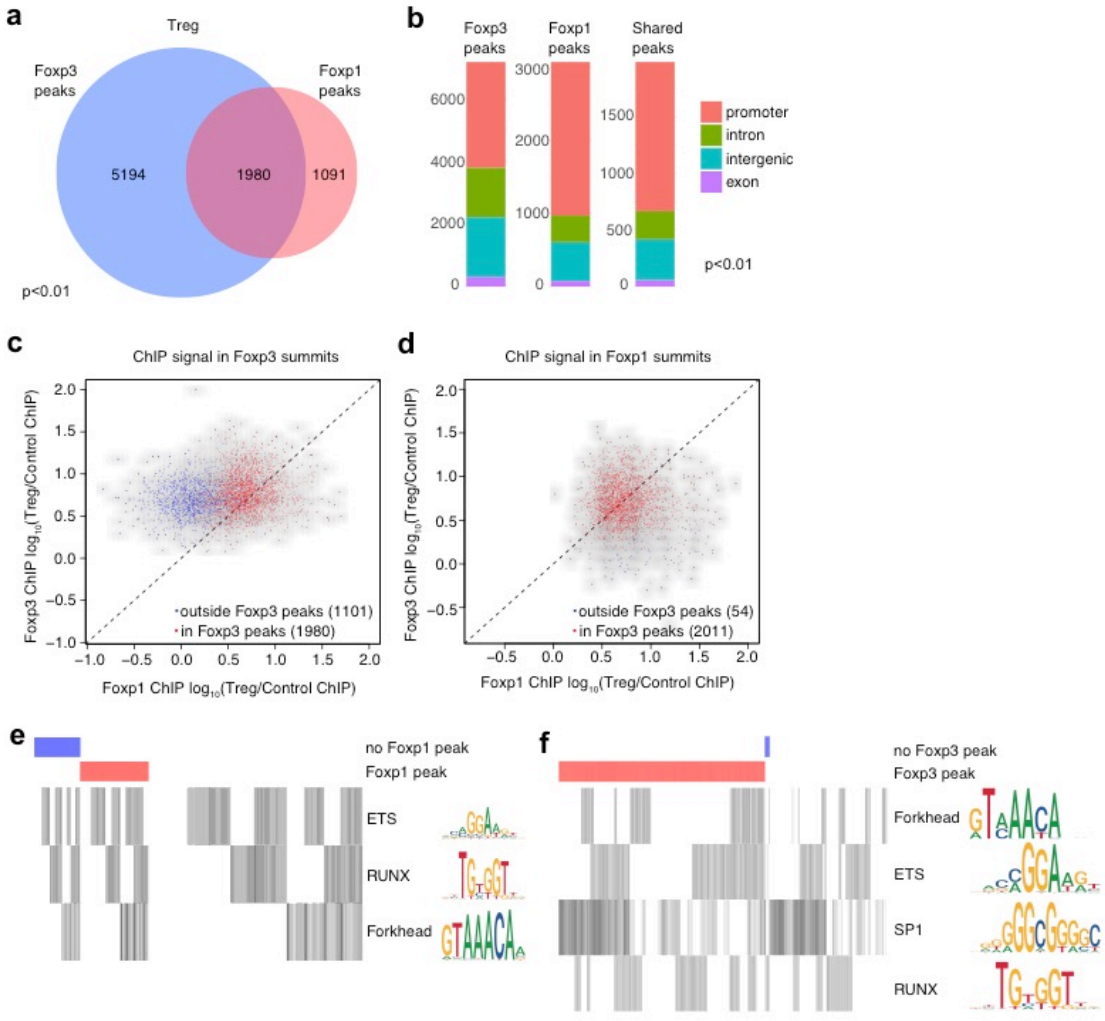

Figure 3.2. Foxp1 and Foxp3 Share a Majority of Binding Sites that are Enriched for Forkhead and Ets Family Consensus Sequences.

(A) Venn diagram of Foxp1 and Foxp3 bound sites in Treg cells ($p<0.01$). (B) Genomic distribution of Foxp1 and Foxp3 bound sites ($p<0.01$). (C) Scatterplot of Foxp3 and Foxp1 ChIP signal at Foxp3 summits. Data are shown for Foxp3 summits bound only by Foxp3 (blue) and Foxp3 summits that overlap with Foxp1 peaks (red). (D) Scatterplot of Foxp3 and Foxp1 ChIP signal at Foxp1 summits. Data are shown for Foxp1 summits bound only by Foxp1 (blue) and Foxp1 summits that overlap with Foxp3 peaks (red). (E, F) Homer analysis of Foxp3 (E) and Foxp1 (F) bound sites to identify enriched transcription factor motifs.

24.90% of Foxp1 and 28.25% of Foxp3 peaks contained canonical Ets family motifs, prompting us to consider the possibility that Foxp3 or Foxp1 might be present in transcription factor complexes where a different transcription factor present in the complex is responsible for DNA binding (Figure 3.2E). This possibility seemed highly likely, given the fact that a relatively small percentage of Foxp3 and Foxp1 peaks contained the Forkhead motif and based on several published examples in which cofactor presence is required for Foxp3 DNA binding [15, 128]. Many Ets family transcription factors were highly expressed at the mRNA level in Treg cells, including Elf1, 2, 4, Elk3, 4, and Ets1. Mass spectrometric analysis of Foxp3 protein complexes in Treg cell nuclei identified Ets family members as components of these complexes [80]. In summary, analysis of overlapping Foxp3 and Foxp1 binding sites revealed significant enrichment of the canonical Forkhead motif and several Ets-family motifs.

Sequences Bound Exclusively by Foxp3 are Associated Predominantly with Differentially Upregulated Genes in Activated Treg Cells.

1101 significantly bound Foxp3 peaks did not overlap with any Foxp1 peaks called at a very relaxed threshold ($p<0.1$) and 54 significantly bound Foxp1 peaks did not overlap with any Foxp3 peaks called at a very relaxed threshold ($p<0.1$). These peaks were found predominantly in intronic and intergenic regions, with very few associated with promoters (Figure 3.3A). Analysis of previously published DNase-seq data revealed that the 1101 Foxp3-only peaks were significantly less accessible than all Foxp3-bound peaks in Treg cells, but were more accessible in activated Treg cells than in naive Treg cells and were even more accessible in activated Tconv cells (Figure 3.3B-D)[77]. To determine whether the genes associated with peaks bound exclusively by Foxp3 were differentially expressed in Treg cells, we analyzed RNA-seq data from $CD62L^{hi}$ naïve and $CD44^{hi}$ activated splenic Treg cells and $CD4^{+}$ Tconv cells (Fan, X. *et al*., in preparation). A subset of genes associated with the 1101 Foxp3-only peaks was very significantly upregulated in activated Treg and Tconv cells relative to naïve cells and included

CD83, *CD44*, and *Itgb1* (Figure 3.3F, cluster 1). We performed GO pathway analysis on each cluster and found that cluster 1 was enriched for regulation of signaling, immune system development, positive regulation of signal transduction and lymphocyte activation GO pathways (Figure 3.4A). Many genes were significantly upregulated in Treg cells relative to Tconv cells and these were known Treg signature genes, including *Ctla4*, *Ikzf2*, *Gpr15*, *Hdac9, Ccr8*, and *Il1r2*. A small number of the genes associated with Foxp3-only peaks were significantly downregulated in activated Treg cells relative to activated Tconv cells, and these included *Ikzf1* and *Foxp1* itself (Figure 3.3F, cluster 2). Overall, the genes associated with Foxp3-only peaks were more highly expressed in activated cells relative to naïve cells and were more highly expressed in Treg cells than in Tconv cells (Figure 3.3E, Table 3.1).

Further analysis of motif enrichment in DNA sequences bound by Foxp3 revealed very significant enrichment for Runx-family motifs at peaks bound exclusively by Foxp3 but not at peaks bound by Foxp1. Of the 1101 Foxp3-only peaks, 340 contained the Runx motif 5' ACCACA 3'. Previous studies have shown that Foxp3 is present in supramolecular complexes with both Foxp1 and Runx1 [80, 128, 129]. To elucidate interactions between Foxp3, Runx1 and Foxp1, we immunoprecipitated each protein from nuclear lysates of EL4 cells retrovirally transduced with Foxp3. Both Foxp1 and Runx1 were co-immunoprecipitated with Foxp3 (Figure 3.3G). Runx1 was co-immunoprecipitated with Foxp1 two-fold less than with Foxp3 (Figure 3.3G). Similarly, Foxp1 was co-immunoprecipitated with Runx1 two-fold less than with Foxp3 (Figure 3.3G). These results support the idea that Runx1 and Foxp1 may be enriched in different Foxp3 complexes. To further evaluate the possibility that Runx1 may be mediating Foxp3 complex binding at a certain subset of Foxp3 target sequences, we performed Runx1 ChIP-qPCR in Treg cells and Tconv cells. We analyzed four Runx1 motif-containing regions that were bound by Foxp3, including the *CNS2* enhancer that was previously reported to require Runx1 for efficient Foxp3 binding (Figure 3.4B)[15]. We also analyzed three regions bound by Foxp3 and

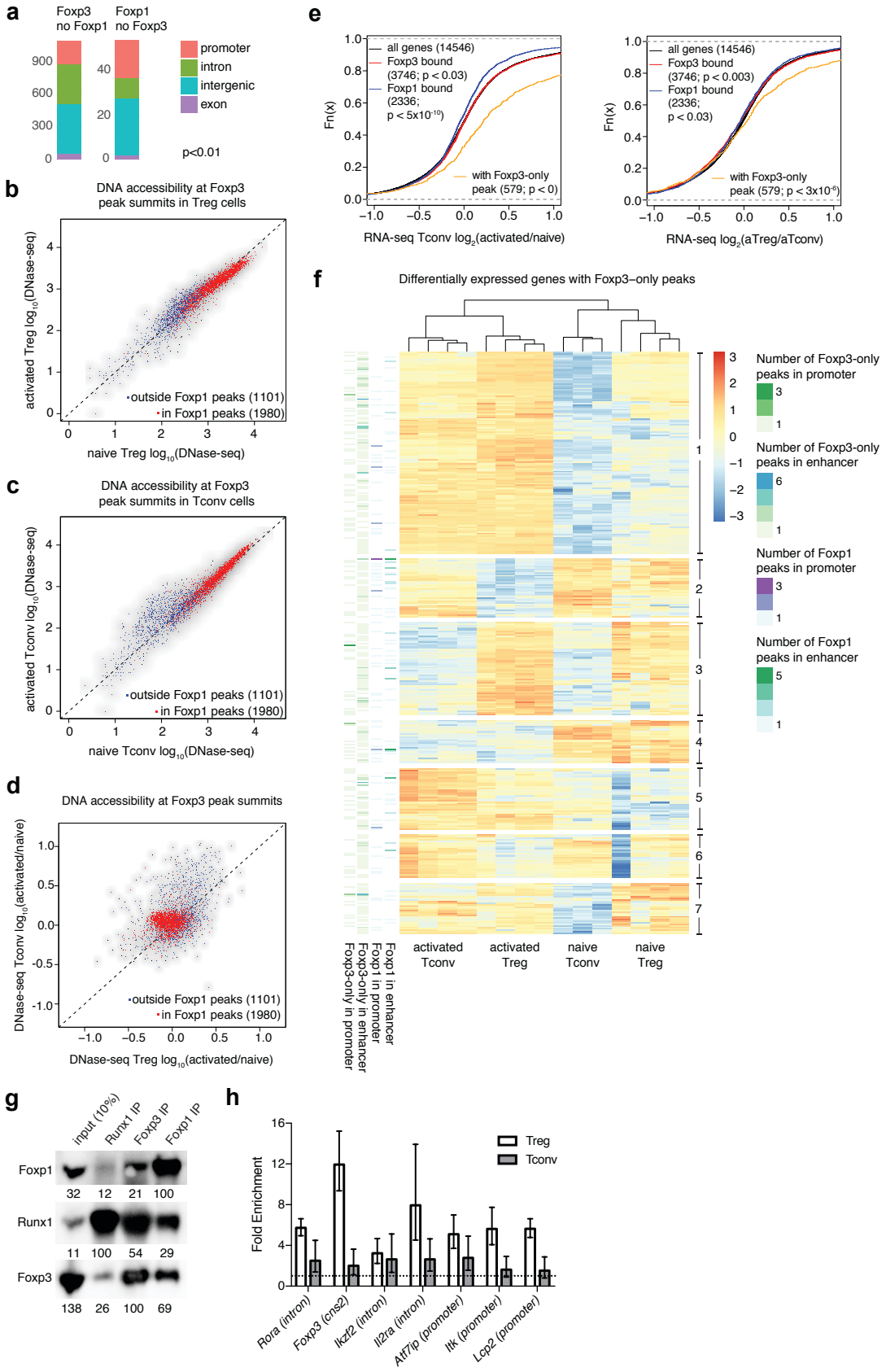
a
Foxp3 no Foxp1
Foxp1 no Foxp3
promoter
intron
intergenic
exon
p<0.01
b
DNA accessibility at Foxp3 peak summits in Treg cells
activated Treg log10(DNase-seq)
naive Treg log10(DNase-seq)
outside Foxp1 peaks (1101)
in Foxp1 peaks (1980)
c
DNA accessibility at Foxp3 peak summits in Tconv cells
activated Tconv log10(DNase-seq)
naive Tconv log10(DNase-seq)
d
DNA accessibility at Foxp3 peak summits
DNase-seq Tconv log10(activated/naive)
DNase-seq Treg log10(activated/naive)
e
all genes (14546)
Foxp3 bound (3746; p < 0.03)
Foxp1 bound (2336; p < 5x10-10)
with Foxp3-only peak (579; p < 0)
Fn(x)
RNA-seq Tconv log2(activated/naive)
Foxp3 bound (3746; p < 0.003)
Foxp1 bound (2336; p < 0.03)
with Foxp3-only peak (579; p < 3x10-6)
RNA-seq log2(aTreg/aTconv)
f
Differentially expressed genes with Foxp3–only peaks
Number of Foxp3-only peaks in promoter
Number of Foxp3-only peaks in enhancer
Number of Foxp1 peaks in promoter
Number of Foxp1 peaks in enhancer
Foxp3-only in promoter
Foxp3-only in enhancer
Foxp1 in promoter
Foxp1 in enhancer
activated Tconv
activated Treg
naive Tconv
naive Treg
g
input (10%)
Runx1 IP
Foxp3 IP
Foxp1 IP
Foxp1
Runx1
Foxp3
h
Treg
Tconv
Fold Enrichment
Rora (intron)
Foxp3 (cns2)
Ikzf2 (intron)
Il2ra (intron)
Atf7ip (promoter)
Itk (promoter)
Lcp2 (promoter)

Figure 3.3. Sequences Bound Exclusively by Foxp3 are Associated Predominantly with Differentially Upregulated Genes in Activated Treg Cells.

(A) Genomic distribution of Foxp1-only and Foxp3-only bound sites ($p<0.01$). (B) DNA accessibility in naive and activated Treg cells at regions bound by Foxp3 in Treg cells. Data are shown for regions at which Foxp3 is bound but Foxp1 is not (blue) and regions where both Foxp3 and Foxp1 are bound (red). (C) DNA accessibility in naive and activated Tconv cells at regions bound by Foxp3 in Treg cells. Data are shown for regions at which Foxp3 is bound but Foxp1 is not (blue) and regions where both Foxp3 and Foxp1 are bound (red). (D) DNA accessibility in activated versus naive Tconv cells and activated versus naive Treg cells at regions bound by Foxp3 in Treg cells. Data are shown for regions at which Foxp3 is bound but Foxp1 is not (blue) and regions where both Foxp3 and Foxp1 are bound (red). (E) Heatmap comparing gene expression between naive and activated Treg and Tconv cells for genes associated with one or more Foxp3-only bound site ($p<0.01$). (F) Cumulative distribution plot of activated/naïve Tconv gene expression (left) and activated Treg/activated Tconv cell gene expression (right) for all genes, genes bound by Foxp3, genes bound only by Foxp3 and not by Foxp1, and genes bound by Foxp1. (G) Western blot of Foxp3, Runx1 and Foxp1 after Co-IP in nuclear fraction of Foxp3-transduced EL4 cell line. (H) Runx1 ChIP-qPCR in Treg and naive Tconv cells at four loci containing Runx motifs and bound by Foxp3, and at three loci bound by Foxp1 and Foxp3 without a Runx motif.

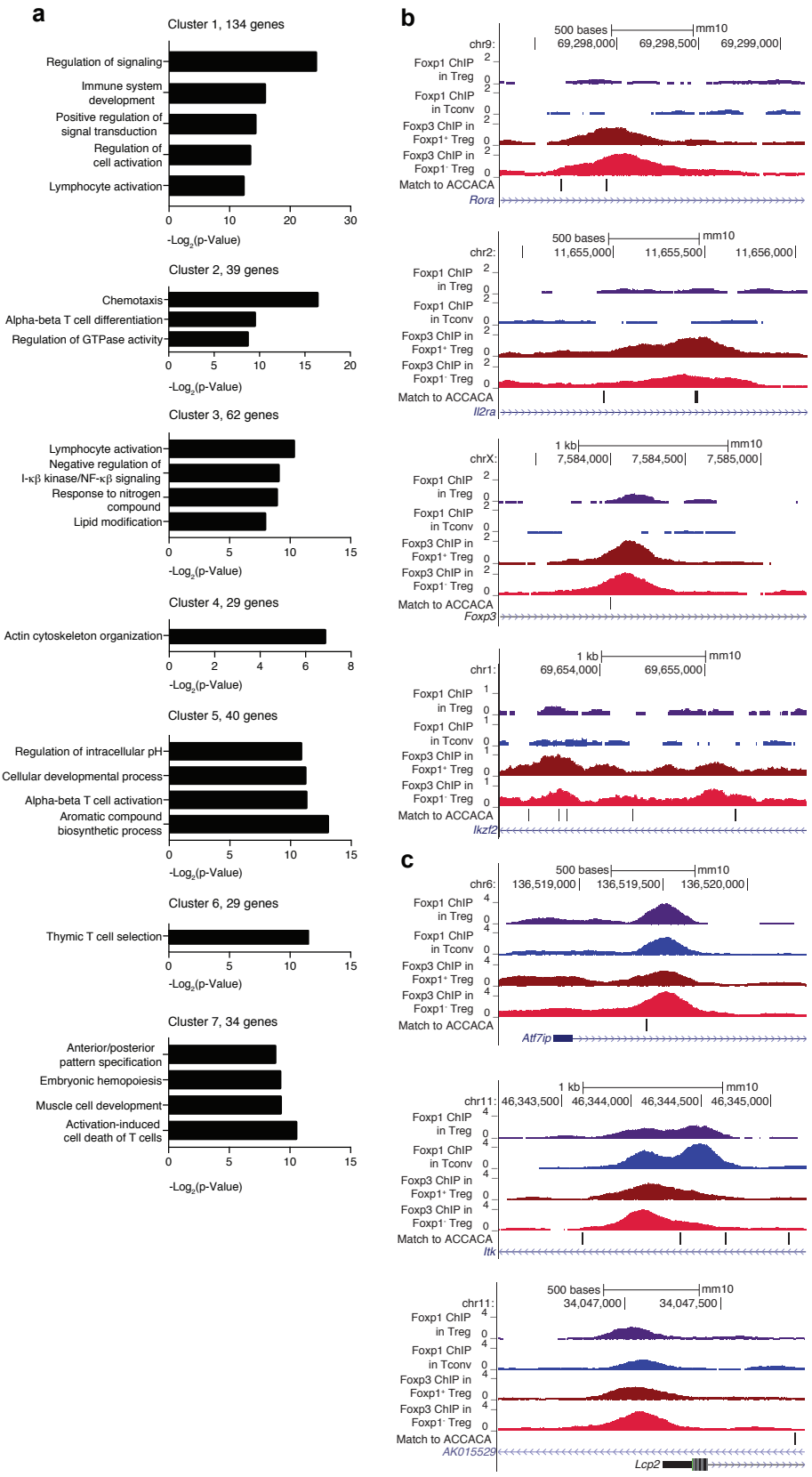
a
Cluster 1, 134 genes
Regulation of signaling
Immune system development
Positive regulation of signal transduction
Regulation of cell activation
Lymphocyte activation
-Log2(p-Value)
Cluster 2, 39 genes
Chemotaxis
Alpha-beta T cell differentiation
Regulation of GTPase activity
-Log2(p-Value)
Cluster 3, 62 genes
Lymphocyte activation
Negative regulation of I-κβ kinase/NF-κβ signaling
Response to nitrogen compound
Lipid modification
-Log2(p-Value)
Cluster 4, 29 genes
Actin cytoskeleton organization
-Log2(p-Value)
Cluster 5, 40 genes
Regulation of intracellular pH
Cellular developmental process
Alpha-beta T cell activation
Aromatic compound biosynthetic process
-Log2(p-Value)
Cluster 6, 29 genes
Thymic T cell selection
-Log2(p-Value)
Cluster 7, 34 genes
Anterior/posterior pattern specification
Embryonic hemopoiesis
Muscle cell development
Activation-induced cell death of T cells
-Log2(p-Value)
b
Foxp1 ChIP in Treg
Foxp1 ChIP in Tconv
Foxp3 ChIP in Foxp1+ Treg
Foxp3 ChIP in Foxp1- Treg
Match to ACCACA
Rora
Il2ra
Foxp3
Ikzf2
c
Atf7ip
Itk
AK015529
Lcp2

Figure 3.4. Analysis of Genes Associated with Foxp3-only Peaks.

(A) GO pathway enrichment analysis for each cluster of genes in Figure 2F. (B) Foxp3 and Foxp1 ChIP-seq tracks at four loci bound by Foxp3 and containing a Runx motif. (C) Foxp3 and Foxp1 ChIP-seq tracks at three loci bound by Foxp3 and Foxp1 and not containing a Runx motif.

Table 3.1. Differential Gene Expression Between Naïve and Activated Treg or Tconv Cells for a Subset of Genes that were Bound by Foxp3 and not Foxp1.

Gene	Average expression in Tconv	Tconv log_2 (activated /naïve)	FDR Tconv	Average expression in Treg	Treg log_2 (activated/ naïve)	FDR Treg	Number of Foxp3-only promoter binding sites	Number of Foxp3-only non-promoter binding sites	Number of Foxp1 promoter binding sites	Number of Foxp1 non-promoter binding sites	Gene cluster
Itgb1	40000	4.569	0.00E+00	14004	2.1819	2.80E-23	NA	1	NA	NA	1
Ctla4	2900	3.918	0.00E+00	25587	1.535	1.40E-31	1	NA	NA	2	1
Nrp1	3300	5.63	0.00E+00	9536	0.9389	8.30E-04	1	1	NA	NA	1
Sell	32000	-3.188	0.00E+00	53219	-2.2724	1.20E-40	1	1	NA	NA	4
Maf	2000	6.37	3.10E-262	2134	4.2359	4.90E-75	NA	1	NA	NA	1
P2rx7	6100	3.761	6.00E-253	10059	0.5801	1.80E-03	NA	1	NA	NA	1
Cd44	8200	3.98	6.80E-238	5505	2.8945	1.30E-47	NA	1	NA	NA	1
Cxcr5	7100	5.812	1.50E-214	5880	2.10145	2.50E-82	1	NA	NA	NA	1
Endod1	3600	4.568	1.10E-203	3743	2.025	4.20E-67	NA	1	NA	NA	1
Plscr1	1300	7.447	1.40E-194	1145	2.1194	2.100E-35	1	1	NA	NA	1
Serpina3g	2000	8.978	2.20E-173	10340	4.1958	9.90E-87	1	NA	NA	NA	1
Tnfsf11	2800	4.593	2.60E-154	2409	3.2303	1.90E-62	NA	1	1	NA	1
Bmp7	1500	4.935	1.40E-132	1963	2.7802	2.70E-89	NA	1	NA	2	1
Cd83	2300	6.085	1.80E-132	20162	3.3672	2.40E-66	NA	1	1	NA	1
Bcl2a1b	1100	2.536	1.10E-114	1169	2.27	3.50E-55	1	NA	NA	NA	1
Ikzf2	1100	6.377	1.40E-105	5442	0.8862	6.90E-02	1	6	1	NA	1
Spry1	2300	4.366	1.00E-104	2596	0.8053	4.20E-04	2	NA	NA	NA	1
Casp4	830	5.236	1.70E-100	382	2.8058	1.40E-13	1	NA	NA	NA	1
Tbc1d4	10000	3.129	7.60E-99	7884	1.3202	1.10E-08	NA	1	NA	NA	1
Srgn	20000	1.347	1.20E-95	27246	1.2624	4.90E-23	NA	1	2	NA	1
Trib1	1800	2.462	1.50E-93	6401	0.3701	8.40E-02	NA	1	NA	NA	1
Il10ra	3500	1.568	2.60E-82	8283	1.395	6.70E-18	1	1	NA	NA	1
Slamf1	2200	1.421	2.20E-70	4868	0.855	4.00E-09	NA	1	NA	1	1
Prelid2	300	3.241	1.70E-53	261	3.4479	2.30E-44	1	NA	NA	NA	1
Il2ra	580	3.542	1.50E-52	36508	-0.4562	5.00E-02	1	3	NA	1	7
Rora	1400	2.893	9.10E-51	676	2.3083	4.50E-07	NA	5	1	1	5

Foxp1 that lacked a Runx1 motif (Figure 3.4C). We found that Runx1 was bound at all loci relative to a control region in Treg cells, but particularly at *Foxp3 CNS2* , where Runx1 binding has been characterized, and at an intronic enhancer in the *Il2ra* locus (Figure 3.3H). Runx1 was bound weakly at all loci containing Runx1 motifs in Tconv cells (Figure 3.3H).

In summary, Foxp3-only bound peaks were associated with increased chromatin accessibility in activated Treg and Tconv cells and with genes that were upregulated in activated cells. Analysis of Foxp3-only binding sites revealed significant enrichment of the Runx-family motif. Consistently, we found that Foxp1 and Runx1 were both present in complexes with Foxp3 but to a much lesser extent with each other. We found Runx1 enrichment by ChIP-qPCR in Treg cells and in Tconv cells at several Foxp3 bound sites containing a Runx motif, suggesting that Runx1 may bind and regulate these loci in a Foxp3 independent manner in cells lacking Foxp3. It is possible that Foxp3 presence in Runx1 transcription factor complexes in Treg cells may modify target loci, as evidenced by the fact that the Foxp3-only peaks were associated with significantly higher chromatin accessibility in Tconv cells relative to Treg cells.

Foxp3 DNA binding and protein abundance are reduced in the context of Foxp1 deficiency

To identify distinct functions of Foxp3 and Foxp1 in Treg cells, we assessed the effect of absence of Foxp1 on DNA binding of Foxp3. We considered that loss of Foxp1, and the resulting inability of these transcription factors to form heterodimeric protein complexes with Foxp1, could lead to a reduction of DNA binding specifically at sites that were normally occupied by both Foxp3 and Foxp1. Alternatively, the change in absolute abundance of Foxp protein due to loss of Foxp1 could lead to an even reduction of DNA binding by Foxp3 protein across all of its normally bound sites. To distinguish between these two possibilities, we generated a conditional Foxp1 allele and crossed it to *Foxp3*$^{YFP\text{-}Cre}$ to generate mice in which Foxp1 is absent in Treg cells (Figure 3.5). When we performed Foxp3-chip on Foxp1-deficient Treg cells we found that Foxp3

binding was reduced genome-wide in the absence of Foxp1, and not just at Foxp1 overlapping sites (Figure 3.6A). In fact, Foxp3 ChIP signal was significantly less reduced in Foxp1-deficient Treg cells at sites bound by Foxp1 than at all Foxp3 bound sites (Figure 3.6B).

Foxp3 protein level is higher in activated Treg cells than in naive Treg cells, though this difference does not result in significant changes in Foxp3 genome occupancy [130]. In the context of Foxp1 loss (Figure 3.6C,D), however, Foxp3 genome occupancy was altered. To investigate whether decreased Foxp3 genome occupancy might be due to a change in Foxp3 protein level, we assessed Foxp3 protein level in Foxp1-deficient and -sufficient $CD62L^{hi}$ naive Treg cells and $CD44^{hi}$ activated Treg cells by flow cytometry and by western blot. We observed a 25% reduction in Foxp3 protein level in Foxp1-deficient naive Treg cells but did not observe a difference in Foxp3 protein level between Foxp1-sufficient and deficient activated Treg cells (Figure 3.6E.F). Foxp3 mRNA level was also reduced in Foxp1 deficient Treg cells, suggesting that the decrease of Foxp3 protein in Foxp1 deficient cells was likely due to altered transcriptional regulation of Foxp3, rather than a change in protein stability. Previous studies examining the role of CBF-β and Runx1 in the Foxp3 dependent transcriptional program found that deficiency in either of these proteins results in greatly reduced Foxp3 mRNA and protein levels, but had no effect on Foxp3 target gene expression [129]. These findings demonstrate that reduction in absolute Foxp3 protein does not always result in reduced Foxp3 genome occupancy. Therefore the reduced genome occupancy observed in Foxp1 deficient Treg cells may be due to reasons independent of Foxp3 protein level.

To assess the impact of Foxp1 loss on gene expression in Treg cells in an unbiased way, we performed RNA-seq of YFP^{+} $CD62L^{hi}$ naïve or $CD44^{hi}$ activated Treg cells isolated from *Foxp3*$^{YFP\text{-}Cre/+}$ *Foxp1*$^{f/f}$ or *Foxp3*$^{YFP\text{-}Cre/+}$ *Foxp1*$^{+/+}$ heterozygous female mice. We observed that *Foxp3*$^{YFP\text{-}Cre}$ *Foxp1*$^{f/f}$ mice, in which all Treg cells lacked Foxp1, had a mild autoimmune phenotype so we performed RNA-seq on Treg cells from heterozygous female mice to control for

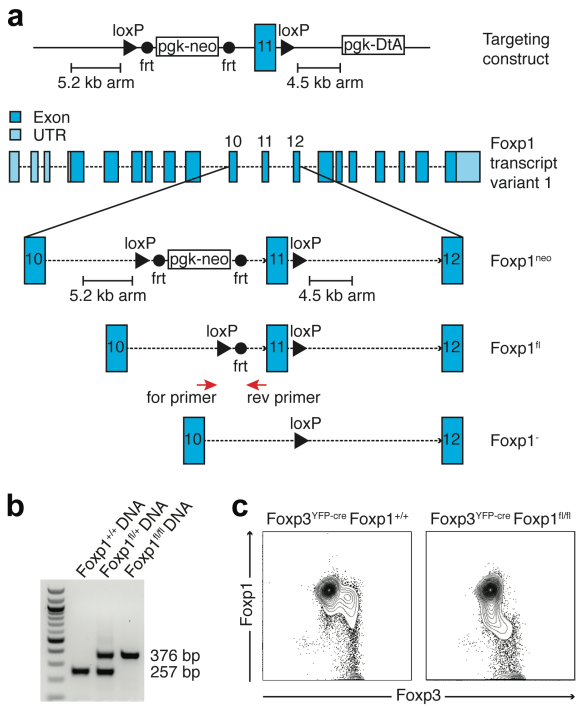

Figure 3.5. Generation of the Conditional *Foxp1* Allele.

(A) Diagram of the targeting vector containing *Foxp1* exon 11 and of the targeting strategy. (B) PCR analysis of homozygous *Foxp1*$^{f/f}$, heterozygous *Foxp1*$^{f/+}$ and homozygous *Foxp1*$^{+/+}$ from tail DNA showing the co-integration of the 3′ downstream *lox*P site (376 bp) and wild-type allele product (257 bp). (C) Representative flow cytometric plots gated on splenic CD4^{+} T cells showing specific Foxp1 deletion in Foxp3^{+} Treg cells when *Foxp1*$^{f/f}$ was crossed to *Foxp3*$^{YFP\text{-}Cre}$.

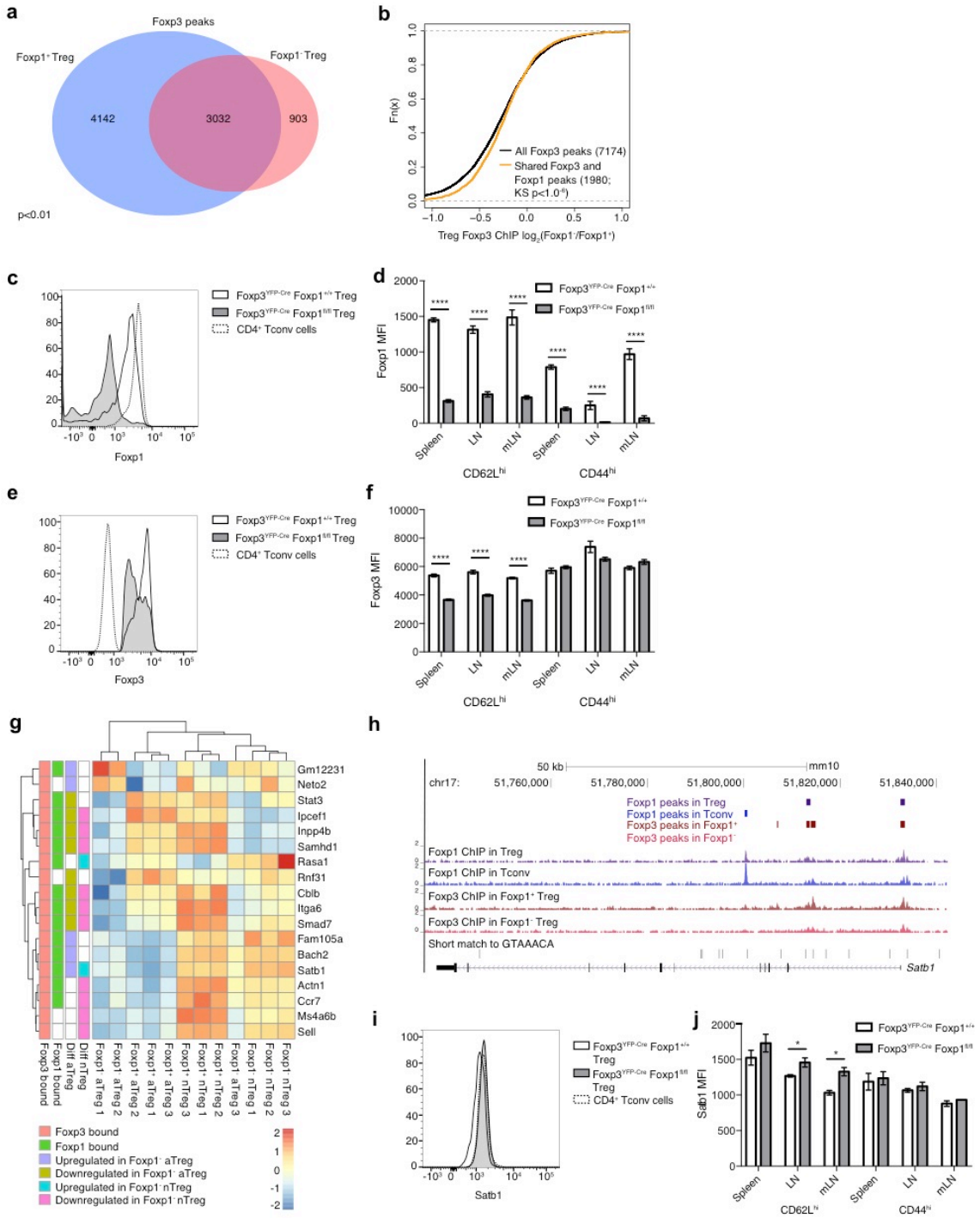

Figure 3.6. Foxp3 DNA Binding and Protein Abundance are Reduced in the Context of Foxp1 Deficiency.

(A) Venn diagram of Foxp3 bound sites in Foxp1$^+$ and Foxp1$^-$ Treg cells ($p<0.01$). (B) Cumulative distribution plot of Foxp3 ChIP binding intensity in Foxp1$^+$/Foxp1$^-$ Treg cells at peaks that overlap with Foxp1 peaks and at Foxp3-only peaks. (C, E) Representative histograms of Foxp1 (C) and Foxp3 (E) protein level in naive Foxp1$^+$ and Foxp1$^-$ Treg cells and in naive Tconv cells. (Figure description continued on following page)

Figure 3.6 – (continued)

(D, F) Summary plots of Foxp1 (D) and Foxp3 (F) MFI in Foxp1^{+} and Foxp1^{-} Treg cells from 8-10 week old male mice (n=5 per group, representative of 3 independent experiments, error bars represent SEM; $^{*}p < 0.05$; $^{**}p < 0.01$, $^{***}p < 0.001$, ns non-significant, unpaired two-tailed Student's t test). (G) Heatmap comparing gene expression between Foxp1^{+} and Foxp1^{-} naive and activated Treg cells from *Foxp3*$^{YFP\text{-}Cre/+}$ *Foxp1*$^{+/+}$ or *Foxp1*$^{f/f}$ heterozygous female mice for a subset of genes associated with Foxp3 ChIP peaks. (H) Foxp3 and Foxp1 ChIP-seq tracks at the *Satb1* locus. (I) Representative histogram of Satb1 protein level in naive Foxp1^{+} and Foxp1^{-} Treg cells and in naive Tconv cells. (J) Summary plot of Satb1 MFI in Foxp1^{+} and Foxp1^{-} Treg cells from 8-10 week old male mice (n=3 per group, representative of 2 independent experiments, error bars represent SEM; $^{*}p < 0.05$; $^{**}p < 0.01$, $^{***}p < 0.001$, ns non-significant, unpaired two-tailed Student's t test).

Table 3.2. Differential Gene Expression Between Naïve or Activated Foxp1 Sufficient and Deficient Treg cells for a Subset of Genes that were Bound by Foxp3.

Gene	Average counts (naïve)	log_2(naïve $Foxp1^+$/ $Foxp1^-$)	FDR (naïve)	Average counts (act)	log_2(act $Foxp1^+$/ $Foxp1^-$)	FDR (act)
Stat3	11135	0.17	0.15	11000	0.36	0.0000022
Neto2	128	-0.043	0.94	100	-0.7	0.024
Gm12231	404	-0.14	0.64	440	-0.47	0.0065
Ipcef1	5341	0.74	3.6E-19	6700	0.9	4.6E-25
Inpp4b	19500	0.82	4.9E-24	18000	0.55	0.00000043
Samhd1	17731	0.76	1.8E-29	17000	0.45	1.1E-10
Rasa1	6449	-0.32	0.00099	6300	0.03	0.85
Rnf31	2320	-0.088	0.58	2300	0.36	0.0015
Cblb	4760	0.3	0.004	4000	0.4	0.00063
Itga6	8155	1	2.10E-31	4700	0.7	8.7E-11
Smad7	4034	0.61	0.00000001	2200	0.45	0.015
Fam105a	8805	-0.16	0.19	5800	-0.22	0.026
Bach2	4133	0.047	0.78	2000	-0.51	0.0054
Satb1	26153	-0.25	0.0014	7100	-0.86	0.00039
Actn1	2255	0.44	0.0000026	1200	-0.26	0.27
Ccr7	23013	0.52	4.2E-09	12000	-0.23	0.23
Ms4a6b	33124	0.35	0.00000054	24000	0.03	0.81
Sell	49222	0.42	0.000000038	12000	0.2	0.6

any cell-extrinsic effects on gene expression. Genes that were differentially expressed ($p<0.001$) between Foxp1 sufficient and deficient naive and activated Treg cells and bound by Foxp3 and Foxp1 included *Itga6*, *Smad7*, and *Satb1* (Figure 3.6G, Table 3.2). The genome organizer Satb1-dependent Treg cell specific super-enhancer activation is crucial for Treg cell lineage specification in the thymus [131]. Satb1 repression in mature Treg cells is crucial for their phenotype and function, with ectopic expression of Satb1 resulting in loss of suppressive function and induction of effector T cell cytokines [132]. Foxp1 and Foxp3 both bound to two alternative Forkhead-motif containing Satb1 promoters in Treg cells, and Foxp1 was not significantly bound to these promoters in Tconv cells (Figure 3.6H). Foxp3 binding was significantly abrogated in Foxp1 deficient Treg cells and Foxp1 deficient Treg cells expressed more Satb1 at the mRNA and protein level than wild-type Treg cells (Figure 3.6I,J), suggesting that Foxp1 plays a role in Foxp3 mediated repression of Satb1 in Treg cells.

Foxp1 Deficiency Causes Treg Cell Activation and Effector Cytokine Production

Treg cell restricted Foxp1 deficiency resulted in mild lymphadenopathy (Figure 3.7A), which was in contrast to the reduced cellularity of spleens and lymph nodes of *CD4*^{Cre}*Foxp1*$^{f/f}$ T cells (Figure 3.8A) [66]. The proportion of CD4$^+$ T cells that were Foxp3$^+$ in lymph nodes was reduced approximately two-fold (Figure 3.8B,C) though the CD4/CD8 ratio remained unchanged (data not shown). Foxp1-deficient Treg cells were very activated based on CD44 expression, and they proliferated more than Foxp1-sufficient Treg cells as measured by Ki-67 expression (Figure 3.7D,E). Foxp1 deficient Treg cells also produced more IFN-γ upon phorbol 12-myristate 13-acetate (PMA) and ionomycin stimulation in vitro than Treg cells expressing Foxp1 (Figure 3.7F). These features of activation are similar to what was observed previously in Foxp1 deficient CD4$^+$ and CD8$^+$ T cells (Figure 3.8B-D)[66].

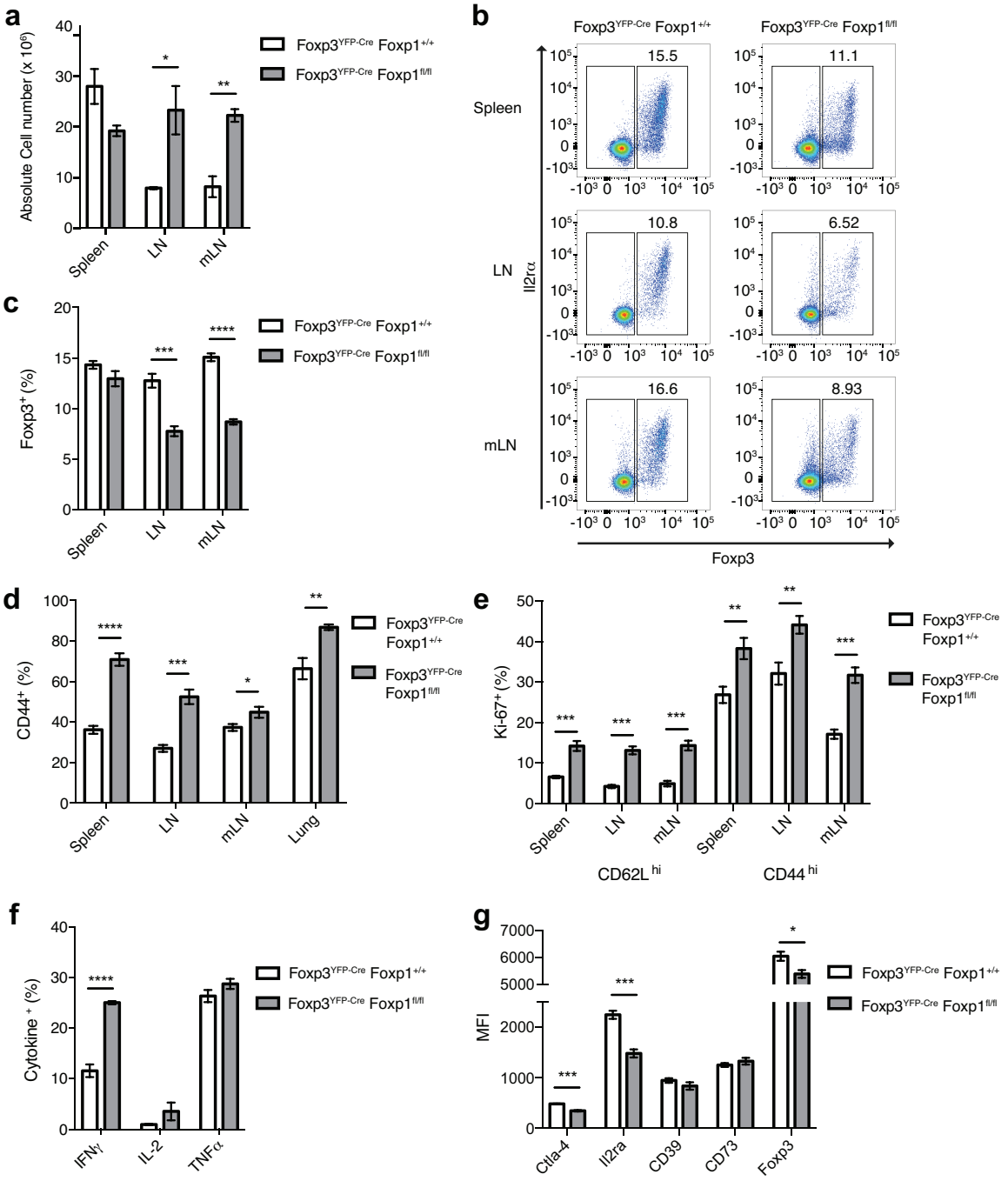

Figure 3.7. Foxp1 Deficiency Causes Treg Cell Activation and Effector Cytokine Production.

(A) Absolute cellularity of spleen, skin-draining lymph nodes and mesenteric lymph nodes of 10 week old mice (n=3, representative of several independent experiments). (B) Representative flow cytometric scatter plots gated on $CD4^+$ T cells from spleen, skin-draining lymph nodes and mesenteric lymph nodes of 10 week old mice showing Foxp3 and IL2r-α protein levels. (C) Summary plot of $Foxp3^+$ T cell frequency among $CD4^+$ T cells in spleen, lymph nodes and mesenteric lymph nodes of 10 week old mice (n=5, representative of several independent experiments). (figure description continued on following page)

Figure 3.7 – (continued)

(D) $CD44^{+}$ Treg cell frequency among $Foxp3^{+}$ Treg cells in various organs (n=5, representative of several experiments). (E) Ki-67^{+} Treg cell frequency among all naive $CD62L^{hi}$ or activated $CD44^{hi}$ Treg cells (n=5, representative of several independent experiments). (F) Protein MFI of several Treg signature proteins (n=5, representative of several experiments). (G) Frequency of cytokine-producing Treg cells among all splenic Treg cells after 3 h *in vitro* stimulation with PMA and ionomycin and with addition of brefeldin-A (n=5, representative of 3 independent experiments). Error bars represent SEM; $^{*}p < 0.05$; $^{**}p < 0.01$, $^{***}p < 0.001$, ns non-significant (unpaired two-tailed Student's t test).

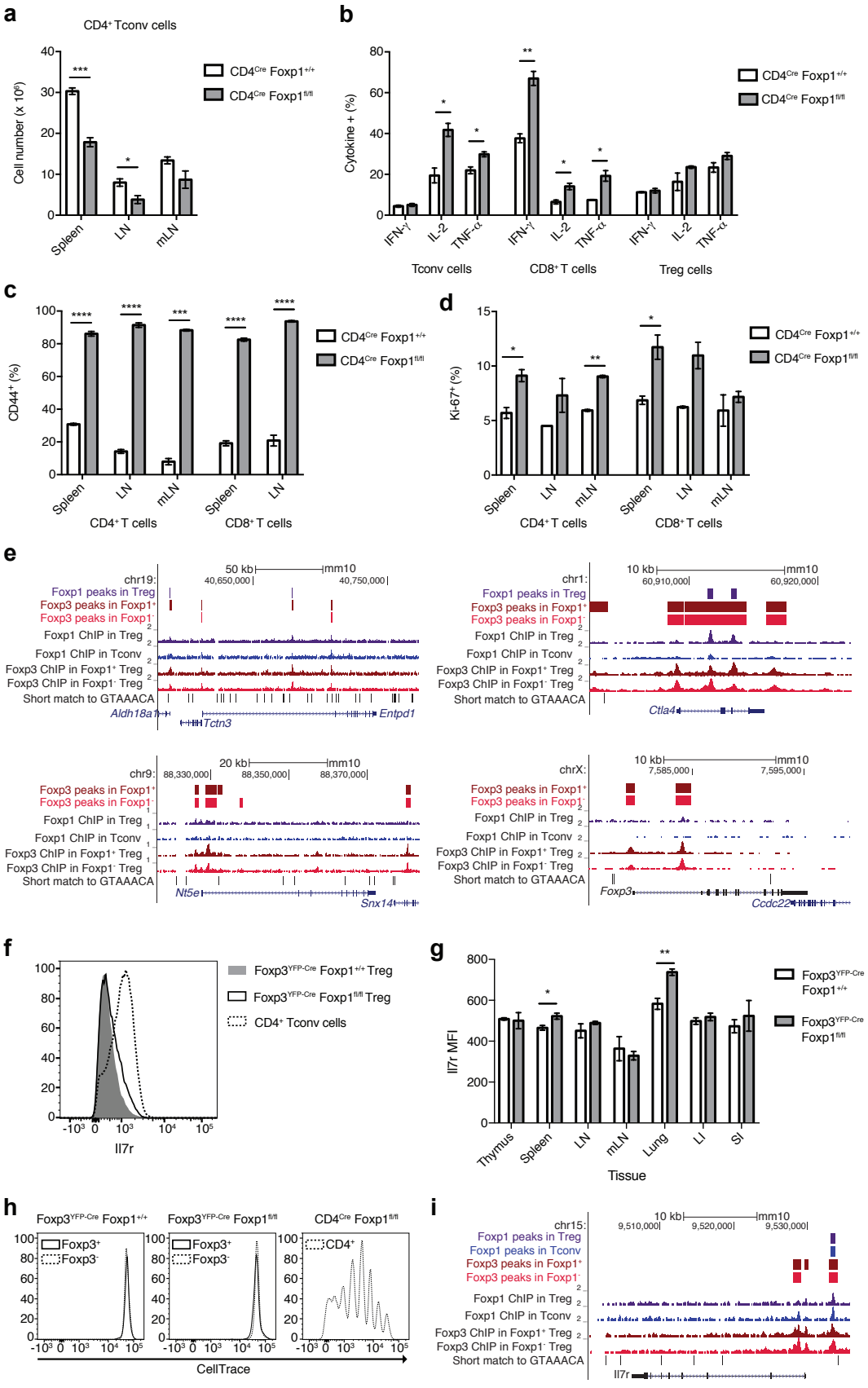
a
CD4+ Tconv cells
Cell number (x 10^6)
CD4Cre Foxp1+/+
CD4Cre Foxp1fl/fl
Spleen
LN
mLN
b
Cytokine + (%)
IFN-γ
IL-2
TNF-α
Tconv cells
CD8+ T cells
Treg cells
c
CD44+ (%)
CD4+ T cells
CD8+ T cells
d
Ki-67+ (%)
e
chr19:
chr1:
chr9:
chrX:
Foxp1 peaks in Treg
Foxp1 peaks in Tconv
Foxp3 peaks in Foxp1+
Foxp3 peaks in Foxp1-
Foxp1 ChIP in Treg
Foxp1 ChIP in Tconv
Foxp3 ChIP in Foxp1+ Treg
Foxp3 ChIP in Foxp1- Treg
Short match to GTAAACA
Aldh18a1
Tctn3
Entpd1
Ctla4
Nt5e
Snx14
Foxp3
Ccdc22
f
Foxp3YFP-Cre Foxp1+/+ Treg
Foxp3YFP-Cre Foxp1fl/fl Treg
CD4+ Tconv cells
Il7r
g
Il7r MFI
Thymus
Spleen
LN
mLN
Lung
LI
SI
Tissue
h
Foxp3YFP-Cre Foxp1+/+
Foxp3YFP-Cre Foxp1fl/fl
CD4Cre Foxp1fl/fl
Foxp3+
Foxp3-
CD4+
CellTrace
i
chr15:
Il7r

Figure 3.8. Comparison of *Foxp3*$^{YFP\text{-}Cre}$*Foxp1*$^{f/f}$ to *CD4*^{Cre}*Foxp1*$^{f/f}$.

(A) CD4$^+$ T cell numbers in lymphoid organs of 10 week old mice (n=3, representative of 2 independent experiments). (B) Frequency of cytokine-producing T cells among all splenic CD4$^+$ Tconv cells or CD8$^+$ T cells from10 week old *CD4*^{Cre}*Foxp1*$^{f/f}$ mice after 3 h *in vitro* stimulation with PMA and ionomycin and with addition of brefeldin-A (n=3, representative of 2 independent experiments). (C) CD44^{hi} cell frequency among splenic or lymph node CD4$^+$ Tconv cell or CD8$^+$ T cells from10 week old *CD4*^{Cre}*Foxp1*$^{f/f}$ mice (n=3, representative of 2 independent experiments). (D) Ki-67$^+$ T cell frequency among CD4$^+$ Tconv cells or CD8$^+$ T cells (n=5, representative of several independent experiments). (E) Representative histograms of IL7r-α protein level in naive Foxp1$^+$ and Foxp1$^-$ Treg cells and in naive Tconv cells. (F) Summary plots of IL7r-α MFI in Foxp1$^+$ and Foxp1$^-$ naive Treg cells from 8-10 week old male mice (n=3 per group, representative of 3 independent experiments). (G) Proliferation of sorted Foxp1$^+$ and Foxp1$^-$ Treg cells or Foxp1$^-$ Tconv cells after 7 d *in vitro* culture with IL-7. Foxp3$^-$ ex-Treg cells and Treg cells that maintained Foxp3 expression are both shown (Representative plots, n=3 with 3 technical replicates each, representative of 2 independent experiments). Error bars represent SEM; $^*p < 0.05$; $^{**}p < 0.01$, $^{***}p < 0.001$, ns non-significant (unpaired two-tailed Student's t test).

Several Treg cell signature proteins were expressed significantly less at the mRNA level in Foxp1-deficient Treg cells, including *Ctla4*, *Il2ra*, *Nt5e*, *Entpd1* and *Foxp3* itself. Foxp3 was bound to all of these loci as well (Figure 3.8E, 3.12E). When we assessed the protein level of these Treg signature genes, we found that Foxp1-deficient Treg cells expressed lower levels of IL2r-α, Ctla-4, and Foxp3, but not CD39 or CD73 (Figure 3.7G).

Foxp1 and Foxp3 are both known to regulate expression of IL7r-α and Foxp1 deficiency in T cells specifically has been shown to result in de-repression of the *Il7ra* locus, increased cell surface expression of IL7r-α and proliferation in response to IL-7 in vitro [68]. We investigated whether Foxp1 deficiency in Treg cells similarly led to increased cell surface IL7r-α expression and proliferation in response to IL-7 and we found that neither protein level nor responsiveness to IL- 7 were affected by Foxp1 deficiency in Treg cells (Figure 3.8F-H). This may be due to Foxp3 mediated repression of IL7r-α expression independent of Foxp1 as Foxp3 binding to the *Il7ra* locus is not reduced in the context of Foxp1 deficiency (Figure 3.8I). Indeed, inverse correlation of Foxp3 and IL7r-α expression in Treg cells has been shown to be consistent, whereas IL2r-α expression is low in certain contexts, including in small intestine lamina propria Treg cells [133, 134].

Foxp1 deficiency causes Treg cell functional impairment

The lymphadenopathy and increased cytokine production by Foxp1 deficient Treg cells that we observed led us to investigate whether Foxp1 deficiency in Treg cells impairs their suppressive function. Indeed, $CD4^+$ and $CD8^+$ T cells were more activated based on CD44 expression and more proliferative in lymphoid organs of mice with Foxp1 deficient Treg cells (Figure 3.9A,B). Without TCR stimulation, T cells did not produce any cytokines examined (data not shown). However, upon transient ex vivo stimulation by PMA plus ionomycin, higher

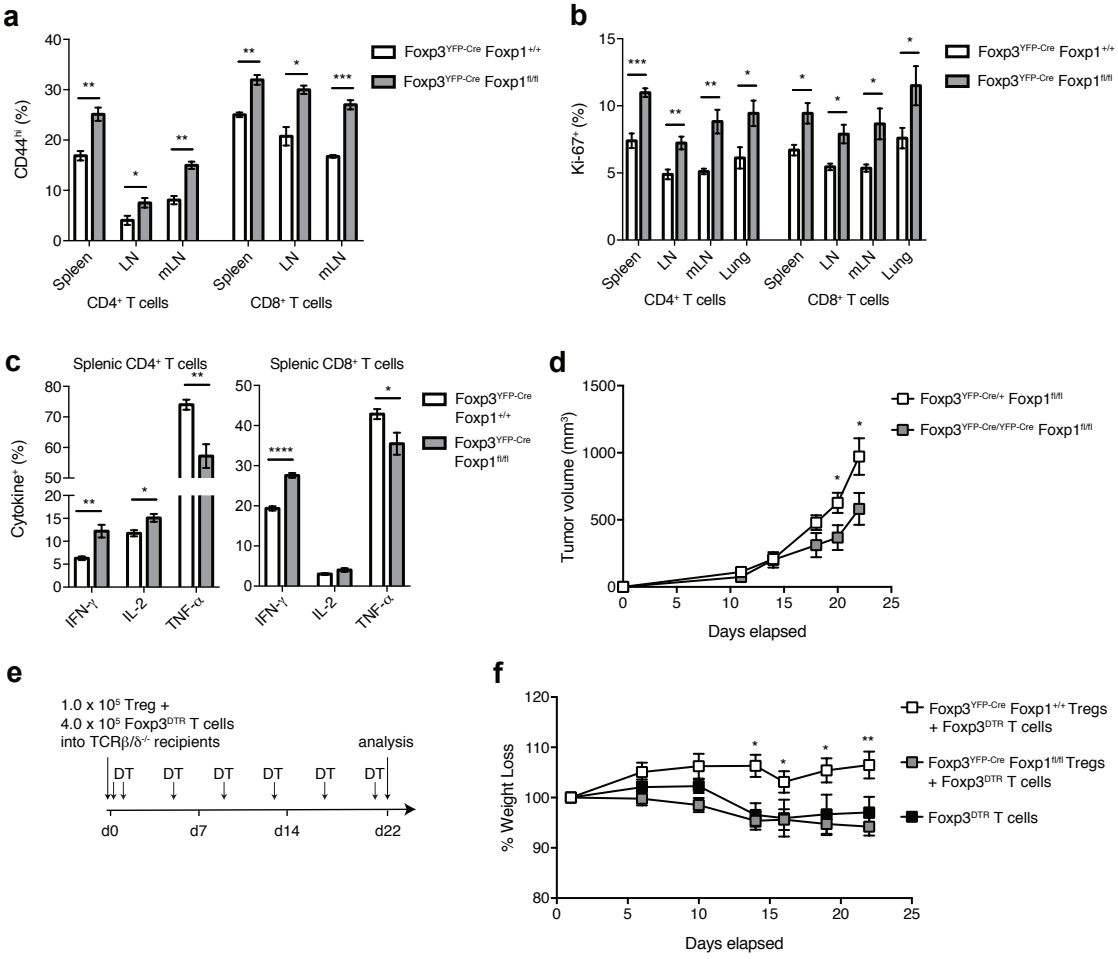

Figure 3.9. Foxp1 Deficiency Causes Treg Cell Functional Impairment.

(A) CD44^{hi} cell frequency among splenic or lymph node CD4$^+$ Tconv cell or CD8$^+$ T cells (n=3, representative of several independent experiments). (B) Ki-67$^+$ T cell frequency among CD4$^+$ Tconv cells or CD8$^+$ T cells (n=5, representative of several independent experiments). (C) Frequency of cytokine-producing T cells among all splenic CD4$^+$ Tconv cells or CD8$^+$ T cells after 3 h *in vitro* stimulation with PMA and ionomycin and with addition of brefeldin-A (n=5, representative of 3 independent experiments). (D) Tumor volume (mm^3) over time of E0771 breast cancer cell line in mammary fat pads of female mice (n=5, representative of 2 independent experiments). (E) Schematic of *in vivo* suppression assay. (F) Weight over time of TCRβδ$^{-/-}$ recipient mice adoptively transferred with Foxp1$^+$ or Foxp1$^-$ Treg cells and *Foxp3*^{DTR} T cells ((n=5, representative of 2 independent experiments). Error bars represent SEM; $^*p < 0.05$; $^{**}p < 0.01$, $^{***}p < 0.001$, ns non-significant (unpaired two-tailed Student's t test).

percentages of splenic CD4+ T cells produced IFN-γ and IL-2 (Figure 3.9C), but not IL-4 or IL-17 (data not shown). Higher percentages of splenic $CD8^+$ T cells were found to produce IFN-γ (Figure 3.9C). Skin-draining lymph node and mesenteric lymph node $CD4^+$ and $CD8^+$ T cells from mice with a Treg cell specific Foxp1 deficiency also produced more IFN-γ *in vitro* (data not shown).

To further assess Treg cell suppressive function, we assessed tumor growth of a breast cancer cell line derived from a spontaneous tumor in a C57/Bl6 mouse injected into the mammary fat pads of female mice. Tumors grew significantly more slowly in female mice with a Treg cell restricted Foxp1 deficiency (Figure 3.9D). To formally assess Treg cell suppressive function, we performed in vivo suppression assays in which Foxp1 deficient or sufficient Treg cells were adoptively co-transferred with *Foxp3*^{DTR} T cells into TCRβδ$^{-/-}$ recipients (Figure 3.9E). We continuously administered diphtheria toxin to these mice to deplete the *Foxp3*^{DTR} Treg cells and measured body weight. Mice that received only *Foxp3*^{DTR} T cells lost weight due to a lack of Treg cells to suppress spontaneous inflammation. Likewise, mice that received Foxp1-deficient Treg cells along with *Foxp3*^{DTR} cells lost weight, while mice that received Foxp1-sufficient Treg cells did not lose weight (Figure 3.9F). We analyzed the lymphoid tissues of these mice and found that fewer Foxp1-deficient Treg cells remained at d22 relative to Foxp1-sufficient Treg cells though the cells that did remain maintained Foxp3 expression (Figure 3.10A,B). These results suggested that Foxp1 might play a role in Treg cell survival. The Tconv and $CD8^+$ T cells from the recipient mice that received Foxp1-deficient Treg cells more readily produced IFN-γ, IL-2 and TNF-α upon transient ex vivo stimulation by PMA plus ionomycin (Figure 3.10C). Collectively, these results suggest that Foxp1 is required for Treg cell suppressive function.

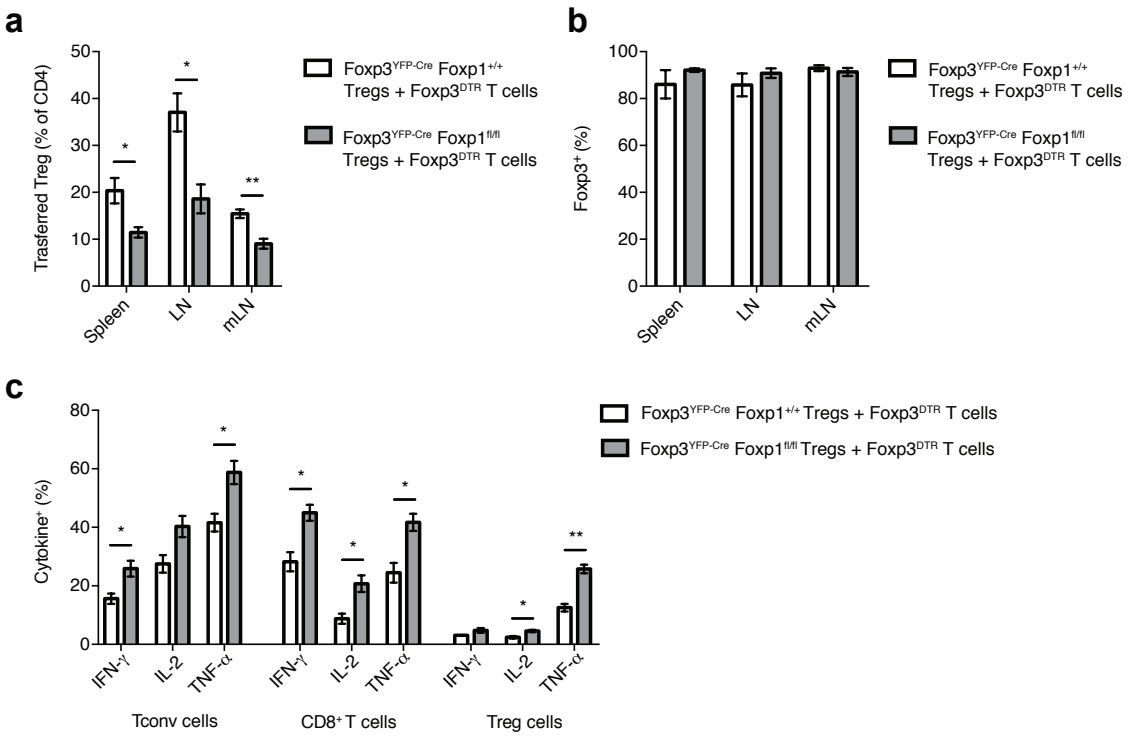

Figure 3.10. *In Vivo* Suppression Assay Analysis.

(A) Frequency of CD45.1xCD45.2 transferred Treg cells of all $CD4^+$ T cells in lymphoid organs on d22 post-transfer. (B) Percentage of CD45.1xCD45.2 transferred Treg cells on d22 post-transfer that maintained expression of Foxp3. (C) Frequency of cytokine-producing T cells among all splenic CD45.1 $CD4^+$ Tconv cells, CD45.1 $CD8^+$ T cells and CD45.1xCD45.2 Treg cells after 3 h *in vitro* stimulation with PMA and ionomycin and with addition of brefeldin-A. In all panels n=4 for $Foxp1^+$ group and n=3 for $Foxp1^-$ group, representative of 2 independent experiments. Error bars represent SEM; $^*p < 0.05$; $^{**}p < 0.01$, $^{***}p < 0.001$, ns non-significant (unpaired two-tailed Student's t test).

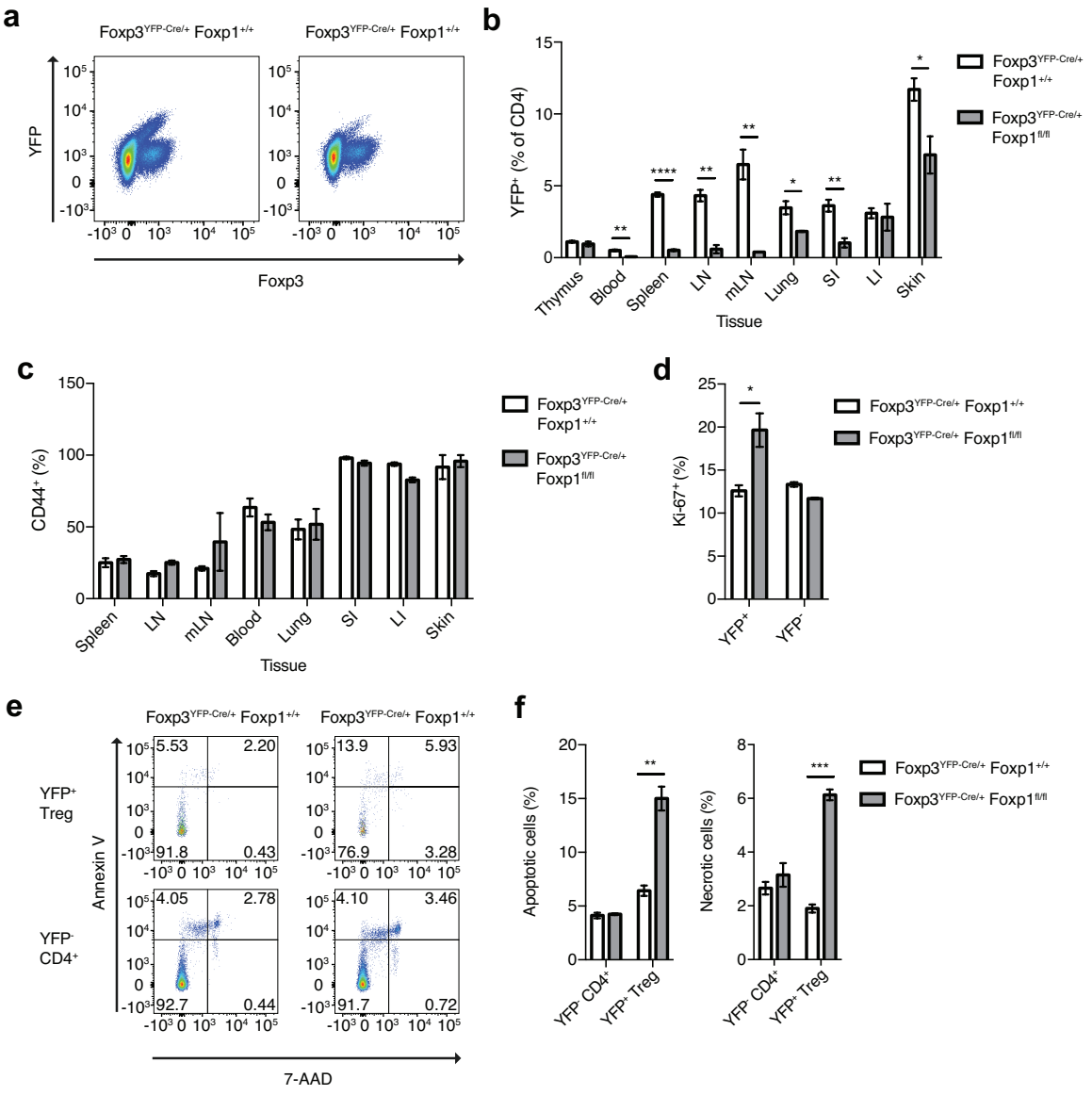

Figure 3.11. Foxp1 Deficient Treg Cells are Severely Disadvantaged in a Competitive Setting and have Increased Apoptotis.

(A) Representative flow cytometric scatter plots gated on $CD4^+$ T cells from spleens of 10 week old *Foxp3*$^{YFP\text{-}Cre/+}$ *Foxp1*$^{+/+}$ or *Foxp1*$^{f/f}$ heterozygous female mice showing Foxp3 and YFP staining. (B) YFP^+ Treg cell frequency of $CD4^+$ T cells in heterozygous female mice in lymphoid and peripheral tissues (n=3, representative of 3 independent experiments).(C) $CD44^{hi}$ cell frequency among YFP^+ Treg cells in lymphoid and peripheral tissues (n=3, representative of several independent experiments). (D) Ki-67^+ cell frequency among YFP^+ and YFP^- Treg cells in heterozygous female mice (n=3, representative of 2 independent experiments).

(figure description continues on following page)

Figure 3.11 – (continued)

(E) Representative flow cytometric scatter plots gated on YFP^+ Treg cells or YFP^- $CD4^+$ T cells from spleens of 10 week old heterozygous female mice showing 7-AAD and Annexin V staining. (F) Summary plot of Annexin V^+ 7-AAD^- apoptotic and Annexin V^+ 7-AAD^+ necrotic YFP^+ Treg cells and YFP^- $CD4^+$ T cells (n=3, representative of 2 independent experiments). Error bars represent SEM; $^*p < 0.05$; $^{**}p < 0.01$, $^{***}p < 0.001$, ns non-significant (unpaired two-tailed Student's t test).

Foxp1 Deficient Treg Cells are Severely Disadvantaged in a Competitive Setting and have Increased Apoptotis

To distinguish between cell-intrinsic and cell-extrinsic effects of Foxp1 deficiency in Treg cells, we analyzed *Foxp3*$^{YFP\text{-}Cre/+}$ *Foxp1*$^{f/f}$ heterozygous female mice. Due to random X-inactivation, approximately half of the Treg cells in these mice were expected to express YFP. Indeed, when *Foxp3*$^{YFP\text{-}Cre/+}$ *Foxp1*$^{+/+}$ heterozygous female mice were examined, 40% of the Treg cells were YFP^{+}, indicating that expression of the *Foxp3*$^{YFP\text{-}Cre}$ protein confers a slight disadvantage to Treg cells in a competitive setting (Figure 3.11A). When we analyzed *Foxp3*$^{YFP\text{-}Cre/+}$ *Foxp1*$^{f/f}$ mice, we found that Foxp1-deficient YFP^{+}Foxp3^{+} thymocytes were not competitively disadvantaged relative to Foxp1-sufficient Foxp3^{+}YFP^{+} thymocytes. However, when we analyzed Treg in the periphery we observed that Foxp1 deficient cells were severely outcompeted by Foxp1-sufficient Treg cells in lymphoid tissues (Figure 3.11A,B). To understand the mechanism underlying the reduced numbers of Foxp1-deficient Treg cells in a competitive setting we assessed activation, proliferation and apoptosis of YFP^{+} Foxp1-deficient Treg cells. Foxp1 deficiency in CD4^{+} Tconv cells and in CD8^{+} T cells leads to cell-intrinsic activation [68]. Conversely, Foxp1-deficient Treg cells in heterozygous mice were activated to the same extent as Foxp1-sufficient Treg cells (Figure 3.11C). This result suggests that the activated Treg cell phenotype observed in *Foxp3*$^{YFP\text{-}Cre}$ *Foxp1*$^{f/f}$ mice (Figure 3.7D) may be cell-extrinsic and due to increased activation of CD4^{+} and CD8^{+} T cells in response to impaired Treg cell suppression.

Despite being comparably activated, YFP^{+} Foxp1-deficient Treg cells from *Foxp3*$^{YFP\text{-}Cre/+}$ heterozygous mice were more proliferative than Foxp1-sufficient Treg cells (Figure 3.11D). Next, we examined apoptosis of YFP^{+} Foxp1-deficient Treg cells from *Foxp3*$^{YFP\text{-}Cre/+}$ heterozygous female mice by annexin V staining. The percentages of annexin V–positive but 7-AAD–negative YFP^{+} Treg cells were significantly higher in Treg cells lacking Foxp1 (Figure 3.11E,F). All apoptotic cells had an activated phenotype based on CD44 expression (data not shown). Foxp1

deficiency is known to increase effector T cell apoptosis *in vivo*. The mechanism by which apoptosis occurs in Foxp1-deficient T cells remains to be elucidated but is not mediated by Fas-FasL interaction [66].

IL-2 Signaling is Impaired in Foxp1 Deficient Treg cells and is Rescued by Constitutive Stat5 Activation *In Vivo*

One observation we made early in our analysis of Foxp1-deficient Treg cells was that they expressed far less Il2r-α than Foxp1-sufficient Treg cells (Figure 3.7F and 3.12A). The lower expression of Il2r-α was observed in YFP^{+} Treg cells from *Foxp3*$^{YFP\text{-}Cre/+}$ *Foxp1*$^{f/f}$ female mice as well, indicating that it was cell-intrinsic (Figure 3.12B). To assess whether the lower Il2r-α expression caused the Foxp1-deficient Treg cells to be less responsive to IL-2, we isolated Treg cells, cultured them in varying concentrations of IL-2 and assessed Stat5b phosphorylation as a measure of functional IL-2 signaling (Figure 3.12C). We found that at low doses of IL-2, Stat5b was significantly less phosphorylated in Foxp1-deficient Treg cells but this difference was absent in saturating IL-2 conditions (Figure 3.12C). The TCR signaling and STAT5 signaling pathways control largely distinct sets of genes and likely control distinct aspects of Treg cell suppressor activity [135]. To test whether the previously characterized Stat5 signaling gene signature was differentially expressed in Foxp1-deficient Treg cells, we analyzed the expression levels of Stat5b-dependent genes in our RNA-seq data. We found that genes upregulated upon constitutive Stat5b activation were more highly expressed by Foxp1-sufficient Treg cells, whereas genes downregulated upon constitutive Stat5b activation were generally more highly expressed in Foxp1-deficient Treg cells (Figure 3.12D). Together, these results demonstrated that IL-2 signaling was impaired in Foxp1-deficient Treg cells in a cell-intrinsic manner at steady state *in vivo*. We further observed that there was a Foxp1 and Foxp3 shared binding site within the *Il2ra*

locus. Foxp3 remained significantly bound to this site but Foxp3 binding at several other sites within the *Il2ra* locus was reduced or lost in the absence of Foxp1 (Figure 3.12E).

To determine whether increasing IL-2 signaling would be sufficient to rescue the competitive disadvantage of Foxp1-deficient Treg cells, we treated *Foxp3*$^{YFP\text{-}Cre/+}$ *Foxp1*$^{f/f}$ heterozygous female mice with IL-2/anti-IL-2 complexes every other day for one week and measured the frequency of YFP$^+$ Treg cells. We found that YFP$^+$ Treg cells from *Foxp3*$^{YFP\text{-}Cre/+}$ *Foxp1*$^{f/f}$ and from *Foxp3*$^{YFP\text{-}Cre/+}$ *Foxp1*$^{+/+}$ mice had similar levels of phospho-Stat5 directly ex vivo. However, Foxp1-deficient Treg cells were still severely outcompeted by Foxp1-sufficient Treg cells (data not shown). To assess whether IL-2 signaling could rescue the competitive disadvantage phenotype in a direct cell-intrinsic manner, we transduced congenically marked Foxp1-sufficient and -deficient Treg cells with a retroviral vector expressing the constitutively active form of Stat5b and co-transferred them at a 1:1 ratio into TCR$\beta\delta^{-/-}$ recipients along with congenically marked *Foxp3*^{DTR} *CD4*$^+$ T cells. We treated the mice with DT continuously to deplete *Foxp3*^{DTR} Treg cells and assessed Foxp1$^-$/Foxp1$^+$ Treg cell ratios in lymphoid organs on d14 (Figure 3.12F). We found that control vector transduced Foxp1-deficient Treg cells adoptively co-transferred with Foxp1-sufficient Treg cells were severely outcompeted in lymph nodes and mesenteric lymph nodes by d14 post-transfer (Figure 3.12G). Foxp1-deficient Treg cells that were localized to the spleen were not strongly outcompeted by Foxp1-sufficient Treg cells. When *Stat5b*^{CA} vector transduced Foxp1-deficient Treg cells were adoptively co-transferred with Foxp1-sufficient Treg cells, they were present at roughly 1:1 ratios in lymph nodes, spleen and blood on d14 (Figure 3.12G). These results suggest that the competitive disadvantage conferred by Foxp1-deficiency in Treg cells is rescued through restoration of IL-2 signaling in these cells. IL-2 signaling is critical for maintenance of Treg cell suppressive function and for competitive fitness of Treg cells [135], both of which are impaired in the context of Foxp1 deficiency, suggesting that a major functional consequence of Foxp1 loss in Treg cells may be dysregulation of Il2r-α expression.

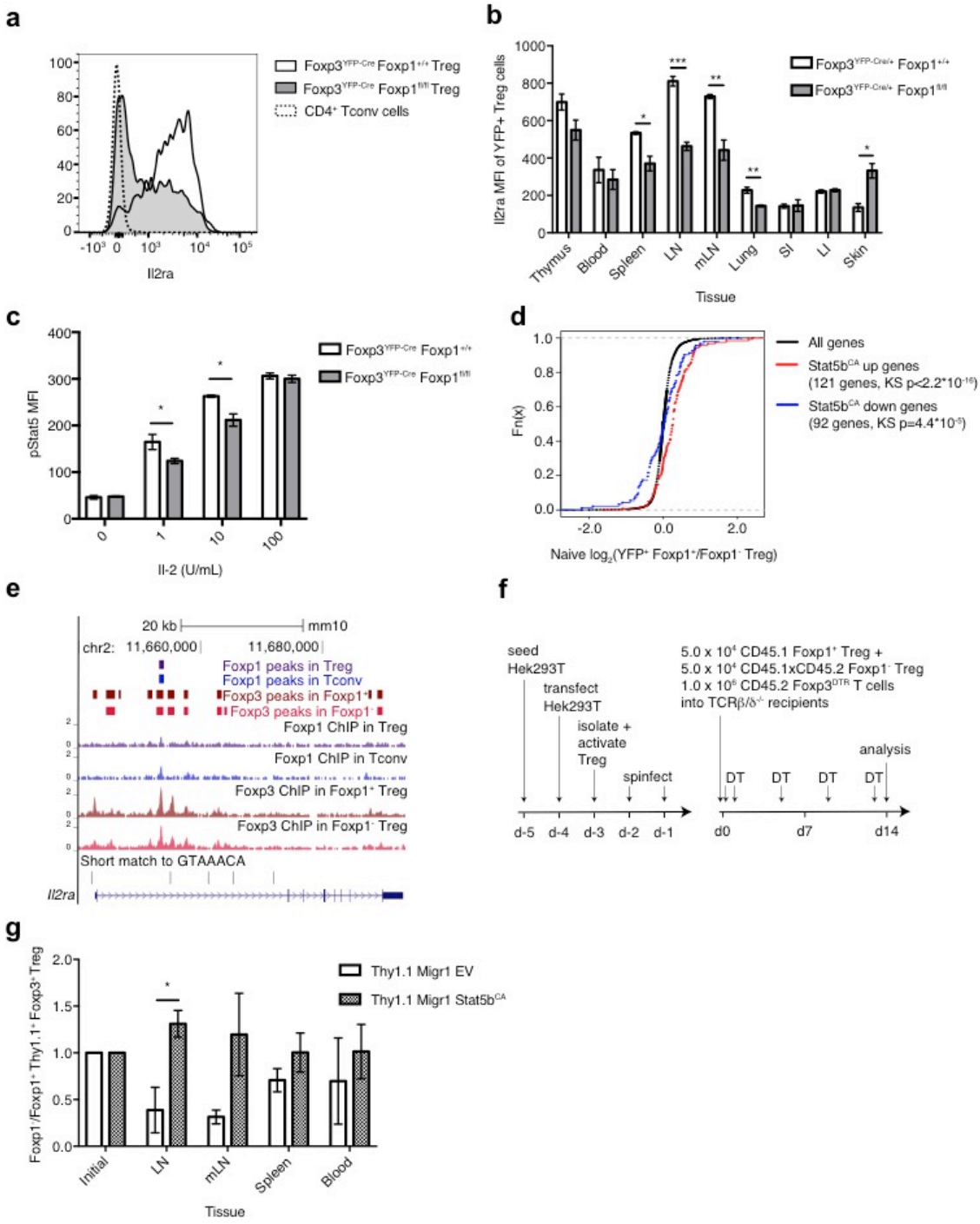

Figure 3.12. IL-2 Signaling is Impaired in Foxp1 Deficient Treg Cells and is Rescued by Constitutive Stat5 Activation *In Vivo.*

(Figure description continued on next page)

Figure 3.12 – (continued)

(A) Representative histograms of IL2r-α protein level in naive Foxp1^{+} and Foxp1^{-} Treg cells and in naive Tconv cells. (B) Summary plot of IL2r-α MFI in YFP^{+} Treg cells from heterozygous females (n=3, representative of 3 independent experiments). (C) IL-2 responsiveness of Foxp1^{+} or Foxp1^{-} sorted Treg cells assessed by pStat5 MFI (n=3, representative of 3 independent experiments). (D) Cumulative distribution plot showing expression of *Stat5b*^{CA} signature genes in naive Foxp1^{+}/Foxp1^{-} Treg cells.(E) Foxp3 and Foxp1 ChIP-seq tracks at the *Il2ra* locus. (F) Schematic of adoptive co-transfer experiment. (G) Ratio of Foxp1^{+}/Foxp1^{-} Treg cells transduced with either control Thy1.1^{+} Migr1 vector or Thy1.1^{+} *Stat5b*^{CA} Migr1 vector and adoptively transferred into TCRβδ$^{-/-}$ mice with *Foxp3*^{DTR} CD4^{+} T cells (n=3 for experimental group, n=2 for control group, representative of 2 independent experiments). Error bars represent SEM; $^{*}p < 0.05$; $^{**}p < 0.01$, $^{***}p < 0.001$, ns non-significant (unpaired two-tailed Student's t test).

DISCUSSION

In Treg cells, Foxp3 is known to bind DNA through a network of cofactors. Foxp3 binding sites have been shown to be significantly enriched for canonical Ets, Runx, C-not and Forkhead motifs and Foxp3 is found in large 400-800 kDa multiprotein complexes[77, 80]. Mass-spectrometric analyses have identified over 350 proteins associated with Foxp3, 30% of which are transcription factors[80]. Foxp3 directly binds a large proportion of the genes encoding its cofactors, as demonstrated by ChIP-seq studies in primary Treg cells [77].

Here, we assessed the role of one of Foxp3's known binding partners, Foxp1, in Treg cell phenotype and function. Foxp1 ChIP-seq in primary Treg and Tconv cells revealed that Foxp1 bound a subset of Foxp3 targets and bound very few loci that were not Foxp3 targets. Foxp1 binding in Treg cells and Tconv cells was highly overlapping and was predominantly found at promoter regions of target loci. These data suggested that some Foxp3 protein complexes in Treg cells contain Foxp1 while others do not. It was also possible that Foxp1 binding and Foxp3 binding to some or all of their shared target loci occurred independently, as Foxp1 binding did occur in Foxp3 deficient Tconv cells and Foxp3 binding to these shared loci was not preferentially abrogated in the absence of Foxp1.

These studies enabled us to uncover a subset of Foxp3 targets that were not bound by Foxp1, which were characterized by increased chromatin accessibility in activated T cells and were specifically enriched for canonical Runx motifs, but not Forkhead motifs, providing further evidence for the idea that Foxp3 may be present in distinct protein complexes with different regulatory functions. Previous work characterizing CBF-β and Runx1 in Treg cells found that their expression is required for maintenance of Foxp3 mRNA and protein expression in Treg cells, but is largely dispensable for the expression of Foxp3 target genes and Treg cell suppressor

function [129]. CBF-β deficiency in Treg cells has no effect on expression of Il2r-α or Ctla-4 but does lead to increased proportions of $Gitr^{hi}$, $Icos^{hi}$, Ki-67^{+} cells, indicative of activation [129].

Despite the fact that Foxp1 was bound only to a subset of Foxp3 bound sites, Foxp1 loss resulted in a redistribution of Foxp3 occupancy genome-wide with an overall reduction in binding (Figure 3.13). Foxp1 therefore somehow functions to maintain Foxp3 occupancy at its target genes, most likely by binding to a subset of its targets, enabling Foxp3 to bind elsewhere. Whether Foxp1 presence in Foxp3 protein complexes causes recruitment of distinct cofactors and differential gene regulation remains an open question. Comparing expression of genes associated with shared Foxp1 and Foxp3 peaks in Foxp1 deficient and sufficient Treg cells to attempt to understand whether these proteins may recruit distinct cofactors that contribute to target gene activation or repression was confounded by the fact that Foxp1 deficiency led to reduced Foxp3 ChIP signal at these loci.

In contrast to Runx1/CBF-β deficiency, Foxp1 deficient Treg cells had dysregulated expression of certain Foxp3 target genes that are part of the core Treg cell signature including *Ctla4* and *Il2ra* and were impaired functionally, providing further evidence that Runx1 and Foxp1 are involved in distinct Foxp3 transcriptional regulation programs. Unlike Foxp1 loss in $CD4^{+}$ and $CD8^{+}$ T cells, which causes a cell-intrinsic loss of quiescence due in part to derepression of *Il7ra* by Foxp1, Foxp1-deficient Treg cells did not become more activated in a cell-intrinsic manner and did not express IL7r-α. Treg cell activation in the context of Foxp1 deficiency appeared to be in response to $CD4^{+}$ and $CD8^{+}$ activation, which was likely caused by the impaired suppressor function of Foxp1-deficient Treg cells. Cell-intrinsic effects of Foxp1

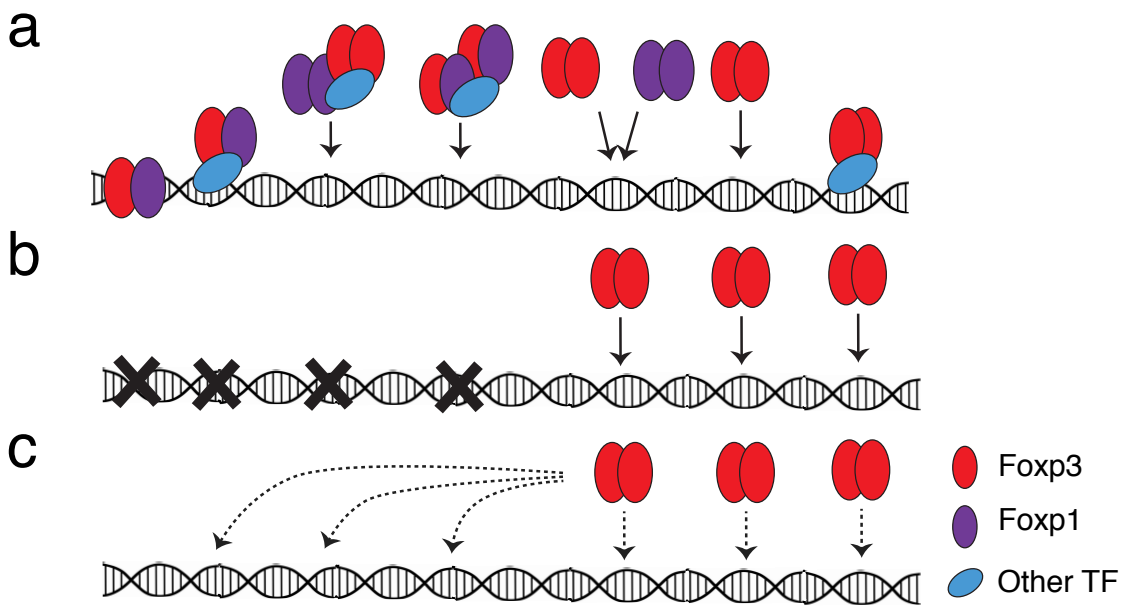

Figure 3.13. Foxp1 Presence in Treg Cells Enables Foxp3 Binding to Additional Sites Genome-wide.

(A) Foxp3 and Foxp1 bind to DNA as heterodimers, homodimers, and as hetero- or homodimers present in the same large supramolecular complexes. (B) In the context of Foxp1 deficiency, Foxp3 binding to sites bound by both Foxp3 and Foxp1 might be reduced if Foxp1 were required for Foxp3 binding. (C) Conversely, Foxp3 binding might be reduced genome-wide if Foxp1 were not required for Foxp3 binding to shared sites. Our data provide support for the second model.

deficiency in Treg cells include increased apoptosis, decreased Ctla-4 and Il2r-α expression and increased Satb1 expression. It remains unclear to what extent Foxp1-mediated regulation of expression of these and other Foxp3 target genes is due to direct DNA binding and regulation of gene expression by Foxp1 and how much is due to indirect regulation. Foxp1 loss in Treg cells leads to both a reduction of Foxp3 expression and an increase of Satb1 expression. Both of these transcription factors have been shown to directly bind and regulate an enormous number of genes in Treg cells and thymocytes, respectively, including one another [77, 131, 132]. This complexity makes it very challenging to tease apart the precise role of Foxp1 in Treg cells.

Though Foxp1 and Foxp3 are highly conserved, they have significant sequence divergence, with very different N-terminal sequences. Foxp3 is also truncated at the C-terminus relative to Foxp1 [57]. These differences may account for differences in cofactor binding between these two proteins and may explain their very distinct functions in T cell development and function. For example, Co-IP experiments revealed that Foxp3 binds to Runx1 more than Foxp1 does (Figure 3.3), though the exact protein domains required for this interaction are not known. Foxp3 binding to Gata-3, NF-κβ, Ets family proteins and other proteins has been fairly well studied, while the cofactors present in Foxp1 transcription factor complexes in T cells are relatively unknown. De novo motif discovery using Homer revealed strong enrichment of the Ets and Sp1 consensus sequences in Foxp1 bound DNA sequences (Figure 3.2), leading us to predict that Foxp1 may interact with these proteins *in vivo* in T cells.

CHAPTER 4: CONCLUSION

The immune system protects against disease by identifying and killing foreign pathogens. It is comprised of multiple cell types that develop in the bone marrow or thymus and then survey the body by circulating through the vascular system or by establishing residence in tissues. The immune system detects a wide variety of agents and it is critical that it distinguishes them from the organism's own healthy cells and tissues. Treg cells are a subset of T cells that are incredibly important because of their ability to suppress the induction and proliferation of effector T cells. Treg cells maintain tolerance to self-antigens through suppression of autoreactive effector T cells, thereby preventing autoimmune disease. Treg cells also maintain immune homeostasis at barrier sites, where foreign antigen is prevalent.

In solid tumors, Treg cells suppress local inflammation, impairing effective anti-tumor responses. Their presence is associated with worse prognosis in ovarian cancer, pancreatic ductal cancer, lung cancer, glioblastoma, non-Hodgkin's lymphoma, melanoma, breast cancer and others. In this thesis, we showed that Treg cells are recruited to and accumulate in breast tumors. Treg cells found in breast tumors are transcriptionally similar to normal breast parenchyma Treg cells though they exhibit a slightly more activated phenotype and express certain chemokine and cytokine receptors more highly population-wide. The most striking difference we identified between tumor and tissue Treg cells is that tumor-associated Treg cells express high levels of the G-protein coupled receptor CCR8. This receptor acts as a functional receptor for CCL1 and CCL18 produced by myeloid cells in breast tumors and it can be induced by interferon or TCR signaling. CCR8 likely marks a highly activated and highly suppressive population of Treg cells whose depletion may lead to an improved anti-tumor immune response.

Treg cells require the X-linked transcription factor Foxp3 for their development, stability and function, and loss of Foxp3 expression, either through genetic manipulation in mice or through mutations in the gene locus in IPEX patients or scurfy mice results in severe

autoimmunity whose direct cause is a lack of Treg cells. One of the ways in which Treg cells suppress effector T cells is by sequestering the IL-2 produced by effector T cells and initiating transcriptional programs in response to IL-2 signaling that result in expression of anti-inflammatory cytokines and upregulation of inhibitory receptors.

Treg cells express the transcription factor Foxp1 that forms heterodimers with Foxp3. Loss of Foxp1 in Treg cells results in a redistribution of Foxp3 occupancy genome-wide, and an impairment in Treg cell stability and function. Foxp3 binding to the *Il2ra* locus is reduced in Foxp1 deficient Treg cells and these cells express lower levels of the IL-2 receptor on their cell surface. They are less responsive to IL-2 *in vitro* and are severely outcompeted by Foxp1 sufficient Treg cells *in vivo*. A constitutively active form of Stat5 that bypasses the need for IL-2 signaling is able to rescue this competitive disadvantage. Foxp1 deficiency in Treg cells leads to their activation and a concomitant activation of effector T cells, leading to mild autoimmunity.

Deepening our understanding of regulatory T cell gene regulation, phenotype and function in the contexts of cancer and autoimmunity will enable development of therapies to modulate the function and localization of these cells. While regulatory T cells are required to prevent autoimmunity, they are detrimental in solid tumors. From this thesis work, we have learned that CCR8 expressing Treg cells are found in human breast tumors and are highly activated and suppressive. We have also learned that Foxp1 is a transcription factor that binds to many Foxp3-bound sites, thereby enabling Foxp3 to bind to additional sites genome-wide and regulate expression of functionally critical genes, such as *Il2ra*.

CHAPTER 5: MATERIALS AND METHODS

Human Samples

Samples were collected from 105 adult treatment-naive women undergoing surgery for primary breast cancer after informed consent and approval from the Institutional Review Board (IRB) at MSKCC. The clinical characteristics of the patients are shown in Table 2.1. NBP was obtained from patients undergoing contralateral prophylactic mastectomies. Peripheral blood mononuclear cells (PBMCs) were obtained from patients prior to their surgical procedures and from buffy coats obtained from the New York Blood Center (NYBC).

Mice

The Foxp1 conditional targeting construct was designed to use 2 site-specific recombinations in vivo: (1) Flp recombinase to delete the neo marker from the mouse germline, and (2) Cre recombinase to conditionally delete *Foxp1* exon 11 flanked by 2 *lox*P sites. $Foxp1^{f/+}$ mice (C57Bl/6/129 mixed background) were backcrossed with C57BL/6 mice for at least 5 generations. Genotypes of $Foxp1^{fl/+}$, $Foxp1^{f/f}$ mice were determined by polymerase chain reaction (PCR) amplification. The wild-type allele was identified by the production of a 376–base pair PCR product and mutated *Foxp1* allele was identified by the production of a 257–base pair PCR product (Table 4.1). $Foxp1^{f/f}$ mice were crossed with $Foxp3^{YFP\text{-}Cre}$ transgenic mice to generate $Foxp3^{YFP\text{-}Cre/+}Foxp1^{fl/+}$ female mice. These mice were bred to $Foxp3^{+}Foxp1^{fl/+}$ male mice. $Foxp3^{YFP\text{-}Cre/+}Foxp1^{f/f}$ and $Foxp3^{YFP\text{-}Cre/+}Foxp1^{+/+}$ female offspring and $Foxp3^{YFP\text{-}Cre}Foxp1^{f/f}$ and $Foxp3^{YFP\text{-}Cre}Foxp1^{+/+}$ male offspring were used in experiments. In mammary tumor experiments, $Foxp3^{YFP\text{-}Cre/YFP\text{-}Cre}Foxp1^{f/f}$ mice were used as experimental mice and $Foxp3^{YFP\text{-}Cre/+}Foxp1^{f/f}$ mice were used as control mice. $Foxp1^{f/f}$ mice were crossed with $CD4^{Cre}$ transgenic mice to generate $CD4^{Cre}Foxp1^{fl/+}$ mice. These mice were crossed to generate $CD4^{Cre}Foxp1^{f/f}$ experimental and

Table 4.1. Genotyping Primer Sequences.

Gene	Forward Primer	Reverse Primer	Figure
Foxp1 fl	GGCAGTGATTCAGCCCTCTG	GGAACCCATAGGTGTAGAATCTG	S3
Foxp3 YFP-Cre	AGGATGTGAGGGACTACCTCCTGTA	TCCTTCACTCTGATTCTGGCAATTT	S3
Foxp3 WT	CCTAGCCCCTAGTTCCAACC	AAGGTTCCAGTGCTGTTGCT	S3
CD4 Cre	CGATGCAACGAGGATGAGG	GCATTGCTGTCACTTGGTCCT	S4

CD4^{Cre}*Foxp1*$^{+/+}$ control mice. *TCRβδ*$^{-/-}$ mice and C57Bl/6 *Ly5.1* mice were purchased from Jackson Laboratories and bred in-house.

Tissue Lymphocyte Isolation

Lymphocytes form tumor and normal tissues were isolated by mincing the freshly obtained surgical specimens and subsequent enzymatic digestion using Liberase TL (Sigma) for 20 min at 37°C. After passing through a 100-μm filter cells were washed twice with PBS prior to staining. PBMC were first enriched for CD4 T cells through negative selection with RosetteSep antibody cocktails (Stem Cell Technologies). For lymphocyte isolation from lung, mice were perfused with PBS and tissues were digested with collagenase A (1mg/ml) and Dnase I (1 unit/ml) for 45 minutes at 37 degrees. For isolation of lamina propria lymphocytes, small and large intestines were first incubated with 1mM EDTA and 1mM DTT in PBS for 15 minutes at 37 degrees. Samples were washed and incubated with collagenase A and Dnase I for 40 min at 37 degrees. Digested cell suspensions were filtered and lymphocyte-containing fractions were isolated using differential Percoll centrifugation.

Flow Cytometry

Single cell suspensions of cells were prepared from spleens, pooled axillary, brachial and inguinal lymph nodes, mesenteric lymph nodes, lungs, and large and small intestines. For exclusion of dead cells, samples were first stained with Ghost Dye (Tonbo) cell viability reagent for 10 min in PBS on ice. Cells were then stained for 30 min on ice in FACS buffer (PBS, 2% FBS, 2 mM EDTA) with antibodies against cell surface proteins. Cells were washed and fixed with Fix/Perm buffer (BD Biosciences) for 20 min on ice or with Foxp3 staining buffer (eBioscience) for 45 min on ice, washed and stained with antibodies against intracellular proteins. Human lymphocytes were stained at 1×10^6 cells per ml for 20 min. For downstream in vitro assays, cells were sorted into fetal bovine serum (FBS). All antibodies were purchased from eBioscience or BioLegend.

Stained cells were either analyzed on a LSRII flow cytometer (BD) or sorted using a FACSAria II (BD). Flow cytometry data were analyzed with FlowJo software (TreeStar).

In Vitro Assays with Human Cells

For in vitro suppression assays, naive $CD4^+$ T cells were isolated from PBMC using the human naive $CD4^+$ T cell isolation kit II (Miltenyi) and cultured with graded numbers of $CD4^+CD25^{hi}$ T_{reg} cells flow cytometry-sorted from breast tumors on 96-well round-bottom plates pre-coated with CD3 and CD28 antibodies in RPMI1640 supplemented with 10% FBS, 2 mM L-glutamine, 1 mM sodium pyruvate, 10 mM HEPES, 2×10^{-5} M 2-mercaptoethanol, 100 U ml^{-1} penicillin, and 100 mg ml^{-1} streptomycin for 80 hr. Proliferation of T cells was assessed by ^{3}H-thymidine incorporation during the final 8 h of culture. For in vitro migration assays, $CD4^+$ T cells were flow cytometry-sorted from breast tumors and resuspended in serum-free RPMI1640 supplemented with 0.1% bovine serum albumin (BSA) and plated on 8 μM Transwell inserts (Corning) placed in 24-well plates containing RPMI1640 containing 0.1% BSA alone or containing RPMI1640 with 0.1% BSA and with either CCL19 as a positive control (100 ng/mL) or CCL1 (1, 10, 100, or 1,000 ng/mL) added. Migration of T cells was assessed by flow cytometry-based staining and cell counting of $CD4^+Foxp3^+$ Treg cells and $CD4^+Foxp3^-$ Tconv cells that had passed through the Transwell after 3 hr of culture at 37°C for 3 hr. Chemotactic index was calculated as number of migrated cells in the given condition normalized to number of migrated cells in the RPMI1640 with 0.1% BSA alone condition. For in vitro induction assays, CD4+ CD25hi Treg cells were isolated from PBMC and cultured in 24- well flat-bottom plates in presence of CD3 and CD28 antibody-coated beads at a 1:1 bead:cell ratio in RPMI1640 supplemented as above. For induction of CCR8 by tumor and NBP slices, 0.4 μM Transwell inserts were placed in each well and thin tumor or NBP slices were laid onto the Transwell surface (Corning). After 120 hr, CCR8 expression was assessed by qPCR as described in Supplemental Experimental Procedures. For induction of CCR8 cells were cultured in 96-well U

bottom plates without or with 1000U/mL recombinant human IFN-α (R&D Systems) and CCR8 expression was assessed by flow cytometry. Quantitative RT-PCR RNA was isolated using the RNeasy Micro Kit (Qiagen) according to the manufacturer's instructions. The isolated RNA was used to synthesize cDNA with the qScript cDNA SuperMix (Quanta-bio). SYBR Green PCR Master Mix (Life Technologies) was used for quantitative RTPCR. PCRs were performed in triplicate (Table 4.2).

***Ex Vivo* Stimulation**

To measure T cell production of cytokines, single cell suspensions were prepared from spleens, lymph nodes and mesenteric lymph nodes and cells were plated at 1 x 10^6 cells in complete RPMI in round-bottom 96 well plates and treated with PMA (50 ng/ml; Sigma) and ionomycin (1 nM; Calbiochem) for 3 h in the presence of GolgiPlug (brefeldin A) and GolgiStop (monensin; BD Biosciences).

***Ex Vivo* IL-2 Responsiveness**

To measure Treg cell responsiveness to IL-2, $CD62L^+$ naïve Treg cells were isolated from lymphoid organs and plated at 1 x 10^5 cells in complete RPMI in round-bottom 96 well plates and treated with IL-2 for 15min at 37 degrees. Cells were prepared for flow cytometric analysis according to the BD Phosflow protocol for mouse splenocytes (BD Biosciences). Cells were stained with anti-Stat5(pY694) (BD Biosciences).

***Ex Vivo* Apoptosis**

To measure T cell apoptosis, single cell suspensions were prepared from spleens, lymph nodes and mesenteric lymph nodes and 1 x 10^6 cells were stained with Annexin V and 7-AAD in Annexin V Binding Buffer (BD Biosciences).

Table 4.2. Primer Sequences for CCR8 and Ligand Quantitative RT-PCR.

Gene	Forward Primer	Reverse Primer
Ccr8	GGGCTTGAGAAGATATCAGGG	TCCAGAACAAAGGCTGTCACT
Ccl1	TTAAGCCCTCATTGGAGCAG	AGATGTGGACAGCAAGAGCA
Ccl18	GTGGAATCTGCCAGGAGGTA	TCCTTGTCCTCGTCTGCA
Rp2	CCCATTAAACTCCAAGGCAA	AAGCTGAGGATGCTCAAAGG
Adar	GGTGGCCTTTTGGAGTACG	CCAACTTTTGCTTGGTAAACG

CellTrace Labeling and Cell Culture

YFP+ Treg cells or CD62L+CD4+ cells were sorted from pooled spleens and lymph nodes of *Foxp3*$^{YFP\text{-}Cre}$*Foxp1*$^{+/+}$, *Foxp3*$^{YFP\text{-}Cre}$*Foxp1*$^{f/f}$, and *CD4*^{Cre}*Foxp1*$^{f/f}$ mice, washed twice with PBS and incubated for 10 min at 37 °C at a density of 1 × 107 cells per ml in PBS with 1 μM CellTrace Violet (Invitrogen), then washed with complete RPMI. CellTrace-labeled cells were cultured for 7 d with or without recombinant mouse IL-7 (3 ng/ml; R&D systems) in complete RPMI. CellTrace profiles, cell viability and maintenance of CD4 or Foxp3 expression were assessed on d7 by flow cytometry.

Treg Cell Transduction

Treg cells were isolated from *Foxp3*$^{YFP\text{-}Cre}$*Foxp1*$^{f/f}$ or *Foxp3*$^{YFP\text{-}Cre}$*Foxp1*$^{+/+}$ mice and seeded in 0.5ml complete DMEM (2 x 10^6) with CD3/CD28 coated beads and 500U/mL hIL-2. Cells were infected 24h and 48h after activation with *Stat5b*^{CA}-*Thy1.1*-Migr1 vector containing virus or *Thy1.1*-Migr1 control vector containing virus in 4ug/mL Polybrene. Infection was performed at 2500 RPM at 37 degrees for 1.5h and media was changed to complete RPMI with 500U hIL-2. Transduction efficiency was assessed 24h after second infection.

Adoptive Transfer

For adoptive transfer experiments, 5 × 10^4 Stat5b^{CA}-Migr1 transduced *Foxp3*$^{YFP\text{-}Cre}$*Foxp1*$^{f/f}$*Ly5.1x2* and *Foxp3*$^{YFP\text{-}Cre}$*Foxp1*$^{+/+}$*Ly5.1* Treg cell populations or 5 × 10^4 EV-Migr1 transduced *Foxp3*$^{YFP\text{-}Cre}$*Foxp1*$^{f/f}$*Ly5.1x2* and *Foxp3*$^{YFP\text{-}Cre}$*Foxp1*$^{+/+}$*Ly5.1* Treg cell populations were transferred together with 1 × 10^6 CD4 T cells isolated from *Foxp3*$^{GFP\text{-}DTR}$*Ly5.2* mice into TCRβδ$^{-/-}$ recipients. Recipients were treated with DT on d0, d1 and every 4 days post-transfer for the duration of the experiment. Treg cell ratios in lymphoid organs were analyzed 2 weeks after adoptive transfer.

In Vivo Suppression Assay

CD4 T cells (4×10^5) isolated from *Foxp3*$^{GFP\text{-}DTR}$*Ly5.1* were transferred together with YFP$^+$ Treg cells (1×10^5) isolated from *Foxp3*$^{YFP\text{-}Cre}$*Foxp1*$^{f/f}$ or *Foxp3*$^{YFP\text{-}Cre}$*Foxp1*$^{+/+}$ mice into *TCRβδ*$^{-/-}$ recipients. Recipients were treated with DT on d0, d1 and every 4 days post-transfer for the duration of the experiment. Weight was monitored throughout the experiment. Treg cell frequencies in lymphoid and non-lymphoid tissues were analyzed at the experimental endpoint.

RNA Sequencing

For human samples, definitions used for cell sorting were for conventional CD4$^+$ T cells: CD45$^+$CD3$^+$CD4$^+$CD8$^-$CD25$^-$; for Treg cells: CD45$^+$CD3$^+$CD4$^+$CD8$^-$CD127$^-$CD25^{high}. Tissue Treg cells were largely of an activated phenotype and for a fair comparison to their peripheral blood counterparts activated Treg cells were defined as CD45$^+$CD3$^+$CD4$^+$CD8$^-$CD45RO$^+$ CD127$^-$CD25^{high}, while resting Treg cells were defined as CD45$^+$CD3$^+$CD4$^+$CD8$^-$CD45RA$^+$ CD127$^-$CD25^{high}. Post sort purity was routinely > 95% pure for the sorted populations. For RNA sequencing, cells were sorted directly into Trizol LS (ThermoFisher) and stored at −80°C prior to RNA extraction. For mouse samples, CD44$^+$ or CD62L$^+$ YFP$^+$ Foxp1$^+$ or Foxp1$^-$ Treg cell populations were FACS-sorted from *Foxp3*$^{YFP\text{-}Cre/+}$*Foxp1*$^{+/+}$ and *Foxp3*$^{YFP\text{-}Cre/+}$*Foxp1*$^{f/f}$ mice directly into Trizol-LS (ThermoFisher) and volume was adjusted post-sort. Samples were stored at −80°C prior to RNA extraction. Total RNA was extracted and assessed for nucleic acid quantity and quality on the Agilent BioAnalyzer. For the first set of human tumor Treg, Tconv and PBMC Treg and Tconv samples, after SMARTer amplification, total RNA was used for poly(A) selection and was used to create Ion Torrent compatible libraries using the Ion ChIP-Seq Kit starting with the end-repair process (Life Technologies), with 12 to 16 cycles of PCR. The resulting barcoded samples were loaded onto template-positive Ion PI™ Ion Sphere™ Particles using the Ion One Touch system II and Ion PI™Template OT2 200kit v2 Kit (Life Technologies).

Enriched particles were sequenced on a Proton sequencing system using the 200bp version 2 chemistry. On average of 70 to 80 million single-end reads were generated per sample. For the second set of human tumor Treg, Tconv and PBMC Treg and Tconv samples, and for all mouse samples, SMARTer amplification with 12-16 cycles of PCR was followed by Illumina TruSeq paired-end library preparation following manufacturer's protocols. Samples were sequenced on the Illumina HiSeq 2500 to an average depth of 20 million 50-bp read pairs per sample.

Chromatin Immunoprecipitation and Sequencing

FACS-sorted cell populations ($2x10^6$ cells for Foxp3-ChIP-seq; $6x10^6$ cells for Foxp1-ChIP-seq) were crosslinked in 1% paraformaldehyde I PBS for 10 minutes at RT. The reaction was quenched by addition of 125mM glycine. Crosslinked cells were lysed and digested nuclei were resuspended in nuclear lysis buffer containing 1% SDS. Cells were sonicated for three rounds of 10x30s with a Bioruptor (Diagenode) on high setting. Following sonication, chromatin was diluted with nuclear lysis buffer to final SDS concentration of 0.1% and pre-cleared for 1h at 4 degrees with rotation with protein A/G magnetic beads (Pierce). 5% of pre-cleared DNA was saved as input. Chromatin was incubated overnight at 4 degrees with rotation with polyclonal antibodies against Foxp3 (Rudensky lab), Foxp1 (EMD Millipore ABE68) or Runx1 (Thermoscientific). Immunocomplexes were incubated with protein A/G magnetic beads for 1h at 4 degrees with rotation. Immunocomplexes were precipitated and washed. After washing, precipitated chromatin and input DNA was decrosslinked overnight at 65 degrees in the presence of proteinase K and DNA fragments were isolated using Qiagen PCR-purification kit. Purified DNA was processed for sequencing on Illumina Hiseq 2500 to an average depth of 30 million 50-bp read pairs per sample. Runx1 ChIP samples were analyzed by q-PCR (Table 4.3)

Nuclear Complex Co-IP

Nuclear complex Co-IP was performed using the Nuclear Complex Co-IP kit (Active Motif). Foxp3-transduced EL4 cell nuclear extracts were prepared according to manufacturer's instructions. 250 ug aliquots of extract were diluted to 500uL in high stringency IP buffer supplemented with NaCl to a final concentration of 150 mM and with 1% detergent. Extracts were pre-cleared for 1h at 4 degrees with rotation with protein A/G magnetic beads. 5% of pre-cleared extract was saved as input. Pre-cleared extracts were incubated with anti-Runx1 (Thermo Scientific, PA5-19638), anti-Foxp1 (CST, D35D10) or anti-Foxp3 (Rudensky lab) overnight at 4 degrees with rotation. Immunocomplexes were incubated with protein A/G magnetic beads for 1h at 4 degrees with rotation. Immunocomplexes were precipitated and washed. Washed beads were boiled in reducing buffer containing SDS for 5 min at 95 degrees. Samples were run on an SDS-Page gel and transferred onto PVDF membrane. Membrane was blocked with 5% milk in TBS-T, incubated with anti-Foxp1 (CST, D35D10), anti-Foxp3 (eBioscience, FJK-16s) and anti-Runx1 (Abcam, 4E7), incubated with appropriate HRP-conjugated secondary antibodies and analyzed.

Statistical Analysis

All statistical analyses (excluding RNA-seq and ChIP-seq analyses) were performed using Prism 7 (GraphPad Software). Differences between individual groups were analyzed for statistical significance using unpaired two-tailed Student's t tests. *, $P \leq 0.05$; **, $P \leq 0.01$; ***, $P \leq 0.001$; ****, $P \leq 0.0001$. Error bars show SEM. For TCGA, whole-tumor and patient-matched NBP gene-expression comparisons, a two-tailed paired Student's t test was used.

Table 4.3. Runx1 ChIP-qPCR Primer Sequences.

Gene	Forward Primer	Reverse Primer
Ikzf2	GCCAGGAAACCATAGCAGTCT	GTGTGCCTGCTGTAGGTAGG
Foxp3 CNS2	GCCAGATGGACGTCACCTAC	CCACAGGTTTCGTTCCGAGA
Il2ra	TCCGTTTCTAAGATTTGAGGGGAA	GGTTGGGCTGCCTGTCTTTT
Rora	CTGATGTCTCCTACCGCAGA	CTGGCACTTCCTGGGTGTAAA
Atf7ip	AACCCTGTTTTTACCGGTTCG	ACTTGTACATCCTTTTCTTGTCCT
Itk	AACATCTGGCTGTTTGTGTTGG	GCTCTGCCAGACCTGACTATG
Lcp2	TTATGAACCCCCAGAGCTGTC	CTGCTGTAGCCAGATCCCCA

Bioinformatic Analyses – Human Samples

RNA-seq

Read alignment and processing followed the method described by Anders et al [136]. Briefly, raw reads were trimmed using Trimmomatic v0.32 with standard settings to remove low-quality reads and adaptor contamination [137]. The trimmed reads were then aligned to the human genome (Ensembl assembly GRCh38) using TopHat2 v2.0.11 implementing Bowtie2 v2.2.2 with default settings [138, 139]. Read alignments were sorted with SAMtools v0.1.19 before being counted to genomic features using HTSeq v0.6.1p1 [136, 140].

Differential gene expression was analyzed using DESeq2 1.12.3 in R version 3.3.1 [141]. Significantly up- and down-regulated genes in all comparisons were defined as expressed genes (threshold of 50 normalized reads) with FDR-adjusted p-value ≤ 0.01 and fold change of at least 2x. To determine transcriptional signatures, the GOrilla tool for discovery of enriched GO terms in ranked gene lists was used [142]. The target gene set was defined as significantly up-regulated expressed genes with FDR adjusted p-value ≤ 0.05 and was compared against a background set of genes defined as genes with average expression across all samples of at least 20 normalized reads.

TCR alpha and beta CDR3 repertoires were extracted from RNA-Seq data using MiXCR software [102] in RNA-Seq mode. Comparative post-analysis of TCR repertoires was performed using VDJtools software [103].

Bioinformatic Analyses – Mouse Samples

Genome

Mouse genome assembly mm10.GRCm38 was used for read alignments. Gene annotations from Ensembl (Mus_musculus.GRCm38.83) were used for all analysis. Unless otherwise noted, all analysis was done using R v3.4.0 (2017-04-21).

RNA-seq

Reads were aligned to the mouse genome using HISAT2 v2.0.1-beta [143] with default parameters including splice sites obtained from gene annotations. Uniquely aligned reads were extracted using grep with parameters "-v 'NH:i:[2-9]'" and SAMtools v1.2 [140] with parameters "view -h -F 4 -q 20 -b" and sorted and indexed using SAMtools.

For analysis of RNA-seq in naïve or activated Foxp1^{+} or Foxp1^{-} Treg samples, reads aligned to genes were counted using Rsubread v1.22.3 [144] in R v3.3.0 (2016-05-03). Read counting for RNA-seq in naïve and activated Tconv and Treg cells was done using R version 3.4.0, Rsubread v1.26.0.

Differential gene expression between any pair of cell states was assessed using DESeq2 v1.16.1 [141], using default FDR adjustment of p-values for multiple hypothesis testing.

ChIP-seq

Transcription factor ChIP-seq datasets for Foxp3 and Foxp1 were generated for Foxp1^{+} and Foxp1^{-} Treg and Foxp1^{+} naïve Tconv cells (described in "Chromatin Immunoprecipitation and Sequencing" section).

Reads were aligned to the mouse genome using Bowtie2 v2.2.5 [139] with parameters "--no-unal -X 500 --no-mixed --no-discordant". Uniquely aligned reads were extracted using SAMtools v1.3.1 with parameters "view -h -bS -F 4 -q 20" and sorted and indexted using SAMtools.

For peak calling, MACS2 v2.1.1.20160309 [145] was used with parameters "-f BAM -B --SPMR -g mm -p 0.1 --keep-dup 'auto' --call-summits". For Foxp1, pooled Foxp1$^+$ Treg and Foxp1$^+$ Tconv ChIP-seq samples were used, with Foxp1$^-$ Treg samples as control, to obtain a list of 55265 putative peaks on standard chromosomes (chr1-chr19, chrX, chrY, chrM), with multiple summits per peak. ChIP-seq fragment length was estimated by MACS2 as 198bp. To obtain peaks with significant coverage in Treg, ChIP-seq reads from each Foxp1$^+$ Treg sample and from pooled control samples were counted in putative peaks using Rsubread v1.26.0, and DESeq2 v1.16.1 was applied to these counts, with FDR adjustment of p-values for multiple hypothesis testing. To estimate sample size factors, DESeq2 was applied to read counts from the same samples in flanking regions of putative peaks, defined by shifting the putative peaks by 2Kb upstream and by 2Kb downstream and taking only those flanking regions that do not overlap with the original putative peaks. This resulted in 3071 Foxp1 peaks in Treg at MACS2 q-value < 0.05 and DESeq2 FDR < 0.01 that contained 4619 summits. The same procedure was applied to each Foxp1$^+$ Tconv sample and pooled control samples and resulted in 1088 Foxp1 peaks in Tconv.

The same procedure for peak calling was applied to pooled Foxp3 ChIP-seq samples from Foxp1$^+$ and Foxp1$^-$ Treg, using Foxp3 ChIP-seq in Foxp1$^+$ and Foxp1$^-$ naïve Tconv cells as controls. This resulted in 141556 putative Foxp3 peaks on standard chromosomes, with estimated ChIP-seq fragment length also 198bp. The same procedure for significant ChIP-seq coverage assessment was applied to each Foxp3 ChIP-seq sample in Foxp1$^+$ Treg cells and pooled control samples. This resulted in 7174 Foxp3 peaks in Foxp1$^+$ Treg at MACS2 q-value < 0.05 and DESeq2 FDR < 0.01 that contained 13997 summits. The same procedure applied to each Foxp3 ChIP-seq sample in Foxp1$^-$ Treg cells and pooled control samples resulted in 3935 Foxp3 peaks in Foxp1$^-$ Treg.

Foxp3-only peaks were defined as those of 7174 Foxp3 peaks in Foxp1$^+$ Treg that did not overlap with any of 55265 putative Foxp1 peaks. This resulted in 1101 Foxp3-only peaks that contained 1956 summits. Foxp1-only peaks were defined as those of 3071 Foxp1 peaks in Treg that did not

overlap with any of 141556 putative Foxp3 peaks. This resulted in 54 Foxp1-only peaks that contained 66 summits.

Each peak was associated with the closest gene according to distance in genomic coordinates, if this distance was not more than 20Kb. Peaks within 2Kb from a transcription start site of any annotated transcript were classified as promoter peaks; the remaining peaks were classified as exonic if overlapping with any exon of any annotated transcript; the remaining peaks were classified as intronic if within a gene body of any annotated gene; the remaining peaks within 20Kb of a gene were classified as intergenic; all the remaining peaks were left unclassified in this classification.

Sequence motifs in 150bp windows around peak summits were identified with HOMER, using script findMotifsGenome.pl with parameters “mm10 -p 1 -size given -len 6,8,10,12 -noknown -mset vertebrates”.

REFERENCES

1. Murphy, K., et al., *Janeway's immunobiology*. 8 ed. 2012, New York: Garland Science.
2. Sakaguchi, S., *Regulatory T Cells: Key Controllers of Immunologic Self-Tolerance.* Cell, 2000. **101**(5): p. 455-458.
3. Josefowicz, S.Z., L. Lu, and A.Y. Rudensky, *Regulatory T Cells: Mechanisms of Differentiation and Function.* Annual Reviews of Immunology, 2012. **30**: p. 531-64.
4. Germain, R.N., *T-cell development and the CD4-CD8 lineage decision.* Nat Rev Immunol, 2002. **2**(5): p. 309-22.
5. Isomura, I., et al., *c-Rel is required for the development of thymic Foxp3+ CD4 regulatory T cells.* J Exp Med, 2009. **206**(13): p. 3001-14.
6. Kim, H.P. and W.J. Leonard, *CREB/ATF-dependent T cell receptor-induced FoxP3 gene expression: a role for DNA methylation.* J Exp Med, 2007. **204**(7): p. 1543-51.
7. Mantel, P.Y., et al., *Molecular Mechanisms Underlying FOXP3 Induction in Human T Cells.* The Journal of Immunology, 2006. **176**(6): p. 3593-3602.
8. Ouyang, W., et al., *Foxo proteins cooperatively control the differentiation of Foxp3+ regulatory T cells.* Nat Immunol, 2010. **11**(7): p. 618-27.
9. Tai, X., et al., *CD28 costimulation of developing thymocytes induces Foxp3 expression and regulatory T cell differentiation independently of interleukin 2.* Nat Immunol, 2005. **6**(2): p. 152-62.
10. Long, M., et al., *Nuclear factor-kappaB modulates regulatory T cell development by directly regulating expression of Foxp3 transcription factor.* Immunity, 2009. **31**(6): p. 921-31.
11. Kretschmer, K., et al., *Inducing and expanding regulatory T cell populations by foreign antigen.* Nat Immunol, 2005. **6**(12): p. 1219-27.
12. Hsieh, C.S., et al., *An intersection between the self-reactive regulatory and nonregulatory T cell receptor repertoires.* Nat Immunol, 2006. **7**(4): p. 401-10.
13. Lathrop, S.K., et al., *Peripheral education of the immune system by colonic commensal microbiota.* Nature, 2011. **478**(7368): p. 250-4.
14. Zheng, S.G., et al., *TGF- Requires CTLA-4 Early after T Cell Activation to Induce FoxP3 and Generate Adaptive CD4+CD25+ Regulatory Cells.* The Journal of Immunology, 2006. **176**(6): p. 3321-3329.
15. Zheng, Y., et al., *Role of conserved non-coding DNA elements in the Foxp3 gene in regulatory T-cell fate.* Nature, 2010. **463**(7282): p. 808-12.
16. Bennett, C.L., et al., *The immune dysregulation, polyendocrinopathy, enteropathy, X-linked syndrome (IPEX) is caused by mutations of FOXP3.* Nat Genet, 2001. **27**(1): p. 20-1.
17. Brunkow, M.E., et al., *Disruption of a new forkhead/winged-helix protein, scurfin, results in the fatal lymphoproliferative disorder of the scurfy mouse.* Nat Genet, 2001. **27**(1): p. 68-73.
18. Chen, Z., et al., *Where CD4+CD25+ T reg cells impinge on autoimmune diabetes.* J Exp Med, 2005. **202**(10): p. 1387-97.
19. Fontenot, J.D., M.A. Gavin, and A.Y. Rudensky, *Foxp3 programs the development and function of CD4+CD25+ regulatory T cells.* Nat Immunol, 2003. **4**(4): p. 330-6.
20. Hori, S., T. Nomura, and S. Sakaguchi, *Control of Regulatory T cell Development by the Transcription Factor Foxp3.* Science, 2003. **299**(5609): p. 1057-61.
21. Kim, J., et al., *Cutting edge: depletion of Foxp3+ cells leads to induction of autoimmunity by specific ablation of regulatory T cells in genetically targeted mice.* J Immunol, 2009. **183**(12): p. 7631-4.

22. Kim, J.M., J.P. Rasmussen, and A.Y. Rudensky, *Regulatory T cells prevent catastrophic autoimmunity throughout the lifespan of mice.* Nat Immunol, 2007. **8**(2): p. 191-7.
23. Kullberg, M.C., et al., *TGF-beta1 production by CD4+ CD25+ regulatory T cells is not essential for suppression of intestinal inflammation.* Eur J Immunol, 2005. **35**(10): p. 2886-95.
24. O'Garra, A., et al., *IL-10–producing and naturally occurring CD4+ Tregs: limiting collateral damage.* Journal of Clinical Investigation, 2004. **114**(10): p. 1372-1378.
25. Pandiyan, P., et al., *CD4+CD25+Foxp3+ regulatory T cells induce cytokine deprivation-mediated apoptosis of effector CD4+ T cells.* Nat Immunol, 2007. **8**(12): p. 1353-62.
26. Borsellino, G., et al., *Expression of ectonucleotidase CD39 by Foxp3+ Treg cells: hydrolysis of extracellular ATP and immune suppression.* Blood, 2007. **110**(4): p. 1225-32.
27. Kobie, J.J., et al., *T Regulatory and Primed Uncommitted CD4 T Cells Express CD73, Which Suppresses Effector CD4 T Cells by Converting 5'-Adenosine Monophosphate to Adenosine.* The Journal of Immunology, 2006. **177**(10): p. 6780-6786.
28. Liang, B., et al., *Regulatory T Cells Inhibit Dendritic Cells by Lymphocyte Activation Gene-3 Engagement of MHC Class II.* The Journal of Immunology, 2008. **180**(9): p. 5916-5926.
29. Kuipers, H., et al., *Contribution of the PD-1 ligands/PD-1 signaling pathway to dendritic cell-mediated CD4+ T cell activation.* Eur J Immunol, 2006. **36**(9): p. 2472-82.
30. Mellor, A.L. and D.H. Munn, *IDO expression by dendritic cells: tolerance and tryptophan catabolism.* Nat Rev Immunol, 2004. **4**(10): p. 762-74.
31. Swann, J.B. and M.J. Smyth, *Immune surveillance of tumors.* J Clin Invest, 2007. **117**(5): p. 1137-46.
32. Bieging, K.T., S.S. Mello, and L.D. Attardi, *Unravelling mechanisms of p53-mediated tumour suppression.* Nat Rev Cancer, 2014. **14**(5): p. 359-70.
33. Khong, H.T. and N.P. Restifo, *Natural selection of tumor variants in the generation of "tumor escape" phenotypes.* Nature Immunology, 2002. **3**(11): p. 999-1005.
34. Azuma, T., et al., *B7-H1 is a ubiquitous antiapoptotic receptor on cancer cells.* Blood, 2008. **111**(7): p. 3635-43.
35. LeBlanc, H., et al., *Tumor-cell resistance to death receptor--induced apoptosis through mutational inactivation of the proapoptotic Bcl-2 homolog Bax.* Nat Med, 2002. **8**(3): p. 274-81.
36. Massague, J., *TGFbeta in Cancer.* Cell, 2008. **134**(2): p. 215-30.
37. del Campo, A.B., et al., *Immune escape of cancer cells with beta2-microglobulin loss over the course of metastatic melanoma.* Int J Cancer, 2014. **134**(1): p. 102-13.
38. Krock, B.L., N. Skuli, and M.C. Simon, *Hypoxia-induced angiogenesis: good and evil.* Genes Cancer, 2011. **2**(12): p. 1117-33.
39. Chang, C.H., et al., *Metabolic Competition in the Tumor Microenvironment Is a Driver of Cancer Progression.* Cell, 2015. **162**(6): p. 1229-41.
40. Michalek, R.D., et al., *Cutting edge: distinct glycolytic and lipid oxidative metabolic programs are essential for effector and regulatory CD4+ T cell subsets.* J Immunol, 2011. **186**(6): p. 3299-303.
41. Barsoum, I.B., et al., *A mechanism of hypoxia-mediated escape from adaptive immunity in cancer cells.* Cancer Res, 2014. **74**(3): p. 665-74.
42. Turley, S.J., V. Cremasco, and J.L. Astarita, *Immunological hallmarks of stromal cells in the tumour microenvironment.* Nat Rev Immunol, 2015. **15**(11): p. 669-82.
43. Feig, C., et al., *Targeting CXCL12 from FAP-expressing carcinoma-associated fibroblasts synergizes with anti-PD-L1 immunotherapy in pancreatic cancer.* Proc Natl Acad Sci U S A, 2013. **110**(50): p. 20212-7.

44. Gajewski, T.F., et al., *Cancer Immunotherapy Targets Based on Understanding the T Cell-Inflamed Versus Non-T Cell-Inflamed Tumor Microenvironment.* Adv Exp Med Biol, 2017. **1036**: p. 19-31.
45. Lanitis, E., et al., *Mechanisms regulating T-cell infiltration and activity in solid tumors.* Ann Oncol, 2017. **28**(suppl_12): p. xii18-xii32.
46. Galon, J., et al., *Type, density, and location of immune cells within human colorectal tumors predict clinical outcome.* Science, 2006. **313**(5795): p. 1960-1964.
47. Gao, J., et al., *Loss of IFN-gamma Pathway Genes in Tumor Cells as a Mechanism of Resistance to Anti-CTLA-4 Therapy.* Cell, 2016. **167**(2): p. 397-404 e9.
48. Zaretsky, J.M., et al., *Mutations Associated with Acquired Resistance to PD-1 Blockade in Melanoma.* N Engl J Med, 2016. **375**(9): p. 819-29.
49. Spranger, S., et al., *Density of immunogenic antigens does not explain the presence or absence of the T-cell-inflamed tumor microenvironment in melanoma.* Proc Natl Acad Sci U S A, 2016. **113**(48): p. E7759-E7768.
50. Hannenhalli, S. and K.H. Kaestner, *The evolution of Fox genes and their role in development and disease.* Nat Rev Genet, 2009. **10**(4): p. 233-40.
51. Myatt, S.S. and E.W. Lam, *The emerging roles of forkhead box (Fox) proteins in cancer.* Nat Rev Cancer, 2007. **7**(11): p. 847-59.
52. Pierrou, S., et al., *Cloning and characterization of seven human forkhead proteins: binding site specificity and DNA bending.* EMBO Journal, 1994. **13**(20): p. 5002-5012.
53. Takahashi, K. and S. Yamanaka, *Induction of pluripotent stem cells from mouse embryonic and adult fibroblast cultures by defined factors.* Cell, 2006. **126**(4): p. 663-76.
54. Tootle, T.L. and I. Rebay, *Post-translational modifications influence transcription factor activity: a view from the ETS superfamily.* Bioessays, 2005. **27**(3): p. 285-98.
55. Slattery, M., et al., *Cofactor binding evokes latent differences in DNA binding specificity between Hox proteins.* Cell, 2011. **147**(6): p. 1270-82.
56. Kaestner, K.H., W. Knochel, and D.E. Martinez, *Unified nomenclature for the winged helix/forkhead transcription factors.* Genes & Development, 2000. **14**: p. 142-146.
57. Lam, E.W., et al., *Forkhead box proteins: tuning forks for transcriptional harmony.* Nat Rev Cancer, 2013. **13**(7): p. 482-95.
58. Santos, M.E., et al., *Alternative splicing and gene duplication in the evolution of the FoxP gene subfamily.* Mol Biol Evol, 2011. **28**(1): p. 237-47.
59. Shu, W., et al., *Characterization of a new subfamily of winged-helix/forkhead (Fox) genes that are expressed in the lung and act as transcriptional repressors.* J Biol Chem, 2001. **276**(29): p. 27488-97.
60. Tamura, S., et al., *Foxp1 gene expression in projection neurons of the mouse striatum.* Neuroscience, 2004. **124**(2): p. 261-7.
61. Wang, B., et al., *Foxp1 regulates cardiac outflow tract, endocardial cushion morphogenesis and myocyte proliferation and maturation.* Development, 2004. **131**(18): p. 4477-87.
62. Zhang, Y., et al., *Foxp1 coordinates cardiomyocyte proliferation through both cell-autonomous and nonautonomous mechanisms.* Genes Dev, 2010. **24**(16): p. 1746-57.
63. Lai, C.S.C., et al., *A forkhead-domain gene is mutated in a severe speech and language disorder.* Nature, 2001. **413**: p. 519-523.
64. Rousso, D.L., et al., *Foxp-mediated suppression of N-cadherin regulates neuroepithelial character and progenitor maintenance in the CNS.* Neuron, 2012. **74**(2): p. 314-30.
65. Shu, W., et al., *Foxp2 and Foxp1 cooperatively regulate lung and esophagus development.* Development, 2007. **134**(10): p. 1991-2000.
66. Feng, X., et al., *Foxp1 is an essential transcriptional regulator for the generation of quiescent naive T cells during thymocyte development.* Blood, 2010. **115**(3): p. 510-518.

67. Hu, H., et al., *Foxp1 is an essential transcriptional regulator of B cell development.* Nat Immunol, 2006. **7**(8): p. 819-26.
68. Feng, X., et al., *Transcription factor Foxp1 exerts essential cell-intrinsic regulation of the quiescence of naive T cells.* Nat Immunol, 2011. **12**(6): p. 544-50.
69. Shi, B., et al., *Foxp1 Negatively Regulates T Follicular Helper Cell Differentiation and Germinal Center Responses by Controlling Cell Migration and CTLA-4.* J Immunol, 2018. **200**(2): p. 586-594.
70. Wang, H., et al., *The transcription factor Foxp1 is a critical negative regulator of the differentiation of follicular helper T cells.* Nat Immunol, 2014. **15**(7): p. 667-75.
71. Wei, H., et al., *Cutting Edge: Foxp1 Controls Naive CD8+ T Cell Quiescence by Simultaneously Repressing Key Pathways in Cellular Metabolism and Cell Cycle Progression.* J Immunol, 2016. **196**(9): p. 3537-41.
72. Stephen, T.L., et al., *Transforming growth factor beta-mediated suppression of antitumor T cells requires FoxP1 transcription factor expression.* Immunity, 2014. **41**(3): p. 427-439.
73. Wiehagen, K.R., *Forkhead Transcription Factors Foxp1 and Foxp4 Regulate T Cell Development and Function.* Publicly Accessible Penn Dissertations, 2013: p. 943.
74. Teichmann, S.A. and M.M. Babu, *Gene regulatory network growth by duplication.* Nat Genet, 2004. **36**(5): p. 492-6.
75. Koh, K.P., M.S. Sundrud, and A. Rao, *Domain requirements and sequence specificity of DNA binding for the forkhead transcription factor FOXP3.* PLoS One, 2009. **4**(12): p. e8109.
76. Lu, M.M., et al., *Foxp4: a novel member of the Foxp subfamily of winged-helix genes co-expressed with Foxp1 and Foxp2 in pulmonary and gut tissues.* Mechanisms of Development, 2002. **119**: p. S197,S202.
77. Samstein, R.M., et al., *Foxp3 exploits a pre-existent enhancer landscape for regulatory T cell lineage specification.* Cell, 2012. **151**(1): p. 153-66.
78. Li, B., et al., *FOXP3 is a homo-oligomer and a component of a supramolecular regulatory complex disabled in the human XLAAD/IPEX autoimmune disease.* Int Immunol, 2007. **19**(7): p. 825-35.
79. Li, S., J. Weidenfeld, and E.E. Morrisey, *Transcriptional and DNA Binding Activity of the Foxp1/2/4 Family Is Modulated by Heterotypic and Homotypic Protein Interactions.* Molecular and Cellular Biology, 2003. **24**(2): p. 809-822.
80. Rudra, D., et al., *Transcription factor Foxp3 and its protein partners form a complex regulatory network.* Nat Immunol, 2012. **13**(10): p. 1010-9.
81. Plitas, G., et al., *Regulatory T Cells Exhibit Distinct Features in Human Breast Cancer.* Immunity, 2016. **45**(5): p. 1122-1134.
82. Sather, B.D., et al., *Altering the distribution of Foxp3(+) regulatory T cells results in tissue-specific inflammatory disease.* J Exp Med, 2007. **204**(6): p. 1335-47.
83. Chaudhry, A., et al., *CD4+ regulatory T cells control TH17 responses in a Stat3-dependent manner.* Science, 2009. **326**(5955): p. 986-91.
84. Nishikawa, H. and S. Sakaguchi, *Regulatory T cells in cancer immunotherapy.* Curr Opin Immunol, 2014. **27**: p. 1-7.
85. Roychoudhuri, R., R.L. Eil, and N.P. Restifo, *The interplay of effector and regulatory T cells in cancer.* Curr Opin Immunol, 2015. **33**: p. 101-11.
86. DeNardo, D.G. and L.M. Coussens, *Inflammation and breast cancer. Balancing immune response: crosstalk between adaptive and innate immune cells during breast cancer progression.* Breast Cancer Res, 2007. **9**(4): p. 212.
87. Coussens, L.M. and J.W. Pollard, *Leukocytes in mammary development and cancer.* Cold Spring Harb Perspect Biol, 2011. **3**(3).

88. Chin, Y., et al., *Phenotypic analysis of tumor-infiltrating lymphocytes from human breast cancer.* Anticancer Res, 1992. **12**(5): p. 1463-6.
89. Bates, G.J., et al., *Quantification of regulatory T cells enables the identification of high-risk breast cancer patients and those at risk of late relapse.* J Clin Oncol, 2006. **24**(34): p. 5373-80.
90. Bohling, S.D. and K.H. Allison, *Immunosuppressive regulatory T cells are associated with aggressive breast cancer phenotypes: a potential therapeutic target.* Mod Pathol, 2008. **21**(12): p. 1527-32.
91. Ohara, M., et al., *Possible involvement of regulatory T cells in tumor onset and progression in primary breast cancer.* Cancer Immunol Immunother, 2009. **58**(3): p. 441-7.
92. Joshi, N.S., et al., *Regulatory T Cells in Tumor-Associated Tertiary Lymphoid Structures Suppress Anti-tumor T Cell Responses.* Immunity, 2015. **43**(3): p. 579-90.
93. Klages, K., et al., *Selective depletion of Foxp3+ regulatory T cells improves effective therapeutic vaccination against established melanoma.* Cancer Res, 2010. **70**(20): p. 7788-99.
94. Pastille, E., et al., *Transient ablation of regulatory T cells improves antitumor immunity in colitis-associated colon cancer.* Cancer Res, 2014. **74**(16): p. 4258-69.
95. Teng, M.W., et al., *Conditional regulatory T-cell depletion releases adaptive immunity preventing carcinogenesis and suppressing established tumor growth.* Cancer Res, 2010. **70**(20): p. 7800-9.
96. Bos, P.D., et al., *Transient regulatory T cell ablation deters oncogene-driven breast cancer and enhances radiotherapy.* J Exp Med, 2013. **210**(11): p. 2435-66.
97. Demir, L., et al., *Predictive and prognostic factors in locally advanced breast cancer: effect of intratumoral FOXP3+ Tregs.* Clin Exp Metastasis, 2013. **30**(8): p. 1047-62.
98. Kim, S., et al., *Zonal difference and prognostic significance of foxp3 regulatory T cell infiltration in breast cancer.* J Breast Cancer, 2014. **17**(1): p. 8-17.
99. Liu, F., et al., *CD8(+) cytotoxic T cell and FOXP3(+) regulatory T cell infiltration in relation to breast cancer survival and molecular subtypes.* Breast Cancer Res Treat, 2011. **130**(2): p. 645-55.
100. Liu, S., et al., *Prognostic significance of FOXP3+ tumor-infiltrating lymphocytes in breast cancer depends on estrogen receptor and human epidermal growth factor receptor-2 expression status and concurrent cytotoxic T-cell infiltration.* Breast Cancer Res, 2014. **16**(5): p. 432.
101. Ruffell, B., et al., *Leukocyte composition of human breast cancer.* Proc Natl Acad Sci U S A, 2012. **109**(8): p. 2796-801.
102. Bolotin, D.A., et al., *MiXCR: software for comprehensive adaptive immunity profiling.* Nat Methods, 2015. **12**(5): p. 380-1.
103. Shugay, M., et al., *VDJtools: Unifying Post-analysis of T Cell Receptor Repertoires.* PLoS Comput Biol, 2015. **11**(11): p. e1004503.
104. Pearce, E.L., et al., *Control of effector CD8+ T cell function by the transcription factor Eomesodermin.* Science, 2003. **302**(5647): p. 1041-3.
105. Doyle, J.M., et al., *MAGE-RING protein complexes comprise a family of E3 ubiquitin ligases.* Mol Cell, 2010. **39**(6): p. 963-74.
106. Xie, Q., et al., *Characterization of a novel mouse model with genetic deletion of CD177.* Protein Cell, 2015. **6**(2): p. 117-26.
107. Harner, S., et al., *Cord blood Valpha24-Vbeta11 natural killer T cells display a Th2-chemokine receptor profile and cytokine responses.* PLoS One, 2011. **6**(1): p. e15714.
108. Roos, R.S., et al., *Identification of CCR8, the receptor for the human CC chemokine I-309.* J Biol Chem, 1997. **272**(28): p. 17251-4.

109. Cancer Genome Atlas, N., *Comprehensive molecular portraits of human breast tumours.* Nature, 2012. **490**(7418): p. 61-70.
110. Gobert, M., et al., *Regulatory T cells recruited through CCL22/CCR4 are selectively activated in lymphoid infiltrates surrounding primary breast tumors and lead to an adverse clinical outcome.* Cancer Res, 2009. **69**(5): p. 2000-9.
111. Hossain, D.M., et al., *FoxP3 acts as a cotranscription factor with STAT3 in tumor-induced regulatory T cells.* Immunity, 2013. **39**(6): p. 1057-69.
112. Senovilla, L., et al., *An immunosurveillance mechanism controls cancer cell ploidy.* Science, 2012. **337**(6102): p. 1678-84.
113. Shang, B., et al., *Prognostic value of tumor-infiltrating FoxP3(+) regulatory T cells in cancers: a systematic review and meta-analysis.* Sci Rep, 2015. **5**: p. 15179.
114. Burzyn, D., C. Benoist, and D. Mathis, *Regulatory T cells in nonlymphoid tissues.* Nat Immunol, 2013. **14**(10): p. 1007-13.
115. De Simone, M., et al., *Transcriptional Landscape of Human Tissue Lymphocytes Unveils Uniqueness of Tumor-Infiltrating T Regulatory Cells.* Immunity, 2016. **45**(5): p. 1135-1147.
116. Levine, A.G., et al., *Continuous requirement for the TCR in regulatory T cell function.* Nat Immunol, 2014. **15**(11): p. 1070-8.
117. Huehn, J., et al., *Developmental stage, phenotype, and migration distinguish naive- and effector/memory-like CD4+ regulatory T cells.* J Exp Med, 2004. **199**(3): p. 303-13.
118. Campbell, D.J., *Control of Regulatory T Cell Migration, Function, and Homeostasis.* J Immunol, 2015. **195**(6): p. 2507-13.
119. Lee, J.H., S.G. Kang, and C.H. Kim, *FoxP3+ T cells undergo conventional first switch to lymphoid tissue homing receptors in thymus but accelerated second switch to nonlymphoid tissue homing receptors in secondary lymphoid tissues.* J Immunol, 2007. **178**(1): p. 301-11.
120. Curiel, T.J., et al., *Specific recruitment of regulatory T cells in ovarian carcinoma fosters immune privilege and predicts reduced survival.* Nat Med, 2004. **10**(9): p. 942-9.
121. Faget, J., et al., *Early detection of tumor cells by innate immune cells leads to T(reg) recruitment through CCL22 production by tumor cells.* Cancer Res, 2011. **71**(19): p. 6143-52.
122. Sugiyama, D., et al., *Anti-CCR4 mAb selectively depletes effector-type FoxP3+CD4+ regulatory T cells, evoking antitumor immune responses in humans.* Proc Natl Acad Sci U S A, 2013. **110**(44): p. 17945-50.
123. Ueda, R., *Clinical Application of Anti-CCR4 Monoclonal Antibody.* Oncology, 2015. **89 Suppl 1**: p. 16-21.
124. Kurose, K., et al., *Phase Ia Study of FoxP3+ CD4 Treg Depletion by Infusion of a Humanized Anti-CCR4 Antibody, KW-0761, in Cancer Patients.* Clin Cancer Res, 2015. **21**(19): p. 4327-36.
125. Williams, L.M. and A.Y. Rudensky, *Maintenance of the Foxp3-dependent developmental program in mature regulatory T cells requires continued expression of Foxp3.* Nat Immunol, 2007. **8**(3): p. 277-84.
126. Heinz, S., et al., *Simple combinations of lineage-determining transcription factors prime cis-regulatory elements required for macrophage and B cell identities.* Mol Cell, 2010. **38**(4): p. 576-89.
127. Chen, Y., et al., *DNA binding by FOXP3 domain-swapped dimer suggests mechanisms of long-range chromosomal interactions.* Nucleic Acids Res, 2015. **43**(2): p. 1268-82.
128. Ono, M., et al., *Foxp3 controls regulatory T-cell function by interacting with AML1/Runx1.* Nature, 2007. **446**(7136): p. 685-9.
129. Rudra, D., et al., *Runx-CBFbeta complexes control expression of the transcription factor Foxp3 in regulatory T cells.* Nat Immunol, 2009. **10**(11): p. 1170-7.

130. Arvey, A., et al., *Inflammation-induced repression of chromatin bound by the transcription factor Foxp3 in regulatory T cells.* Nat Immunol, 2014. **15**(6): p. 580-587.
131. Kitagawa, Y., et al., *Guidance of regulatory T cell development by Satb1-dependent super-enhancer establishment.* Nat Immunol, 2017. **18**(2): p. 173-183.
132. Beyer, M., et al., *Repression of the genome organizer SATB1 in regulatory T cells is required for suppressive function and inhibition of effector differentiation.* Nat Immunol, 2011. **12**(9): p. 898-907.
133. Liu, W., et al., *CD127 expression inversely correlates with FoxP3 and suppressive function of human CD4+ T reg cells.* J Exp Med, 2006. **203**(7): p. 1701-11.
134. Feuerer, M., et al., *Genomic definition of multiple ex vivo regulatory T cell subphenotypes.* Proc Natl Acad Sci U S A, 2010. **107**(13): p. 5919-24.
135. Chinen, T., et al., *An essential role for the IL-2 receptor in Treg cell function.* Nat Immunol, 2016. **17**(11): p. 1322-1333.
136. Anders, S., et al., *Count-based differential expression analysis of RNA sequencing data using R and Bioconductor.* Nat Protoc, 2013. **8**(9): p. 1765-86.
137. Bolger, A.M., M. Lohse, and B. Usadel, *Trimmomatic: a flexible trimmer for Illumina sequence data.* Bioinformatics, 2014. **30**(15): p. 2114-20.
138. Kim, D., et al., *TopHat2: accurate alignment of transcriptomes in the presence of insertions, deletions and gene fusions.* Genome Biol, 2013. **14**(4): p. R36.
139. Langmead, B. and S.L. Salzberg, *Fast gapped-read alignment with Bowtie 2.* Nat Methods, 2012. **9**(4): p. 357-9.
140. Li, H., et al., *The Sequence Alignment/Map format and SAMtools.* Bioinformatics, 2009. **25**(16): p. 2078-9.
141. Love, M.I., W. Huber, and S. Anders, *Moderated estimation of fold change and dispersion for RNA-seq data with DESeq2.* Genome Biol, 2014. **15**(12): p. 550.
142. Eden, E., et al., *GOrilla: a tool for discovery and visualization of enriched GO terms in ranked gene lists.* BMC Bioinformatics, 2009. **10**: p. 48.
143. Kim, D., B. Langmead, and S.L. Salzberg, *HISAT: a fast spliced aligner with low memory requirements.* Nat Methods, 2015. **12**(4): p. 357-60.
144. Liao, Y., G.K. Smyth, and W. Shi, *The Subread aligner: fast, accurate and scalable read mapping by seed-and-vote.* Nucleic Acids Res, 2013. **41**(10): p. e108.
145. Zhang, Y., et al., *Model-based analysis of ChIP-Seq (MACS).* Genome Biol, 2008. **9**(9): p. R137.